Electronic Supplementary Information 4

Non-identical Electronic Characters of the Internucleotidic Phosphates in RNA Modulate the Chemical Reactivity of the Phosphodiester Bonds

Jharna Barman[1], Sandipta Acharya[1], Chuanzheng Zhou[1], Subhrangsu Chatterjee[1], Åke Engström[2], and Jyoti Chattopadhyaya[1]*

[1]Department of Bioorganic Chemistry, Box 581, Biomedical Center, Uppsala University, S-751 23 Uppsala, Sweden

[2]Department of Medical Biochemistry and Microbiology, Box 582, Biomedical Center, Uppsala University, S-751 23 Uppsala, Sweden

jyoti@boc.uu.se

Content:

Figure S13

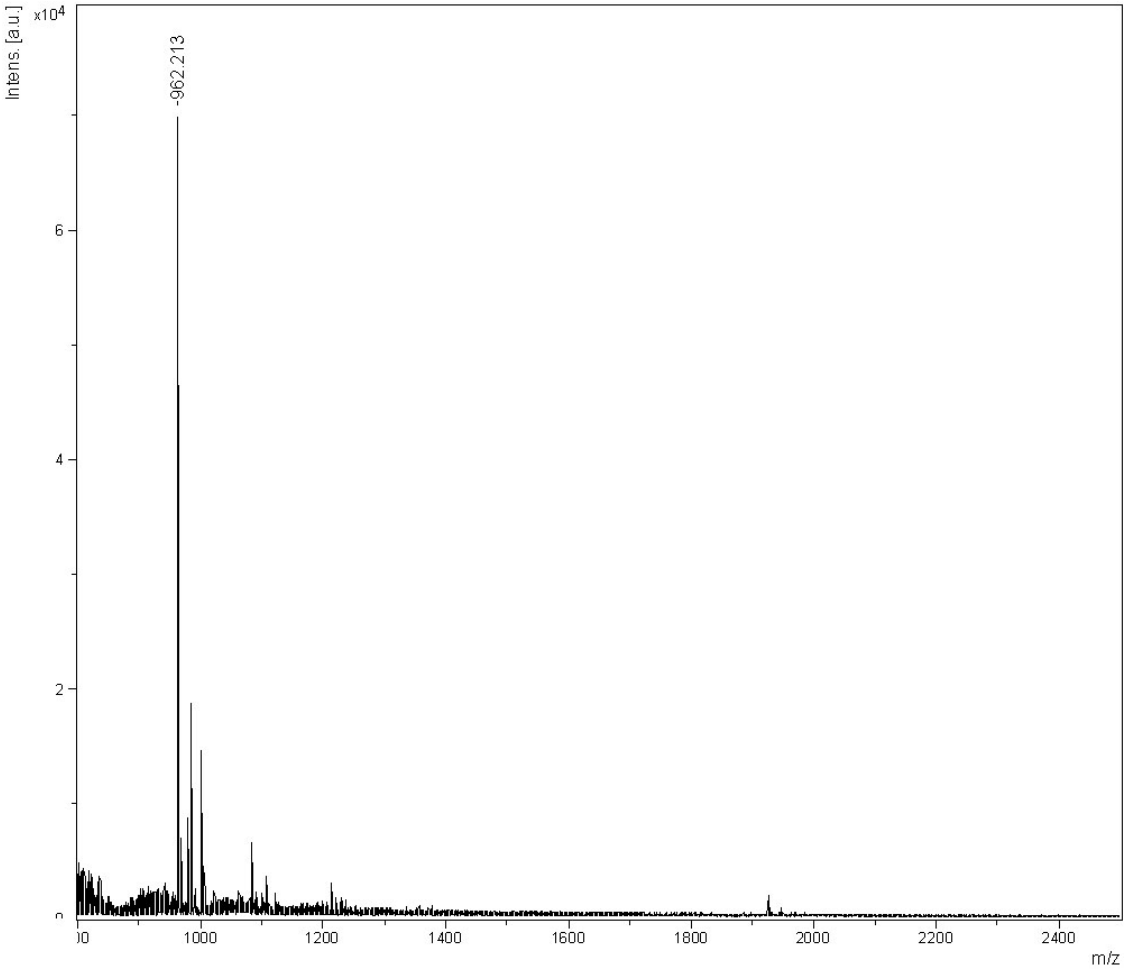

Figure S13(a1): Maldi Tof mass-spectral analysis of the RP-Hplc fraction at **R_T = 21.52** min for alkaline hydrolysis (pH 12.5 / 20ºC) of **5′-r(CAAGAAC)-3′** (**5b**) after **1h** [for Hplc profile, see Fig **S12 (a2)**] showing the main peak at m/z **962.2** for **5′-CAA$_{2'/3'-P}$** [see Table S9(A)].

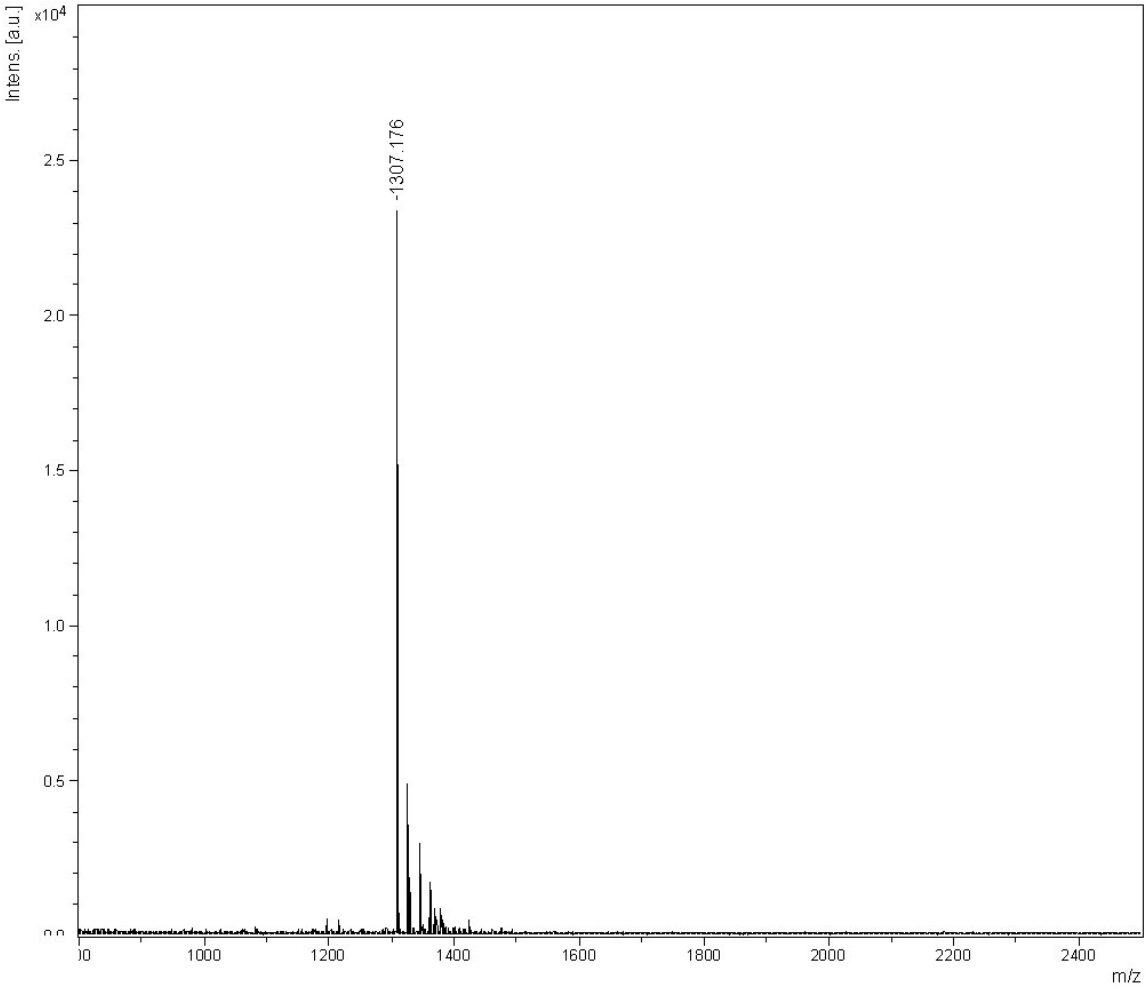

Figure S13(a2): Maldi Tof mass-spectral analysis of the SMART™ RP-Hplc fraction at **R_T = 34.04** min in the **Fig S12(a2i).** Corresponding RP-Hplc fraction is **R_T = 23.86** min in the **Fig S12(a2)** [after **1h** of alkaline hydrolysis (pH 12.5 / 20ºC) of **5′-r(CAAGAAC)-3′**, **5b**]. The main peak at m/z **1307.3** is for **5'-CAAG$_{2', 3'\text{-cMP}}$** [see Table S9(A)].

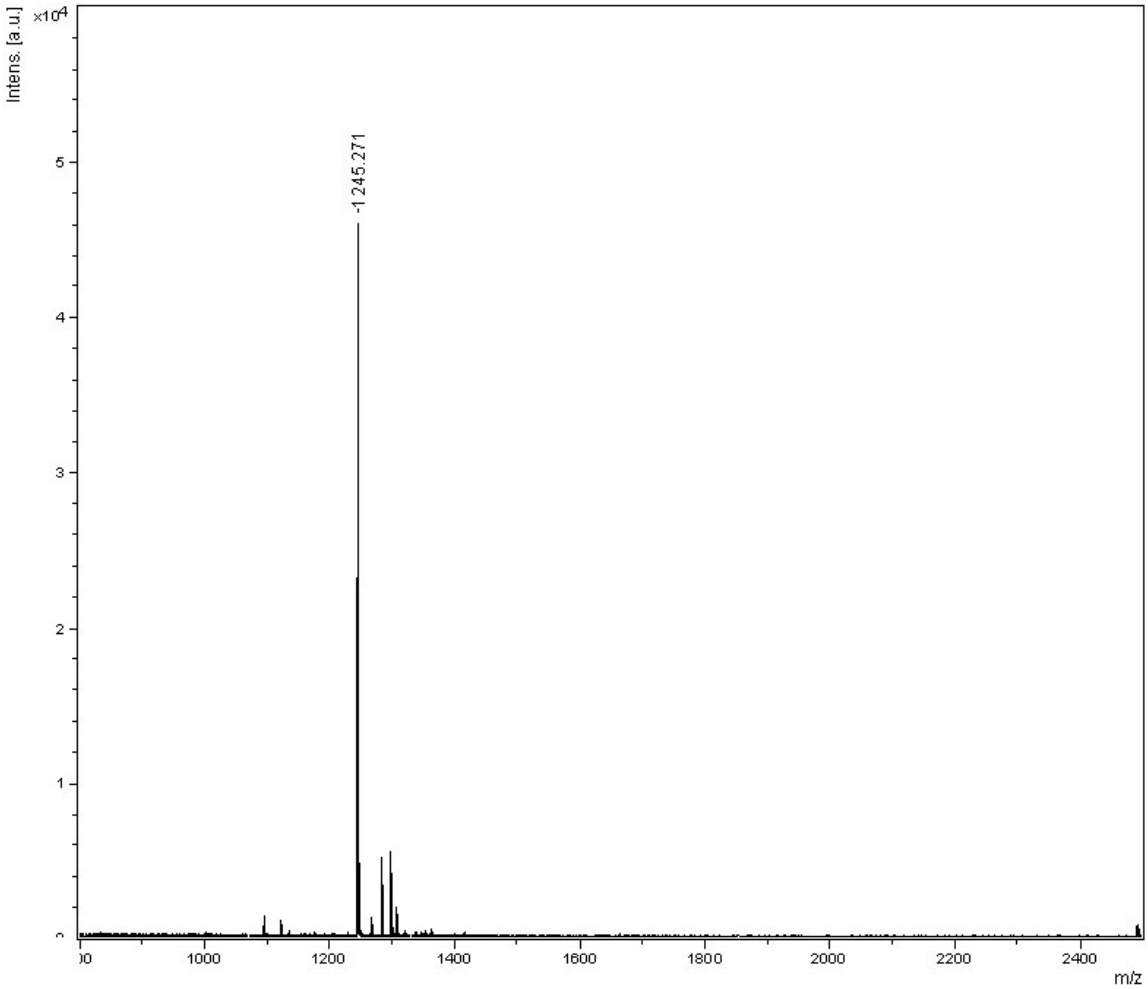

Figure S13(a3): Maldi-Tof mass-spectral analysis of the SMART™ RP-Hplc fraction at **R_T = 34.77** min in the **Fig S12(a2i).** Corresponding RP-Hplc fraction is **R_T = 23.86** min in the **Fig S12(a2)** [after **1h** of alkaline hydrolysis (pH 12.5 / 20ºC) of **5′-r(CAAGAAC)-3′**, **5b**]. The main peak at m/z **1245.3** is for **5'-GAAC-3'** [see Table S9(A)].

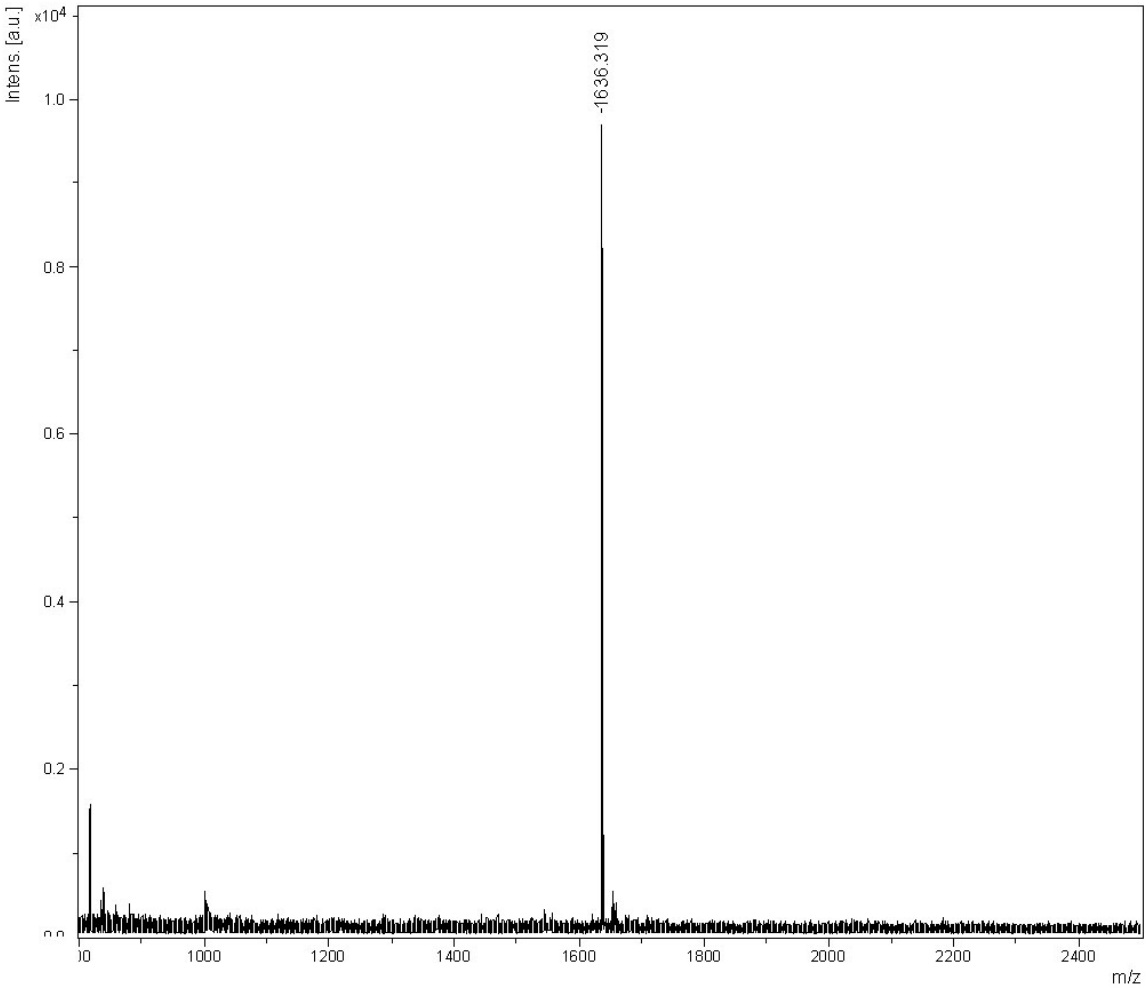

Figure S13(a4): Maldi-Tof mass-spectral analysis of the SMART™ RP-Hplc fraction at **R_T = 27.12** min in the **Fig S12(a2j).** Corresponding RP-Hplc fraction is **R_T = 25.44** min in the **Fig S12(a2)** [after **1h** of alkaline hydrolysis (pH 12.5 / 20ºC) of **5′-r(CAAGAAC)-3′**, **5b**]. The main peak at m/z **1636.3** is for **5'-CAAGA$_{2', 3'\text{-cMP}}$** [see Table S9(A)].

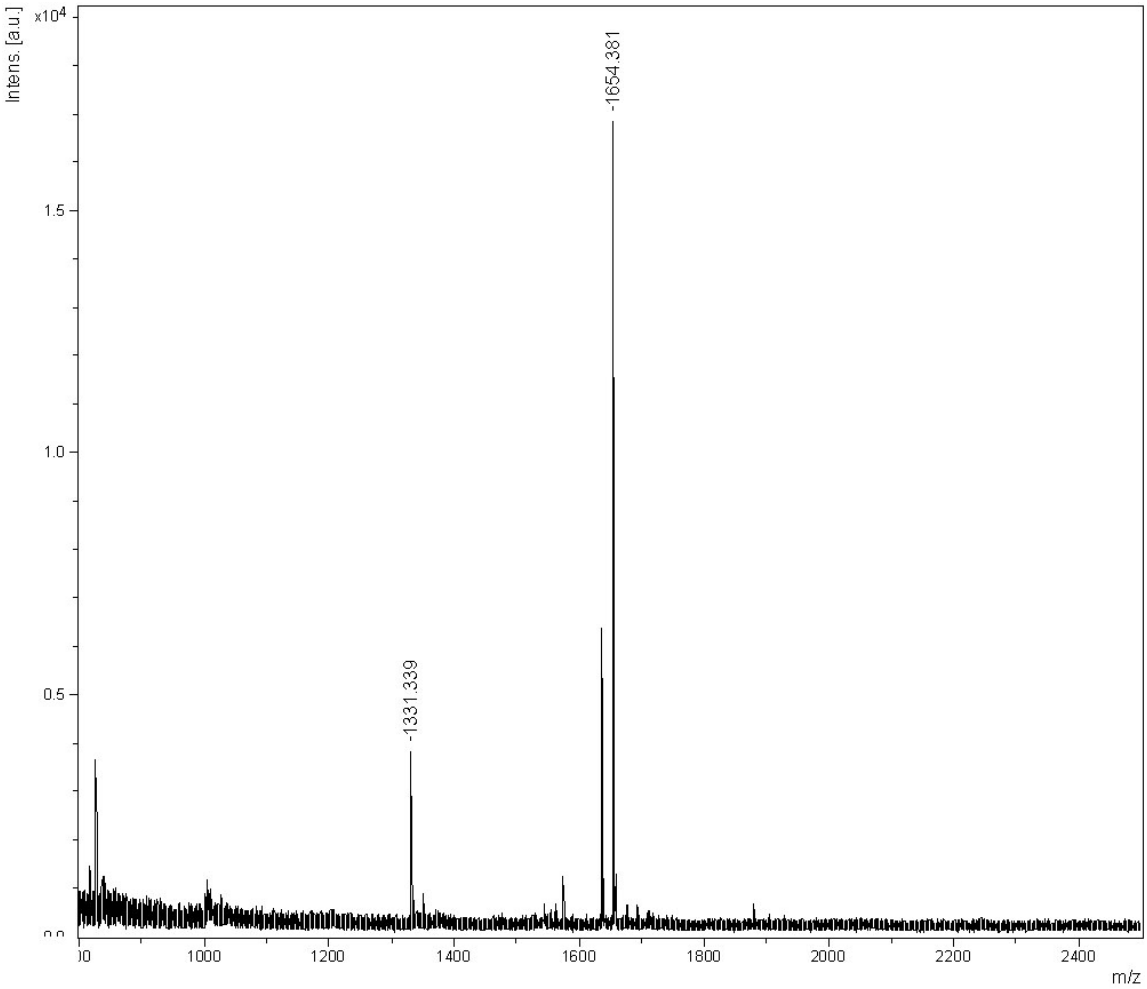

Figure S13(a5): Maldi-Tof mass-spectral analysis of the SMART™ RP-Hplc fraction at **R_T = 27.41** min in the **Fig S12(a2j).** Corresponding RP-Hplc fraction is **R_T = 25.44** min in the **Fig S12(a2)** [after **1h** of alkaline hydrolysis (pH 12.5 / 20ºC) of **5′-r(CAAGAAC)-3′**, **5b**]. The main peak at m/z **1654.4** is for **5'-CAAGA$_{2'/3'-P}$** and at m/z **1636.3** is for **5'-CAAGA$_{2', 3'-cMP}$** [see Table S9(A)].

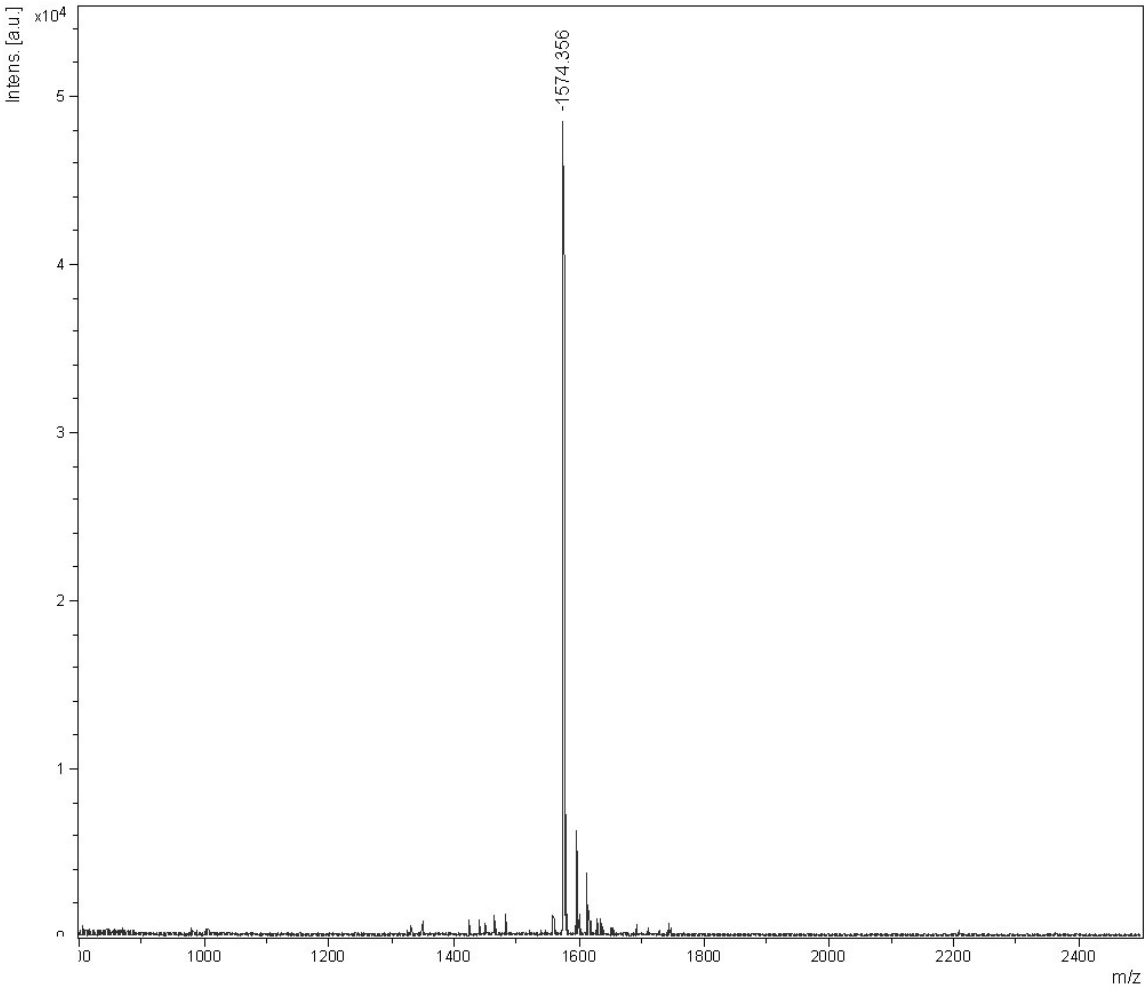

Figure S13(a6): Maldi-Tof mass-spectral analysis of the SMART™ RP-Hplc fraction at **R_T = 27.93** min in the **Fig S12(a2j).** Corresponding RP-Hplc fraction is **R_T = 25.44** min in the **Fig S12(a2)** [after **1h** of alkaline hydrolysis (pH 12.5 / 20ºC) of **5′-r(CAAGAAC)-3′**, **5b**]. The main peak at m/z **1574.4** is for **5′-AGAAC-3′** [see Table S9(A)].

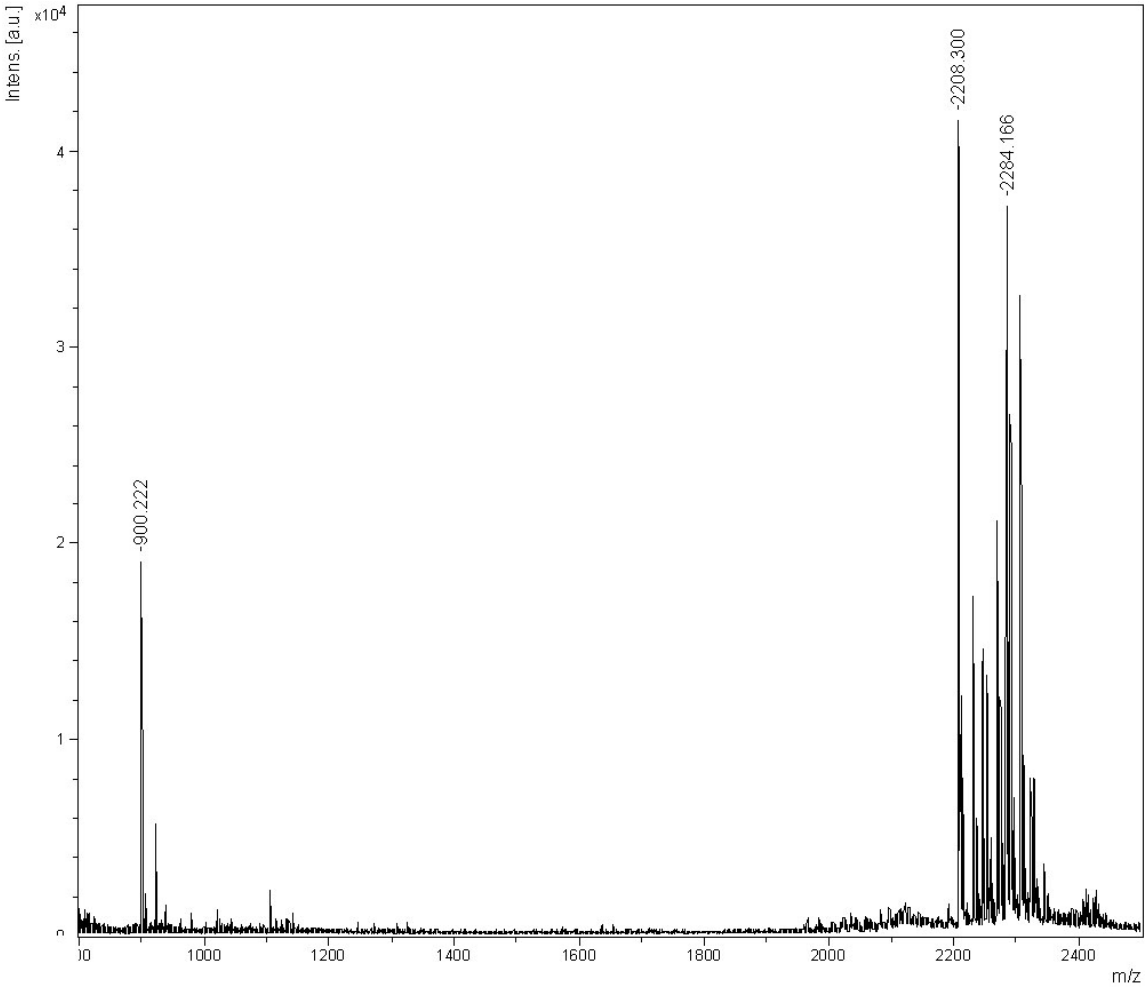

Figure S13(a7): Maldi-Tof mass-spectral analysis of the RP-Hplc fraction at **R_T = 26.21** min for alkaline hydrolysis (pH 12.5 / 20ºC) of **5′-r(CAAGAAC)-3′** (**5b**) after **1h** [for Hplc profile, see Fig **S12 (a2)**] showing the main peak at m/z **900.2** for 5'-AAC-3' (a fragmentation peak of the heptameric peak in the process of recording mass as confirmed by the variation of the laser power in the Maldi Tof)**,** **2208.3** for the parent heptamer and **2284.2** for some non-nucleos(t)idic fragment [see Table S9(A)].

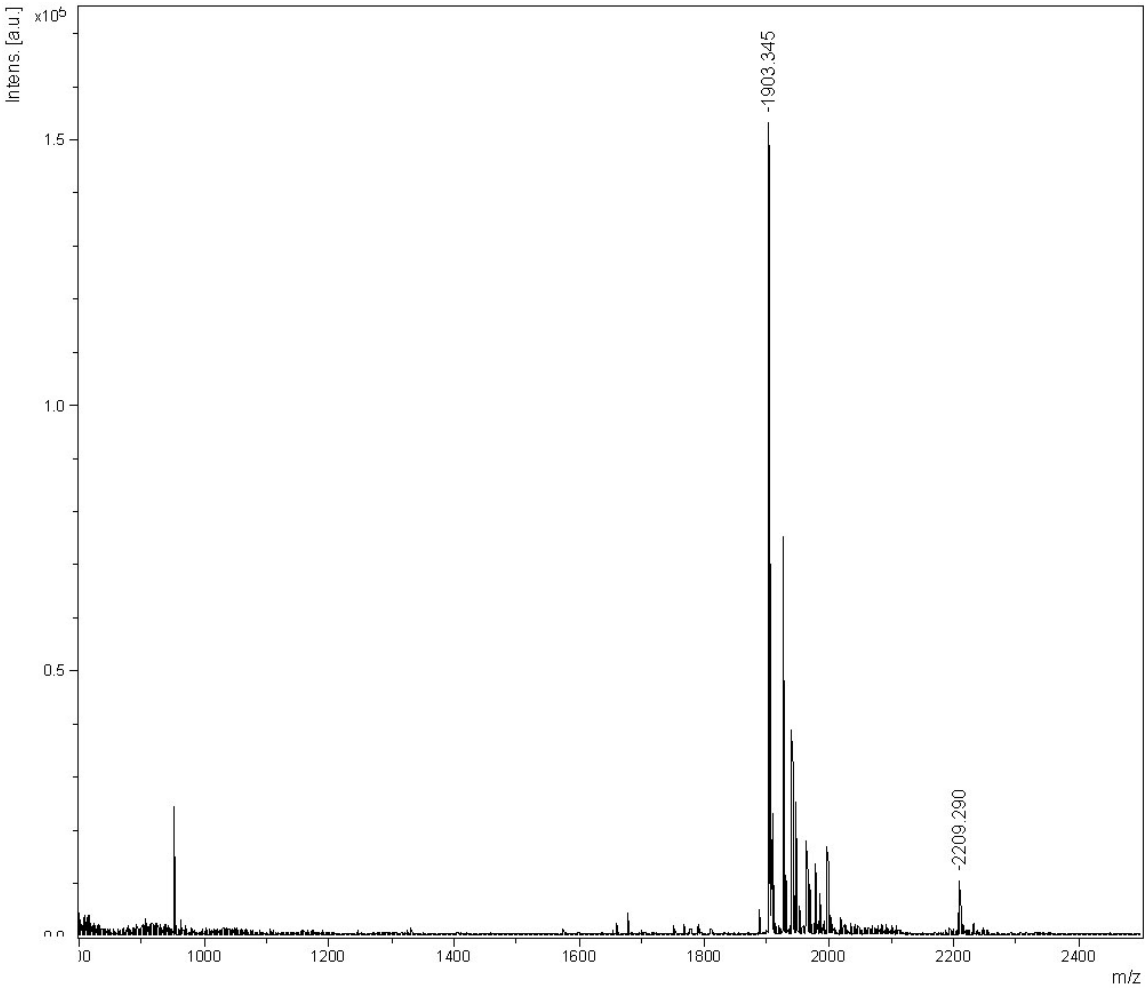

Figure S13(a8): Maldi-Tof mass-spectral analysis of the RP-Hplc fraction at **R_T = 27.10** min for alkaline hydrolysis (pH 12.5 / 20ºC) of **5′-r(CAAGAAC)-3′** (**5b**) after **1h** [for Hplc profile, see Fig **S12 (a2)**] showing the main peak at m/z **1903.3** for **5′-AAGAAC-3′** [see Table S9(A)].

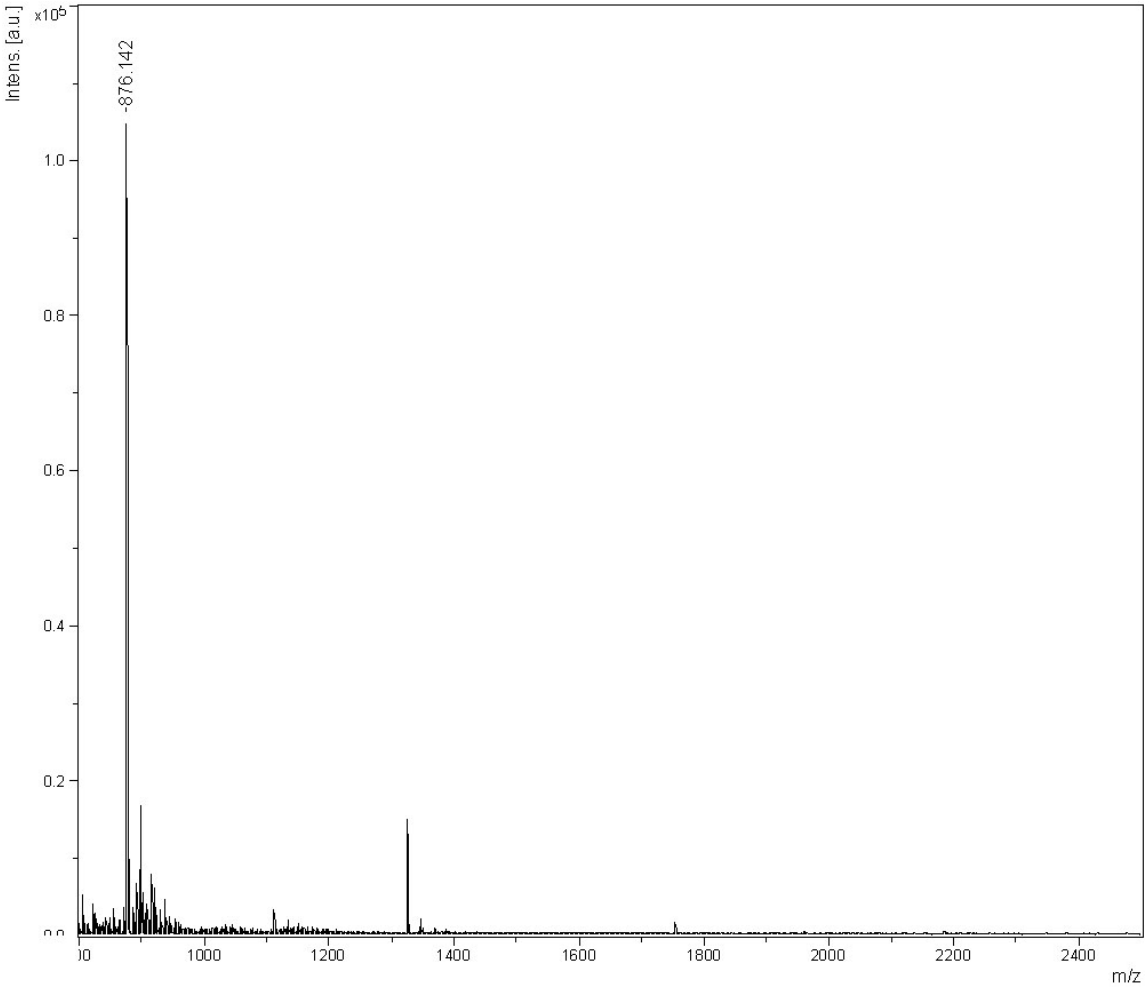

Figure S15(b1): Maldi-Tof mass-spectral analysis of the RP-Hplc fraction at **R_T = 19.87** min for alkaline hydrolysis (pH 12.5 / 20ºC) of **5′-r(CAAGCAC)-3′** (**6b**) after **1h** [for RP-Hplc profile, see Fig **S12 (b2)**] showing the main peak at m/z **876.1** for **5'-CAC-3'** [see Table S9(B)].

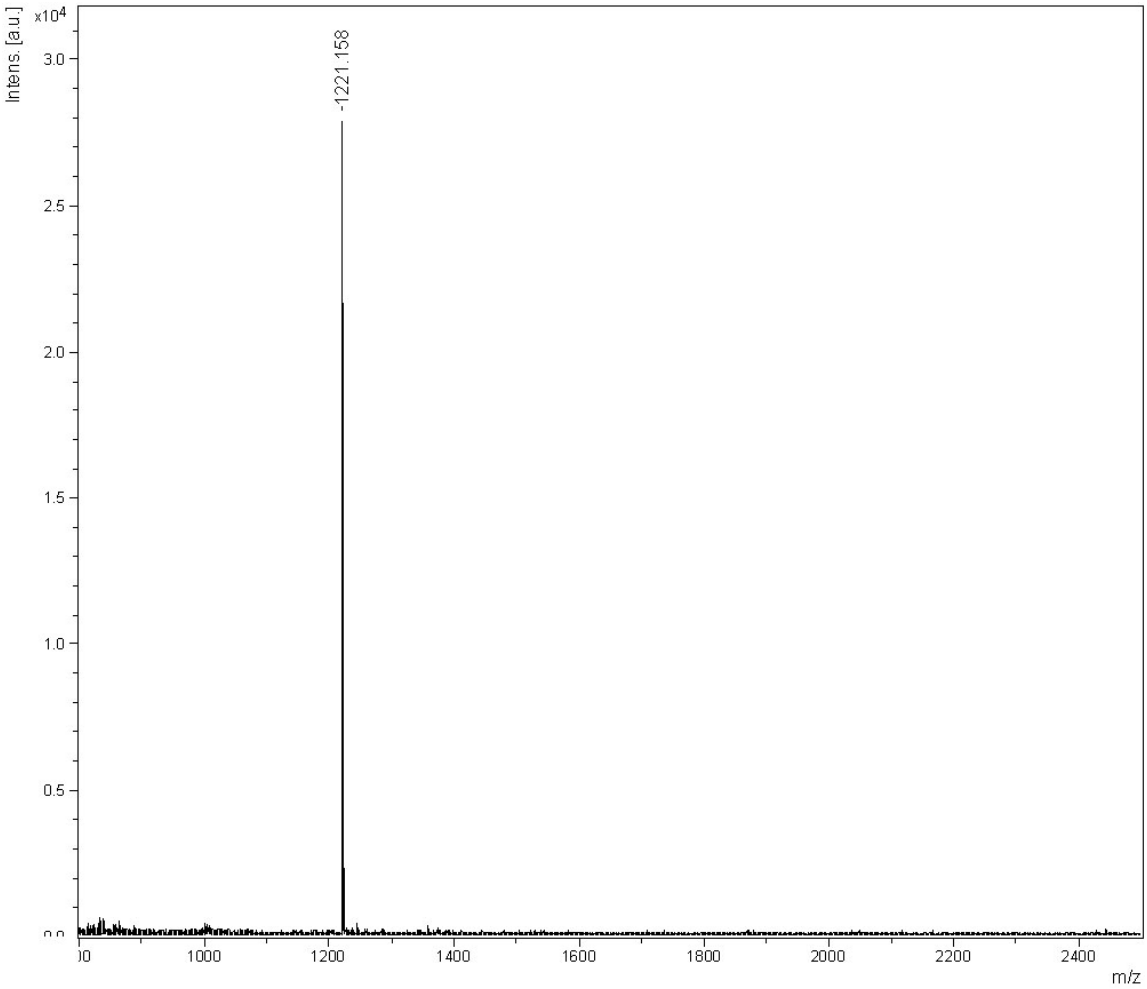

Figure S13(b2): Maldi-Tof mass-spectral analysis of the SMART™ RP-Hplc fraction at **R_T = 20.68** min in the **Fig S12(b2i).** Corresponding RP-Hplc fraction is **R_T = 21.18** min in the **Fig S12(b2)** [after **1h** alkaline hydrolysis (pH 12.5 / 20ºC) of **5′-r(CAAGCAC)-3′**, **6b**]. The main peak at m/z **1221.3** is for **5'-GCAC-3'** [see Table S9(B)].

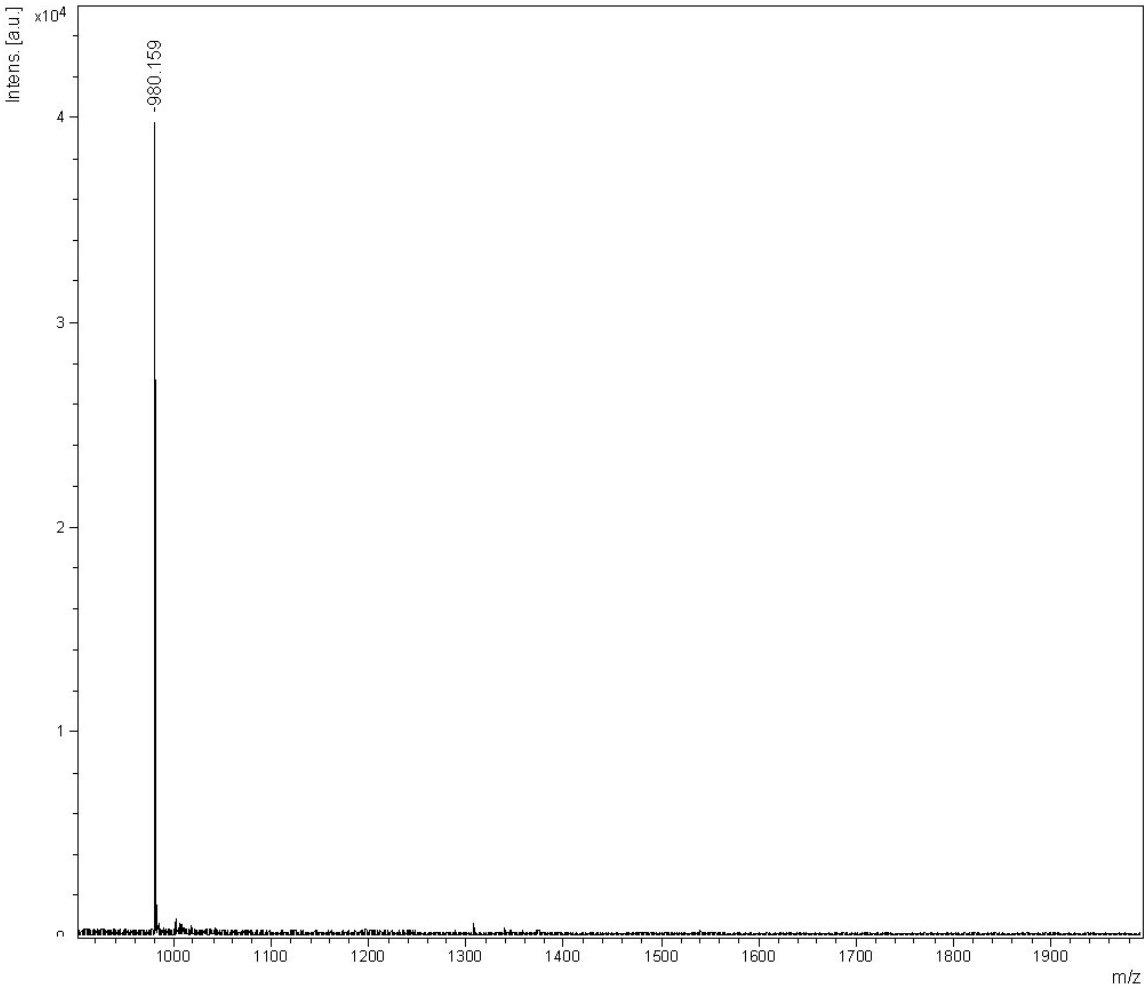

Figure S13(b3): Maldi-Tof mass-spectral analysis of the SMART™ RP-Hplc fraction at **R_T = 22.16** min and **R_T = 22.51** min in the **Fig S12(b2i).** Corresponding RP-Hplc fraction is **R_T = 21.18** min in the **Fig S12(b2)** [after **1h** of alkaline hydrolysis (pH 12.5 / 20ºC) of **5′-r(CAAGCAC)-3′**, **6b**]. The main peak at m/z **980.2** is for **5'-CAA$_{2'/3'-P}$** [see Table S9(B)].

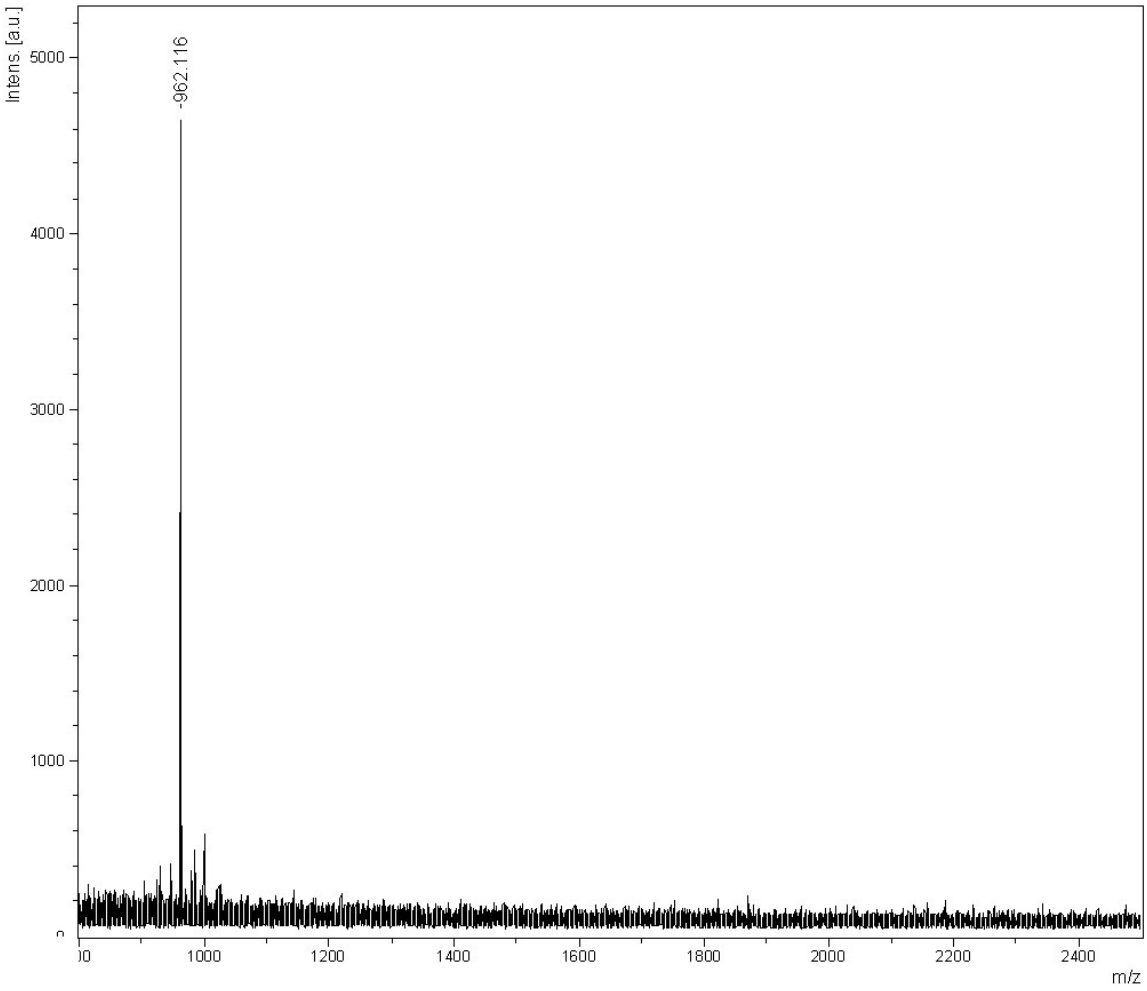

Figure S13(b4): Maldi-Tof mass-spectral analysis of the RP-Hplc fraction at **R_T = 21.77** min for alkaline hydrolysis (pH 12.5 / 20ºC) of **5′-r(CAAGCAC)-3′** (**6b**) after **1h** [for RP-Hplc profile, see Fig **S12 (b2)**] showing the main peak at m/z **962.1** for **5'-CAA$_{2', 3'\text{-cMP}}$** [see Table S9(B)].

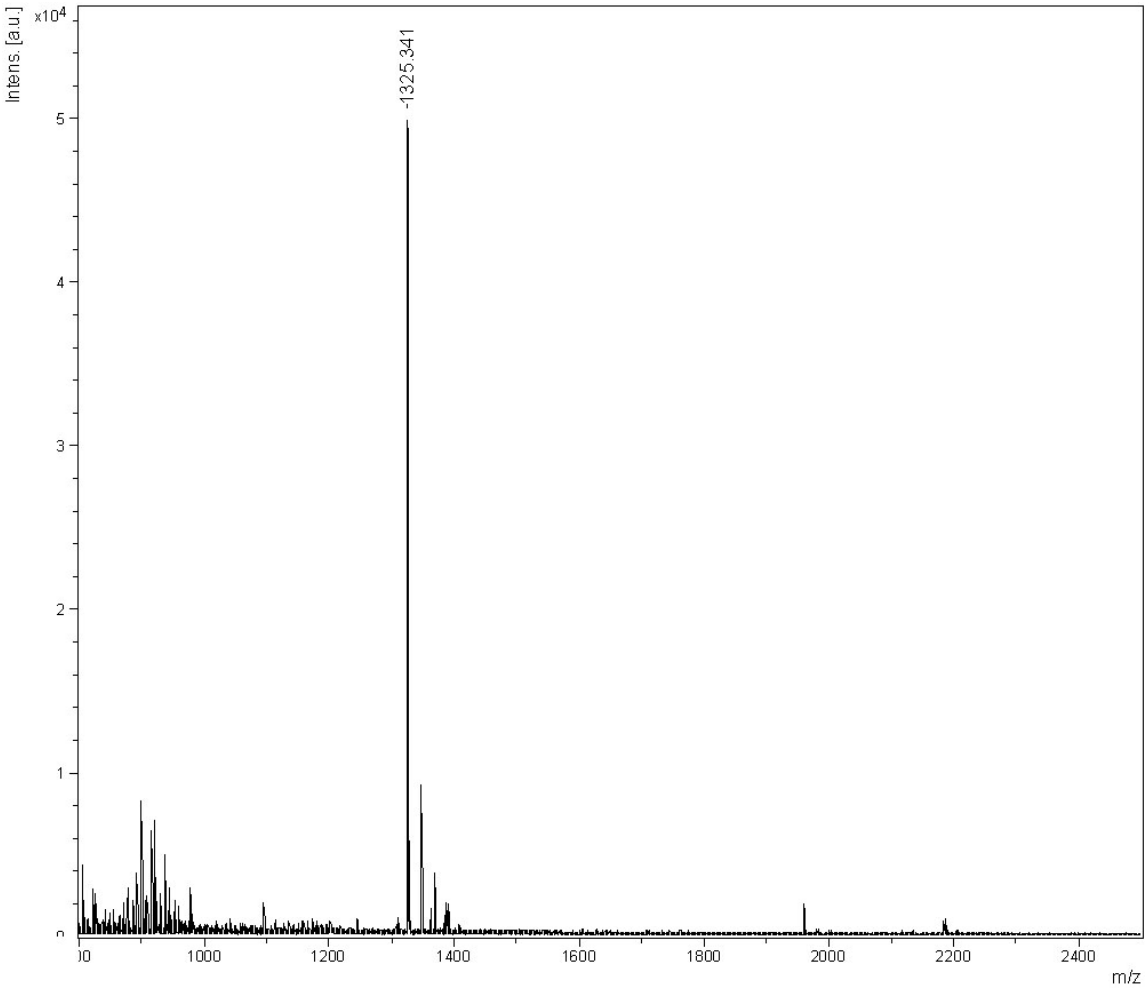

Figure S13(b5): Maldi-Tof mass-spectral analysis of the RP-Hplc fraction at **R_T = 22.76** min for alkaline hydrolysis (pH 12.5 / 20ºC) of **5′-rCAAGCAC-3′** (**6b**) after **1h** [for Hplc profile, see Fig **S12 (b2)**] showing the main peak at m/z **1325.3** for **5'-CAAG$_{2'/3'-P}$** [see Table S9(B)].

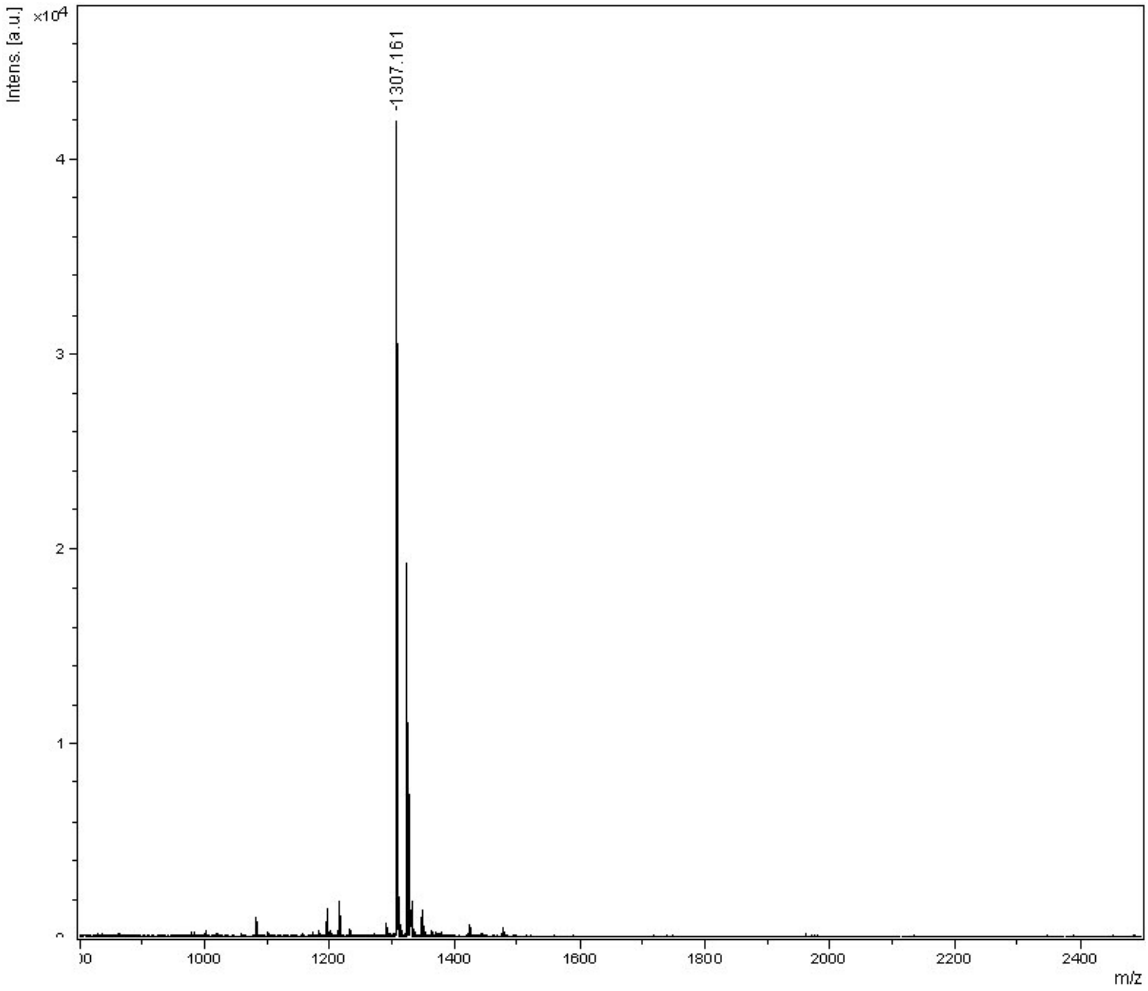

Figure S13(b6): Maldi-Tof mass-spectral analysis of the SMART™ RP-Hplc fraction at **R_T = 29.33** min in the **Fig S12(b2j).** Corresponding RP-Hplc fraction is **R_T = 24.23** min in the **Fig S12(b2)** [after **1h** of alkaline hydrolysis (pH 12.5 / 20ºC) of **5′-r(CAAGCAC)-3′**, **6b**]. The main peak at m/z **1307.2** is for **5'-CAAG$_{2', 3'\text{-cMP}}$** and **1325.2** is for **5'-CAAG$_{2'/3'\text{-P}}$** [see Table S9(B)].

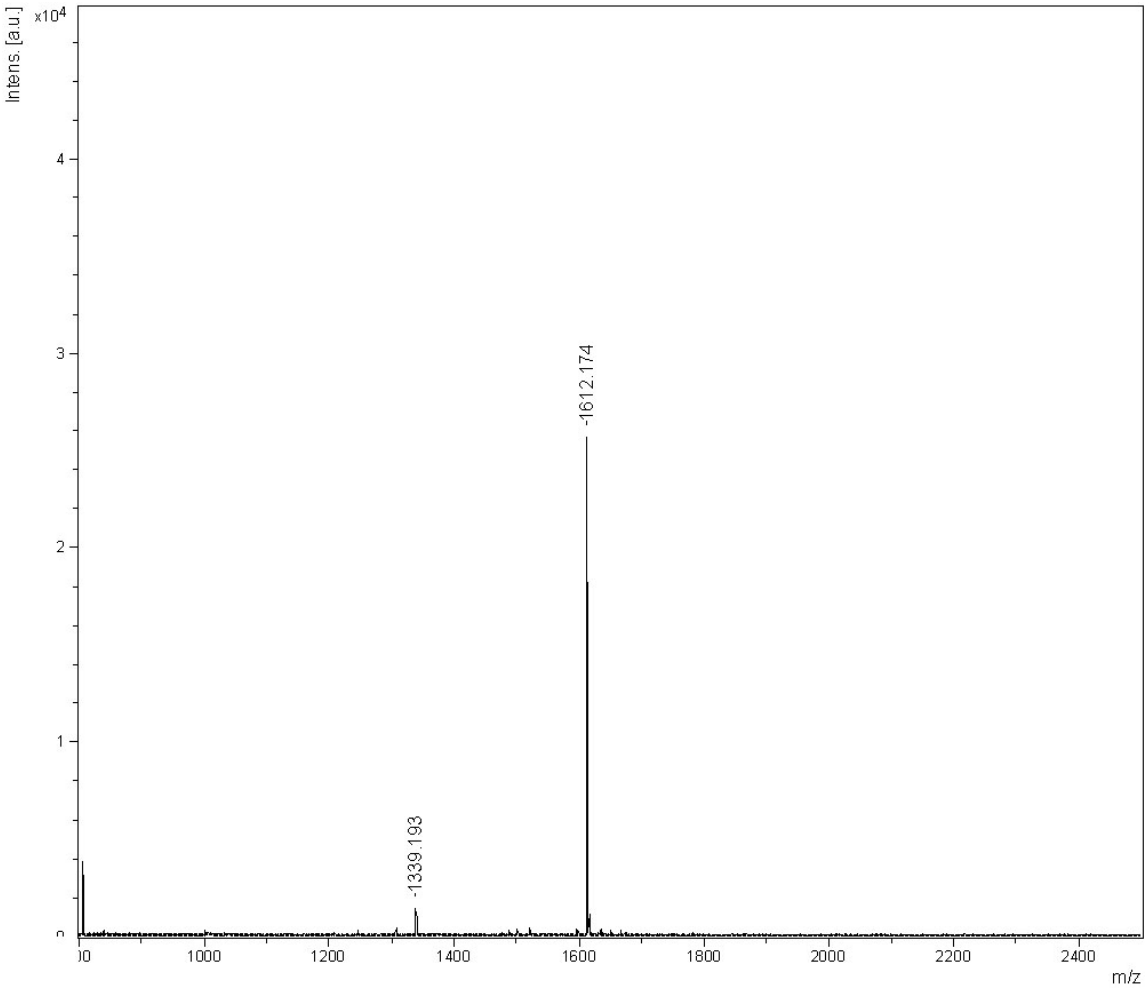

Figure S12(b7): Maldi-Tof mass-spectral analysis of the SMART™ RP-Hplc fraction at **R_T = 30.12** min in the **Fig S12(b2j).** Corresponding RP-Hplc fraction is **R_T = 24.23** min in the **Fig S12(b2)** [after **1h** of alkaline hydrolysis (pH 12.5 / 20ºC) of **5′-r(CAAGCAC)-3′**, **6b**]. The main peak at m/z **1612.2** is for **5'-CAAGC$_{2', 3'\text{-cMP}}$** [see Table S9(B)].

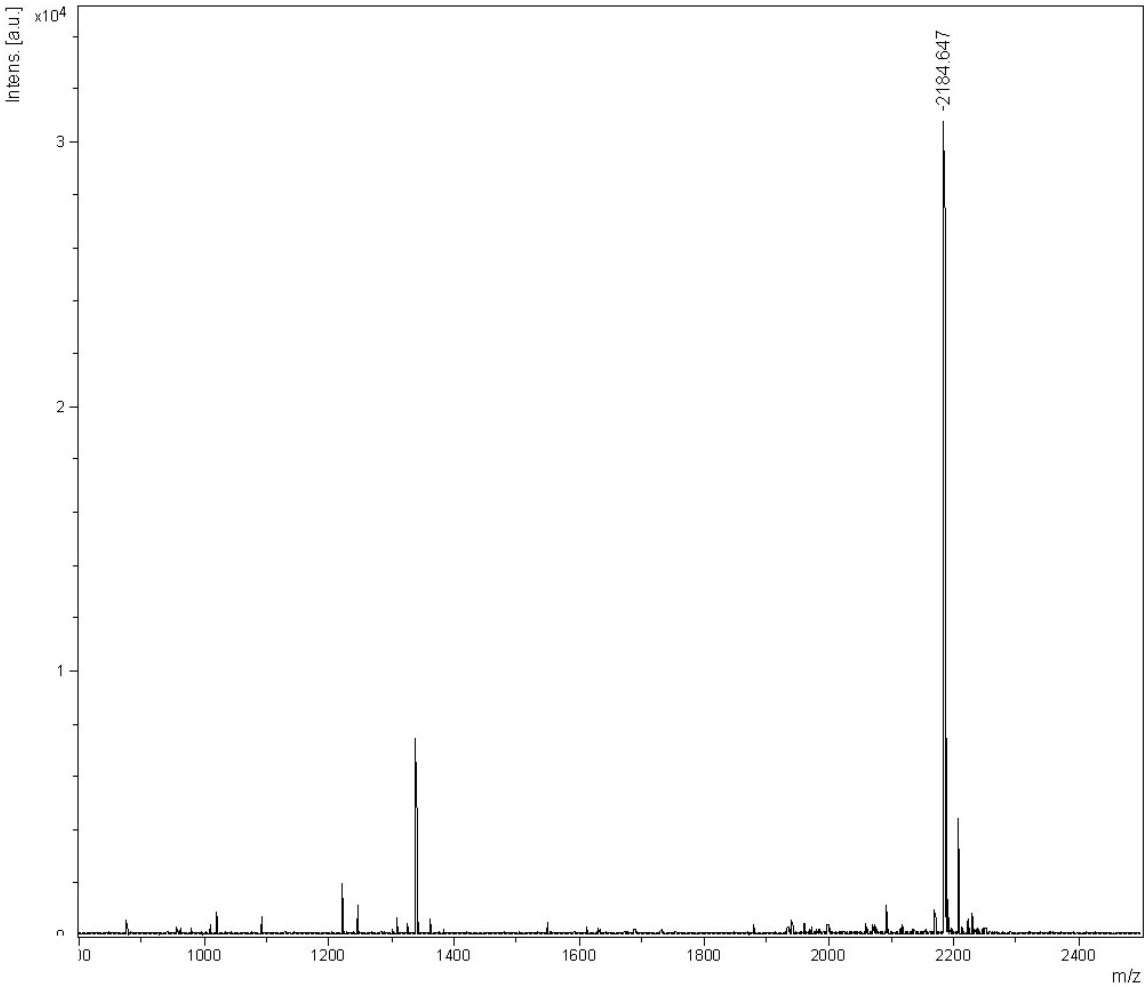

Figure S13(b8): Maldi-Tof mass-spectral analysis of the RP-Hplc fraction at **R_T = 25.27** min for alkaline hydrolysis (pH 12.5 / 20ºC) of **5′-r(CAAGCAC)-3′** (**6b**) after **1h** [for RP-Hplc profile, see Fig S12 (b2)] showing the main peak at m/z **2184.7** for the parent heptamer [see Table S9(B)].

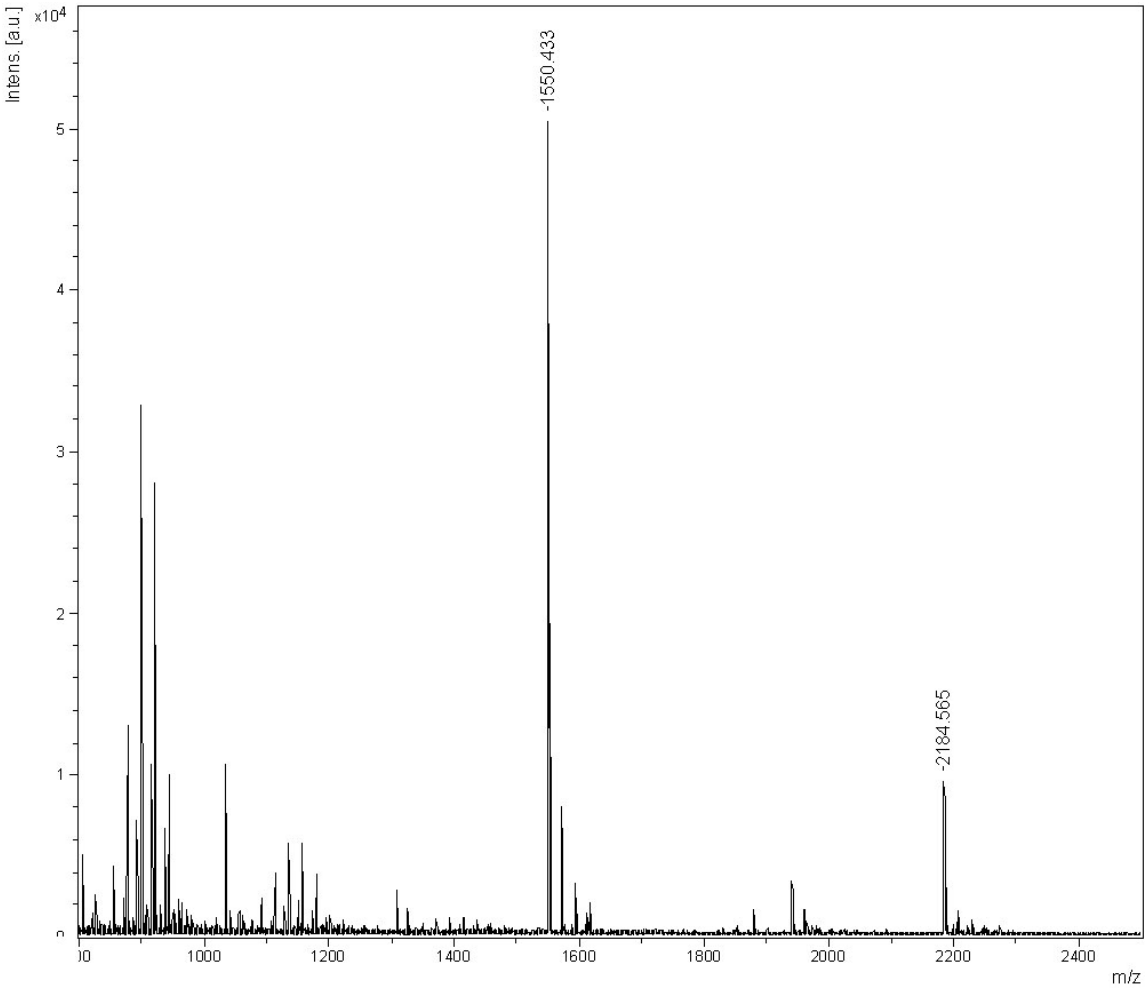

Figure S13(b9): Maldi-Tof mass-spectral analysis of the RP-Hplc fraction at **R_T = ~25.5** min for alkaline hydrolysis (pH 12.5 / 20ºC) of **5′-rCAAGCAC-3′** (**6b**) after **1h** [for Hplc profile, see Fig S12 (b2)] showing the main peak at m/z **1550.4** for **5'-AGCAC-3'**and **2184.6** for the parent heptamer[see Table S9(B)].

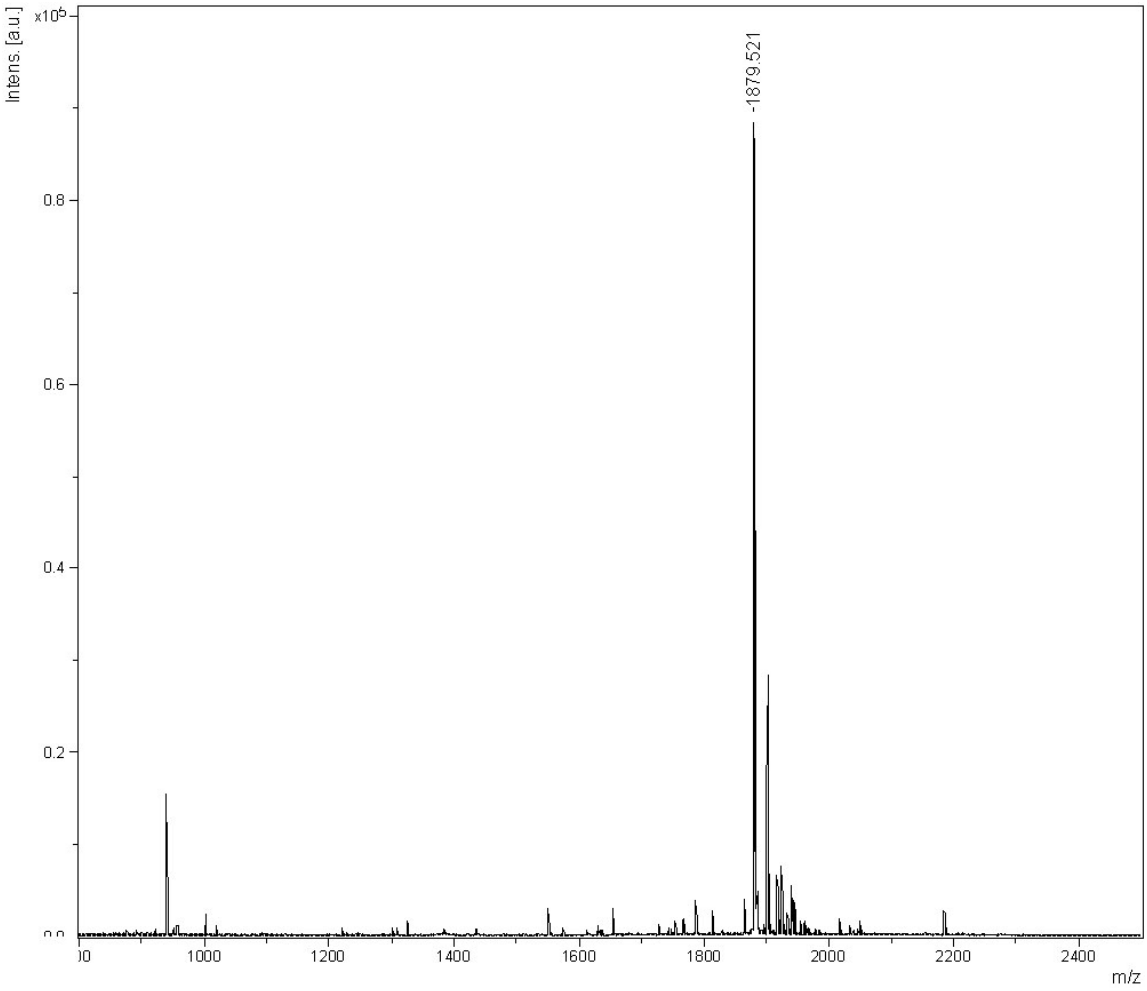

Figure S13(b10): Maldi-Tof mass-spectral analysis of the RP-Hplc fraction at **R_T = 27.11** min for alkaline hydrolysis (pH 12.5 / 20ºC) of **5′-rCAAGCAC-3′** (**6b**) after **1h** [for RP-Hplc profile, see Fig S12 (b2)] showing the main peak at m/z **1879.5** for **5'-AAGCAC-3'** [see Table S9(B)].

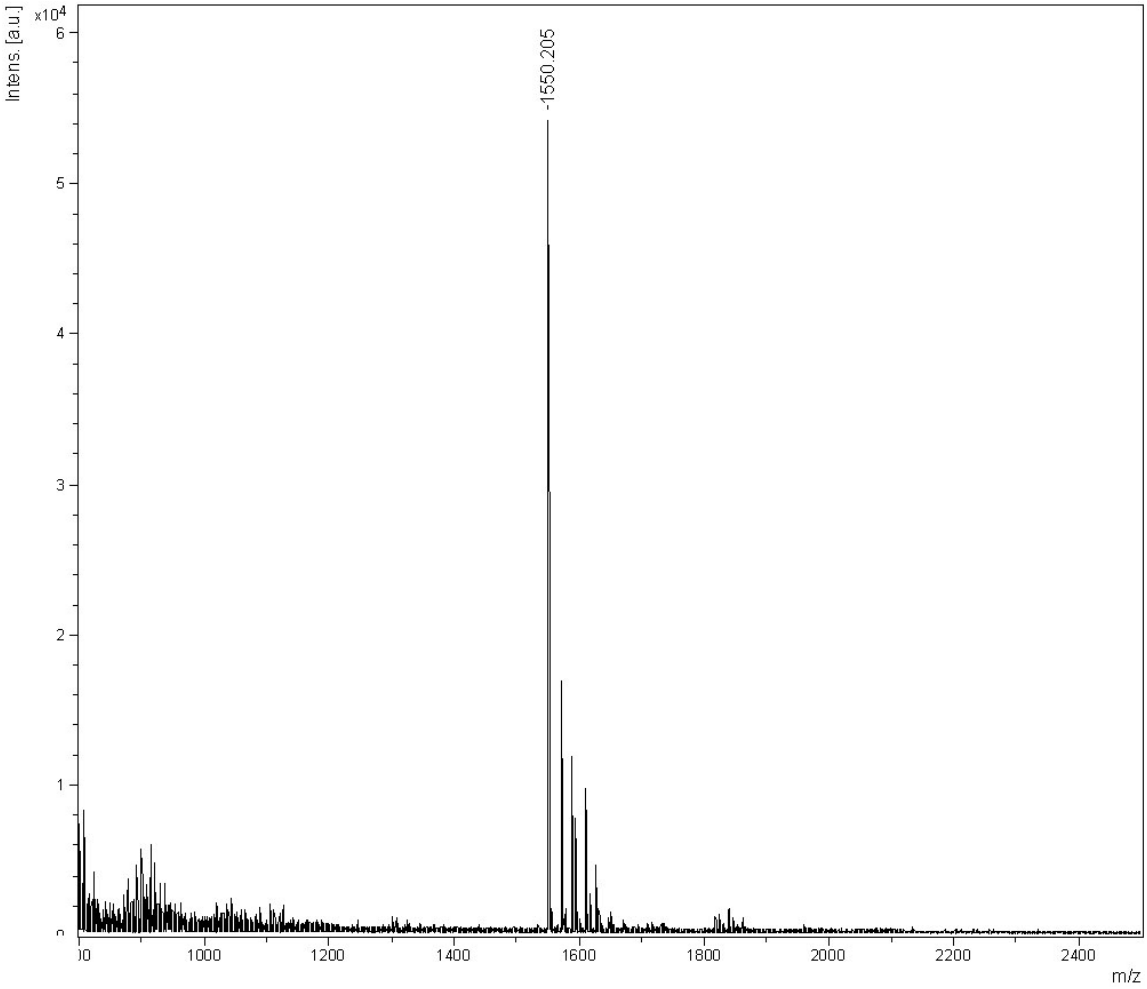

Figure S13(c1): Maldi-Tof mass-spectral analysis of the RP-Hplc fraction at **R_T = 23.18** min for alkaline hydrolysis (pH 12.5 / 20ºC) of **5′-r(CACGAAC)-3′** (**7b**) after **1h** [for RP-Hplc profile, see Fig **S12 (c2)**] showing the main peak at m/z **1550.2** for **5'-CGAAC-3'**and [see Table S9(C)].

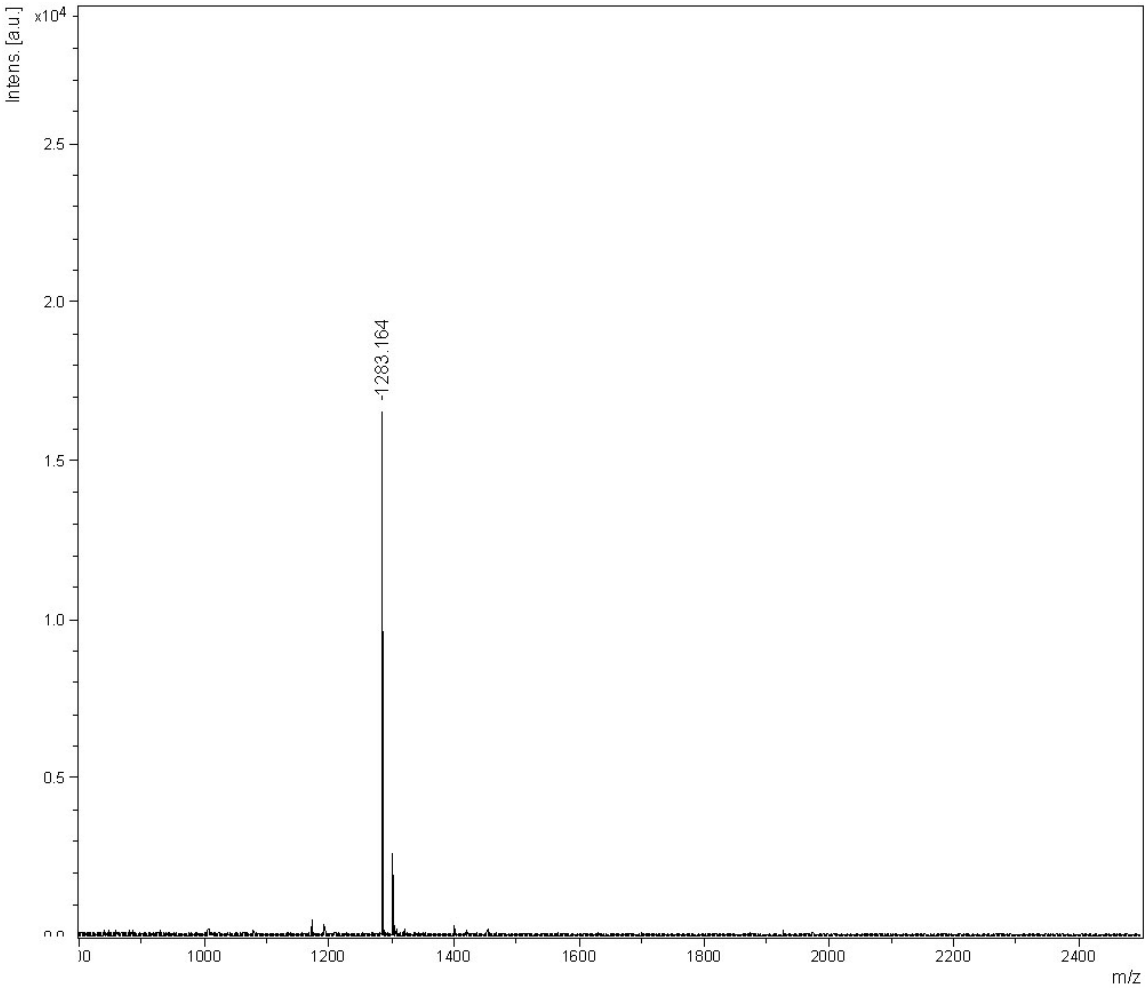

Figure S13(c2): Maldi-Tof mass-spectral analysis of the SMART™ RP-Hplc fraction at **R_T = 30.27** min in the **Fig S13(c2i).** Corresponding RP-Hplc fraction is **R_T = 24.97** min in the **Fig S12(c2)** [after **1h** of alkaline hydrolysis (pH 12.5 / 20ºC) of **5′-r(CACGAAC)-3′**, **7b**]. The main peak at m/z **1283.2** is for **5'-CACG$_{2', 3'\text{-cMP}}$** [see Table S9(C)].

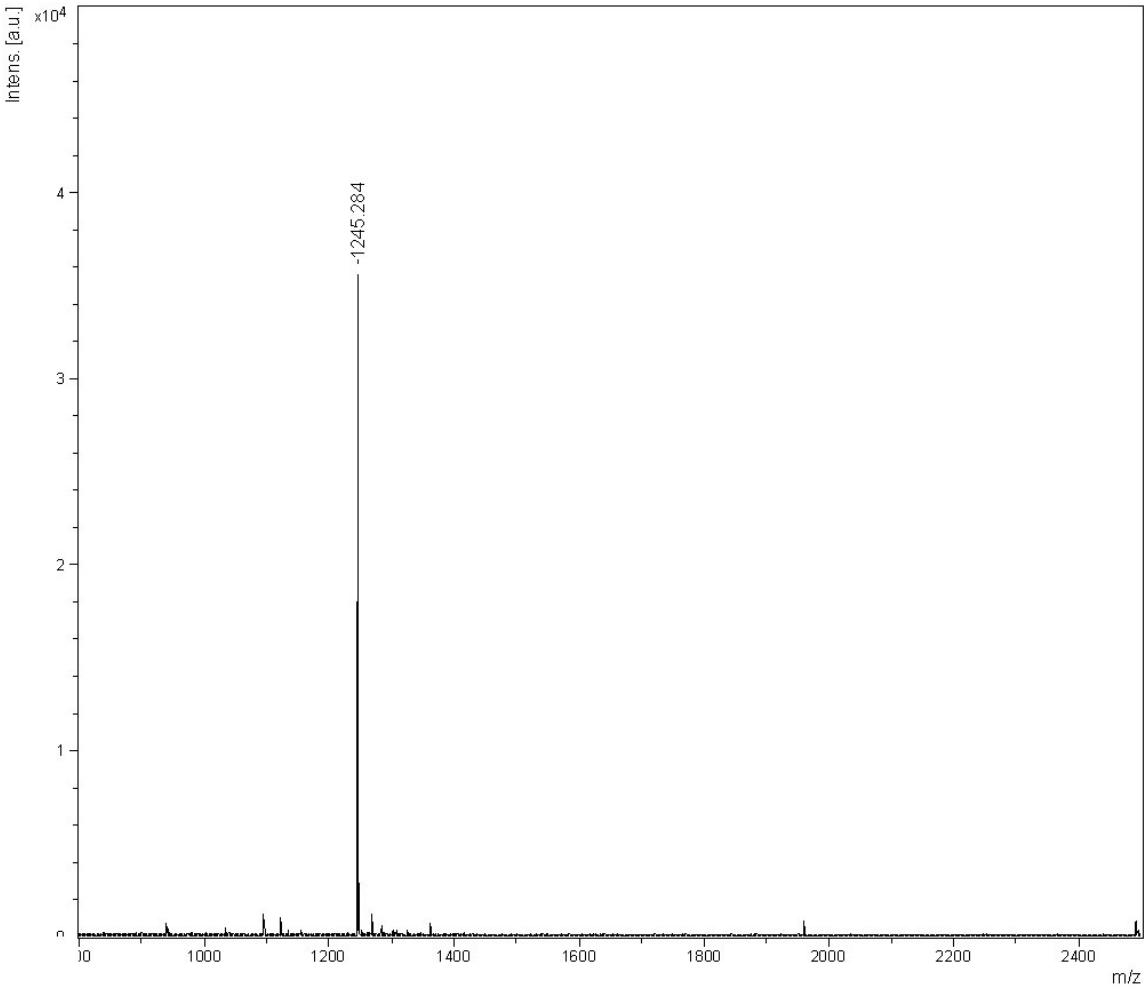

Figure S13(c3): Maldi-Tof mass-spectral analysis of the SMART™ RP-Hplc fraction at **R_T = 31.48** min in the **Fig S12(c2i).** Corresponding RP-Hplc fraction is **R_T = 24.97** min in the **Fig S12(c2)** [after **1h** of alkaline hydrolysis (pH 12.5 / 20ºC) of **5′-r(CACGAAC)-3′**, **7b**]. The main peak at m/z **1245.3** is for **5'-GAAC-3'** [see Table S9(C)].

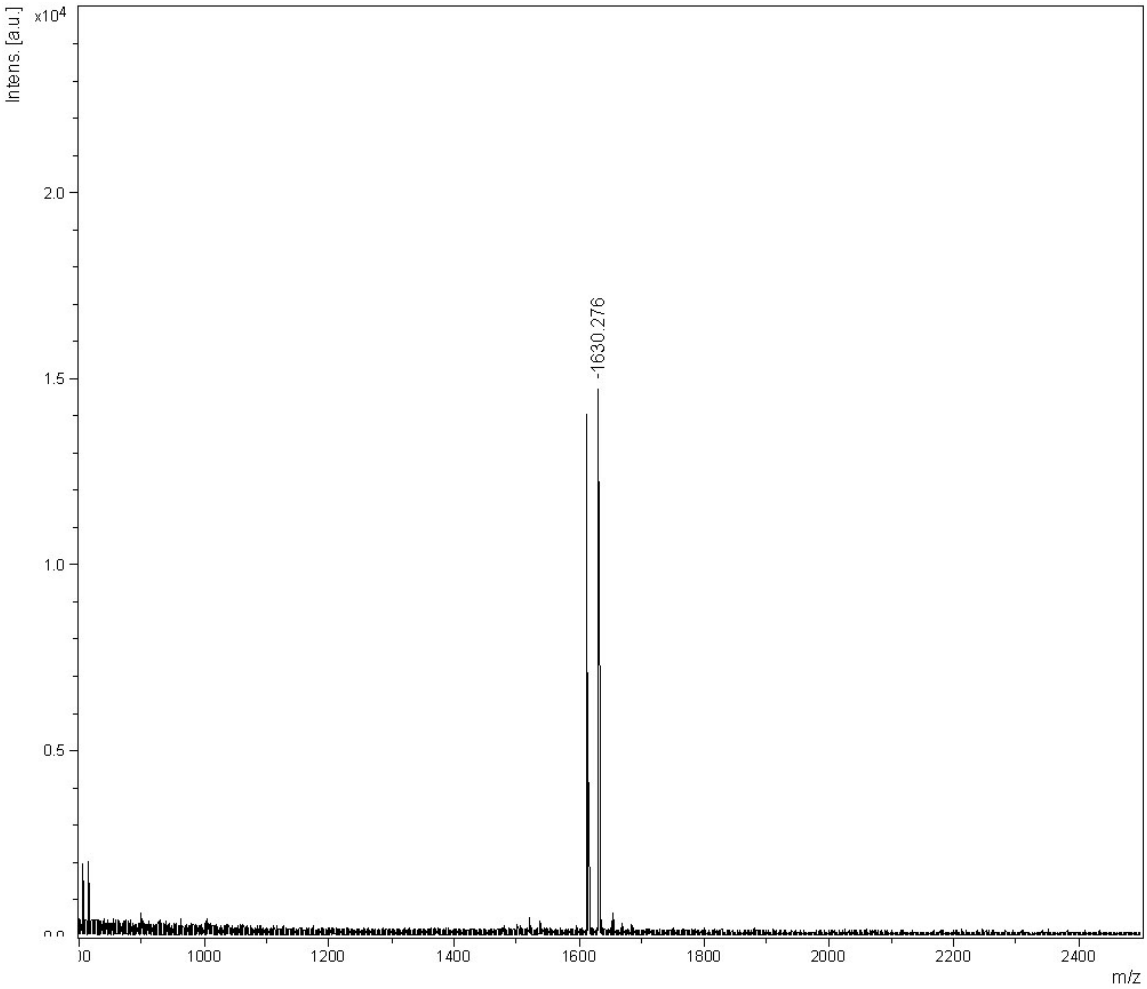

Figure S13(c4): Maldi-Tof mass-spectral analysis of the SMART™ RP-Hplc fraction at **R_T = 30.63** min in the **Fig S12(c2j).** Corresponding RP-Hplc fraction is **R_T = 26.50** min in the **Fig S12(c2)** [after **1h** of alkaline hydrolysis (pH 12.5 / 20ºC) of **5′-r(CACGAAC)-3′**, **7b**]. The main peak at m/z **1612.3** is for **5'-CACGA$_{2', 3'\text{-cMP}}$** and **1630.3** is for **5'-CACGA$_{2'/3'\text{-P}}$** [see Table S9(C)].

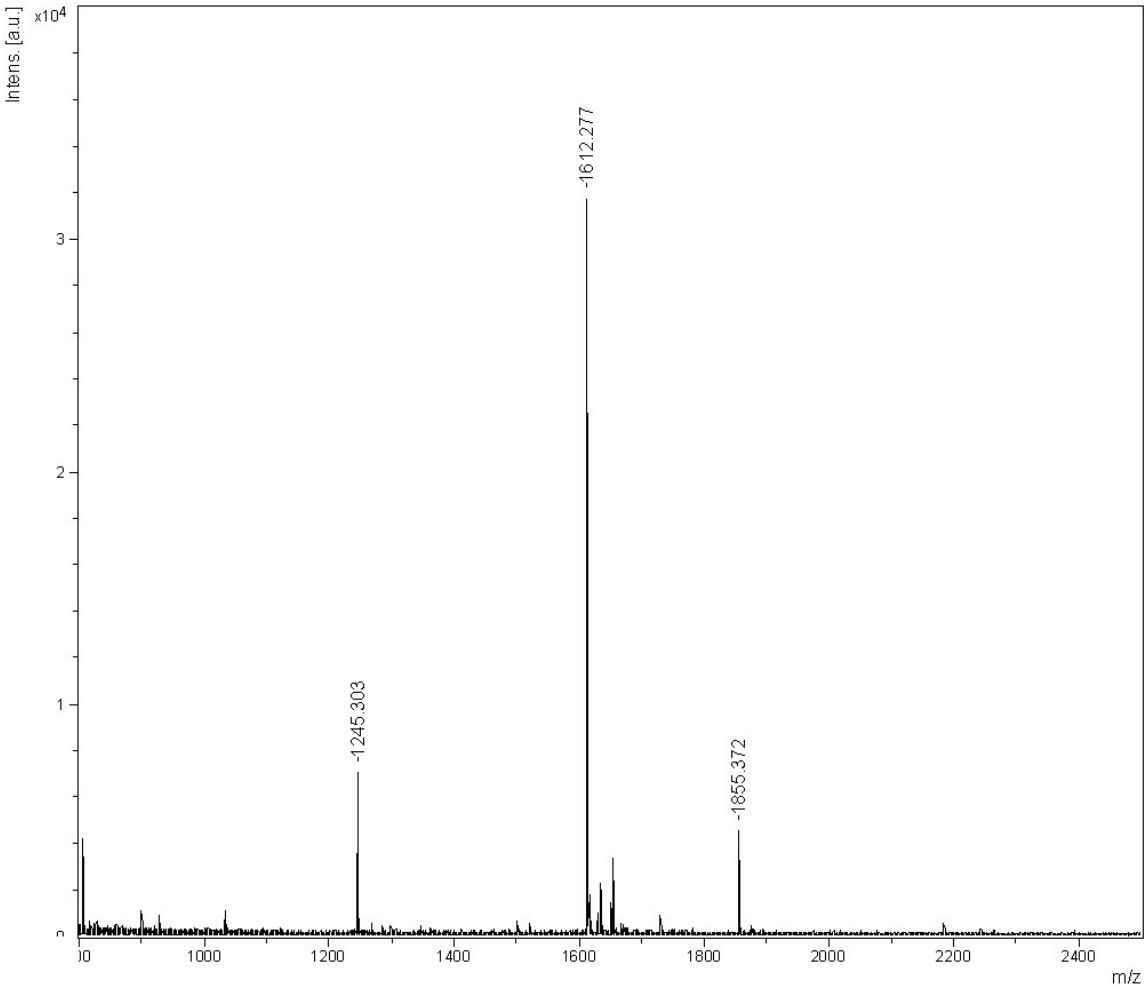

Figure S13(c5): Maldi-Tof mass-spectral analysis of the SMART™ RP-Hplc fraction at **R_T = 30.97** min in the **Fig S12(c2j).** Corresponding RP-Hplc fraction is **R_T = 26.50** min in the **Fig S12(c2)** [after **1h** of alkaline hydrolysis (pH 12.5 / 20ºC) of **5′-r(CACGAAC)-3′**, **7b**]. The main peak at m/z **1612.3** is for **5'-CACGA$_{2', 3'\text{-cMP}}$** [see Table S9(C)].

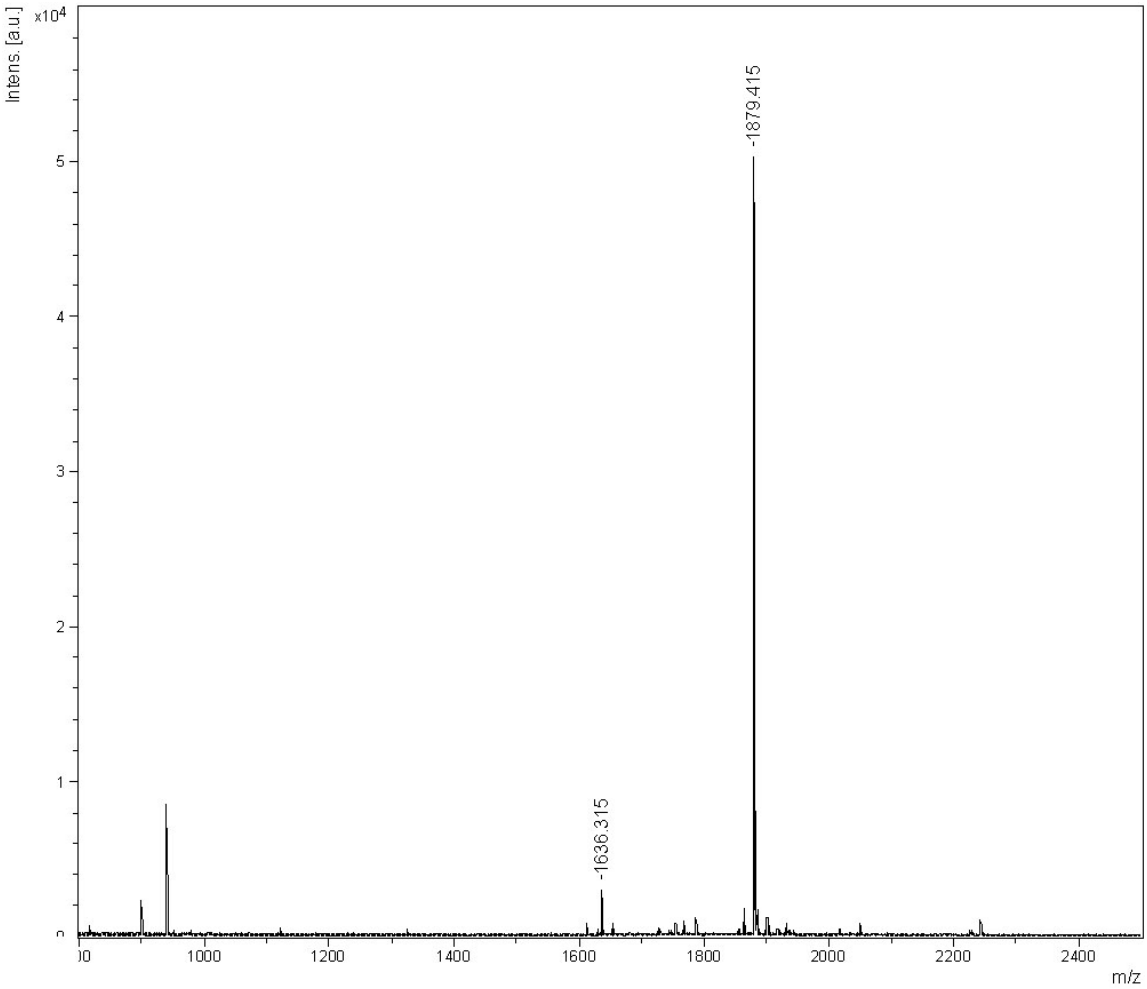

Figure S13(c6): Maldi-Tof mass-spectral analysis of the SMART™ RP-Hplc fraction at **R_T = 31.49** min in the **Fig S12(c6).** Corresponding RP-Hplc fraction is **R_T = 26.50** min in the **Fig S12(c2)** [after **1h** of alkaline hydrolysis (pH 12.5 / 20ºC) of **5′-r(CACGAAC)-3′**, **7b**] the main peak at m/z **1879.4** is for **5'-ACGAAC-3'** [see Table S9(C)].

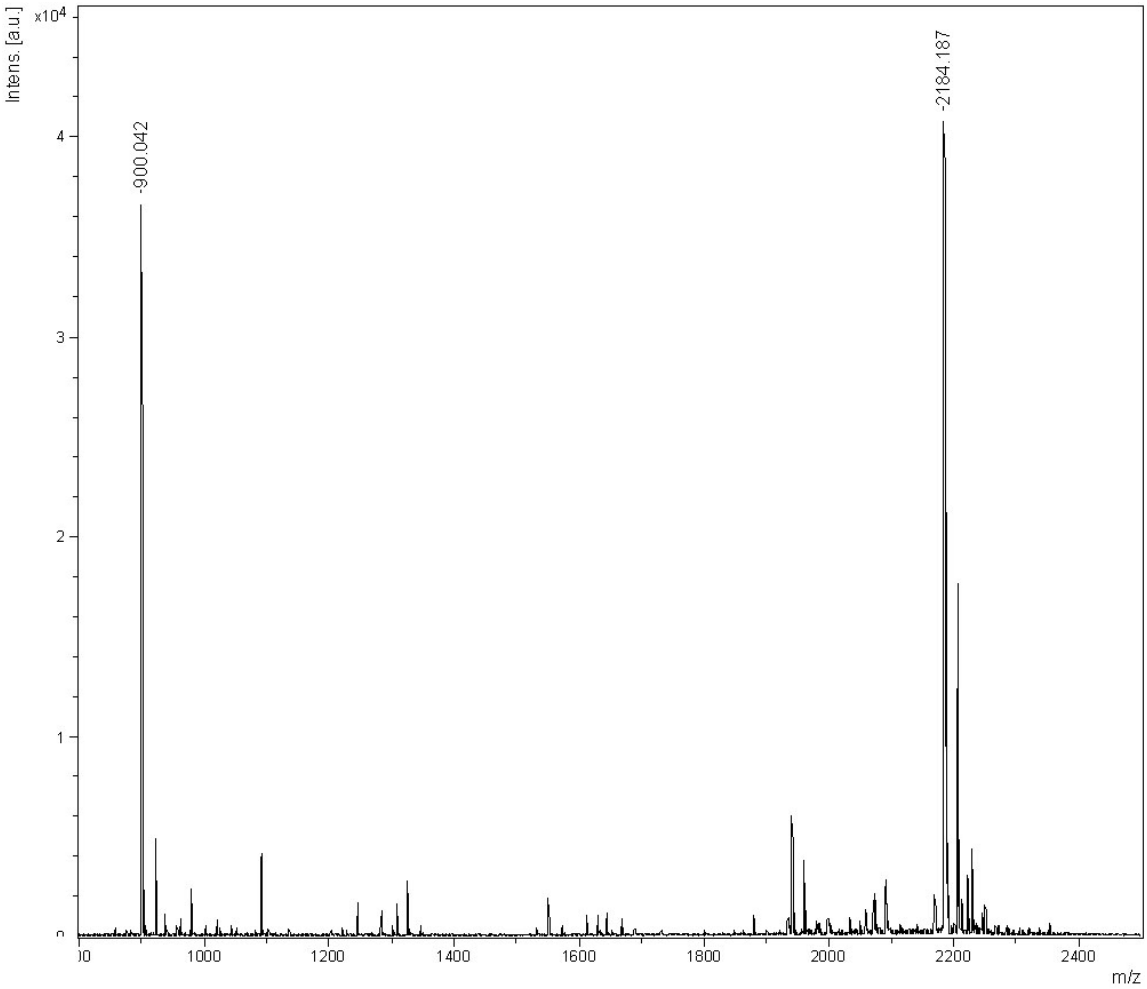

Figure S13(c7): Maldi-Tof mass-spectral analysis of the RP-Hplc fraction at **R_T = 27.36** min for alkaline hydrolysis (pH 12.5 / 20ºC) of **5′-r(CACGAAC)-3′** (**7b**) after **1h** [for Hplc profile, see Fig **S12 (c2)**] showing the main peak at m/z **900.0** for **5'-AAC-3'** (a fragmentation peak of the heptameric peak in the process of recording mass as confirmed by the variation of the laser power in the Maldi Tof) and **2184.2** for the parent heptamer [see Table S9(C)].

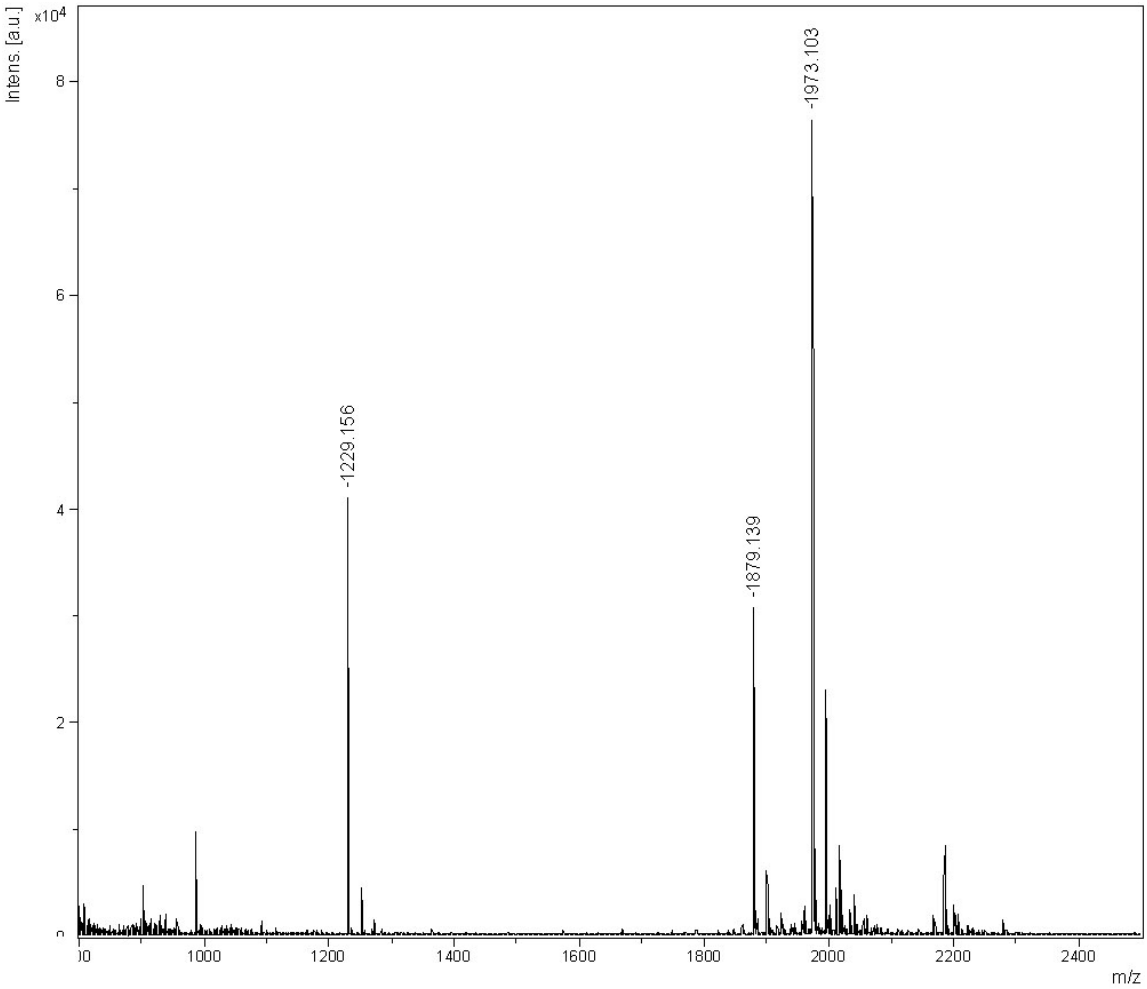

Figure S13(c8): Maldi-Tof mass-spectral analysis of the RP-Hplc fraction at **R_T = 28.06** min for alkaline hydrolysis (pH 12.5 / 20ºC) of **5′-r(CACGAAC)-3′** (**7b**) after **1h** [for Hplc profile, see Fig **S12 (c2)**] showing the main peak at m/z **1229.2** [non nucleos(t)idic fragment], **1879.1** for **5'-ACGAAC-3'** and **1973.1** [non nucleos(t)idic fragment] [see Table S9(C)].

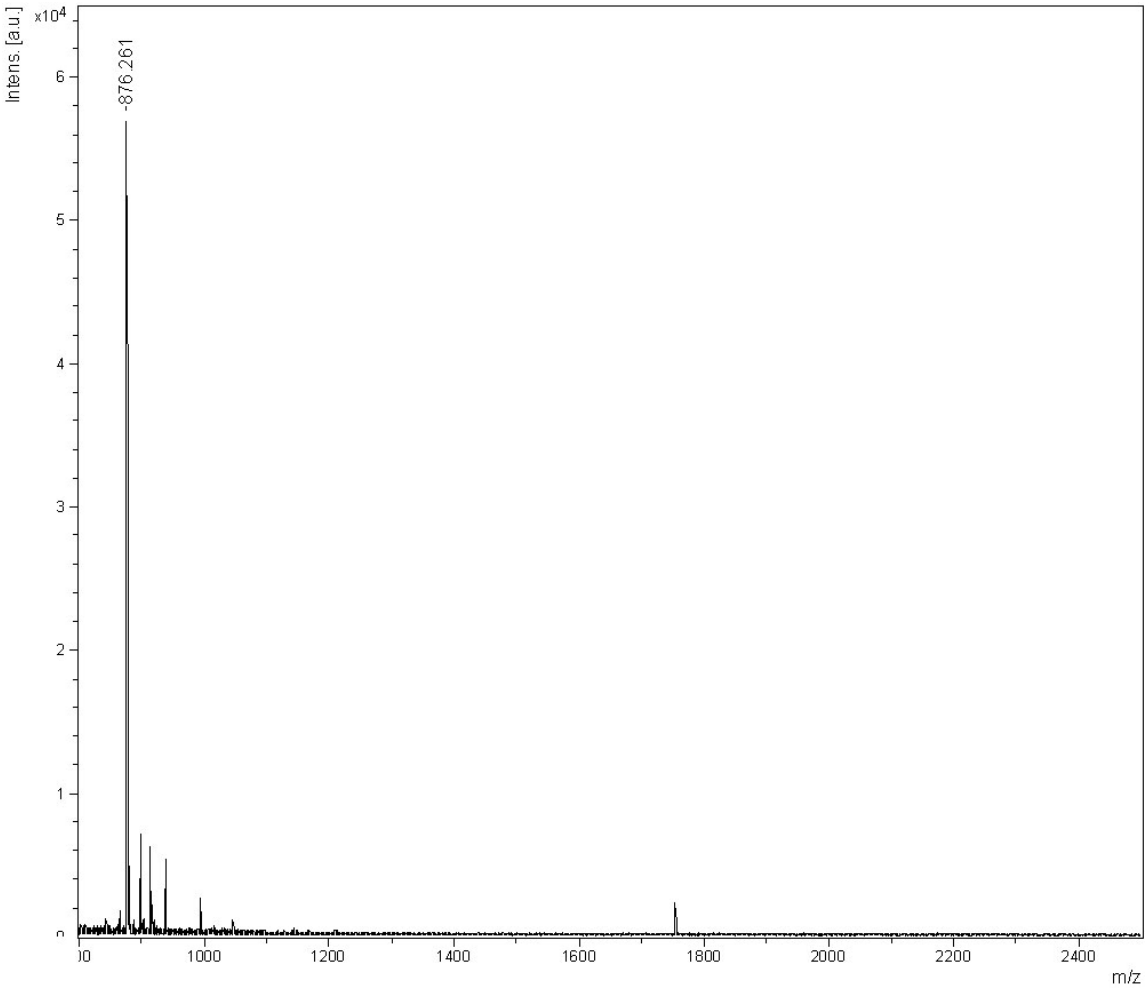

Figure S13(d1): Maldi-Tof mass-spectral analysis of the SMART™ RP-Hplc fraction at **R_T = 18.10** min in the **Fig S12(d2i).** Corresponding RP-Hplc fraction is **R_T = 19.99** min in the **Fig S12(d2)** [after **1h** of alkaline hydrolysis (pH 12.5 / 20ºC) of **5′-r(CACGCAC)-3′**, **8b**]. The main peak at m/z **876.3** is for **5'-CAC-3'** [see Table S9(D)]**.**

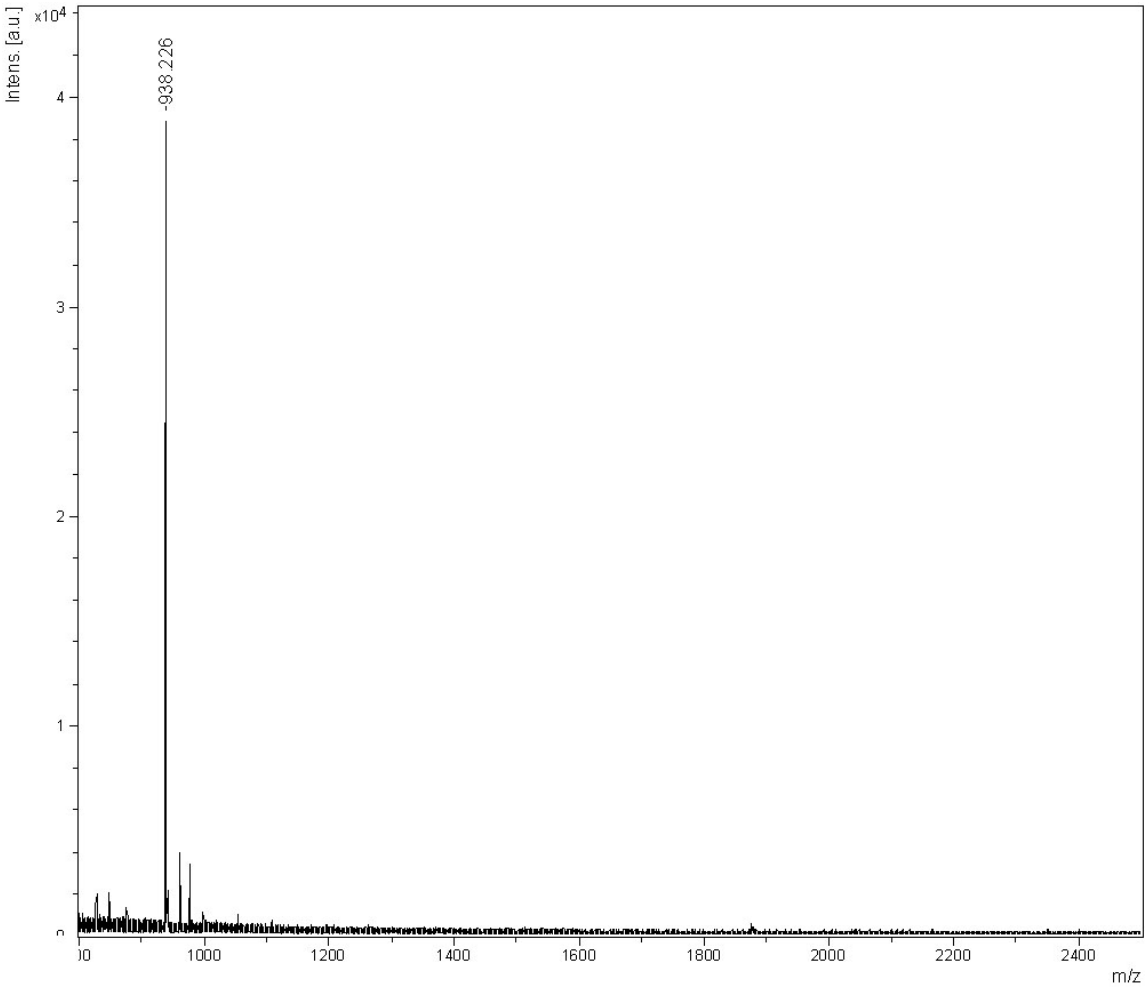

Figure S13(d2): Maldi-Tof mass-spectral analysis of the SMART™ RP-Hplc fraction at **R_T = 18.55** min in the **Fig S12(d2i).** Corresponding RP-Hplc fraction is **R_T = 19.99** min in the **Fig S12(d2)** [after **1h** of alkaline hydrolysis (pH 12.5 / 20ºC) of **5′-r(CACGCAC)-3′**, **8b**]. The main peak at m/z **938.2** is for **5'-CAC$_{2', 3'\text{-cMP}}$** [see Table S9(D)]**.**

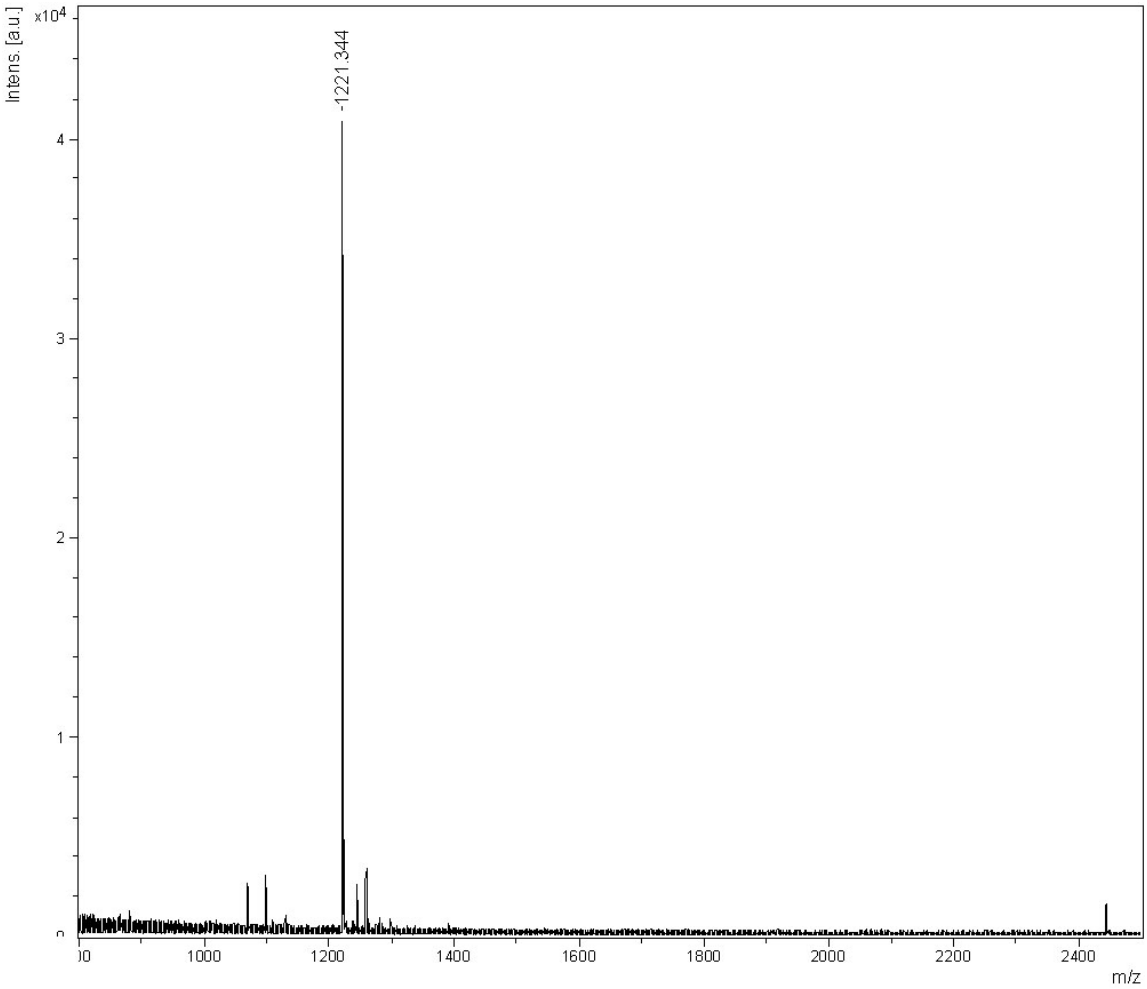

Figure S13(d3): Maldi-Tof mass-spectral analysis of the SMART™ RP-Hplc fraction at **R_T = 20.58** min in the **Fig S12(d2j).** Corresponding RP-Hplc fraction is **R_T = 21.23** min in the **Fig S12(d2)** [after **1h** of alkaline hydrolysis (pH 12.5 / 20ºC) of **5′-r(CACGCAC)-3′**, **8b**]. The main peak at m/z **1221.3** is for **5'-GCAC-3'** [see Table S9(D)]**.**

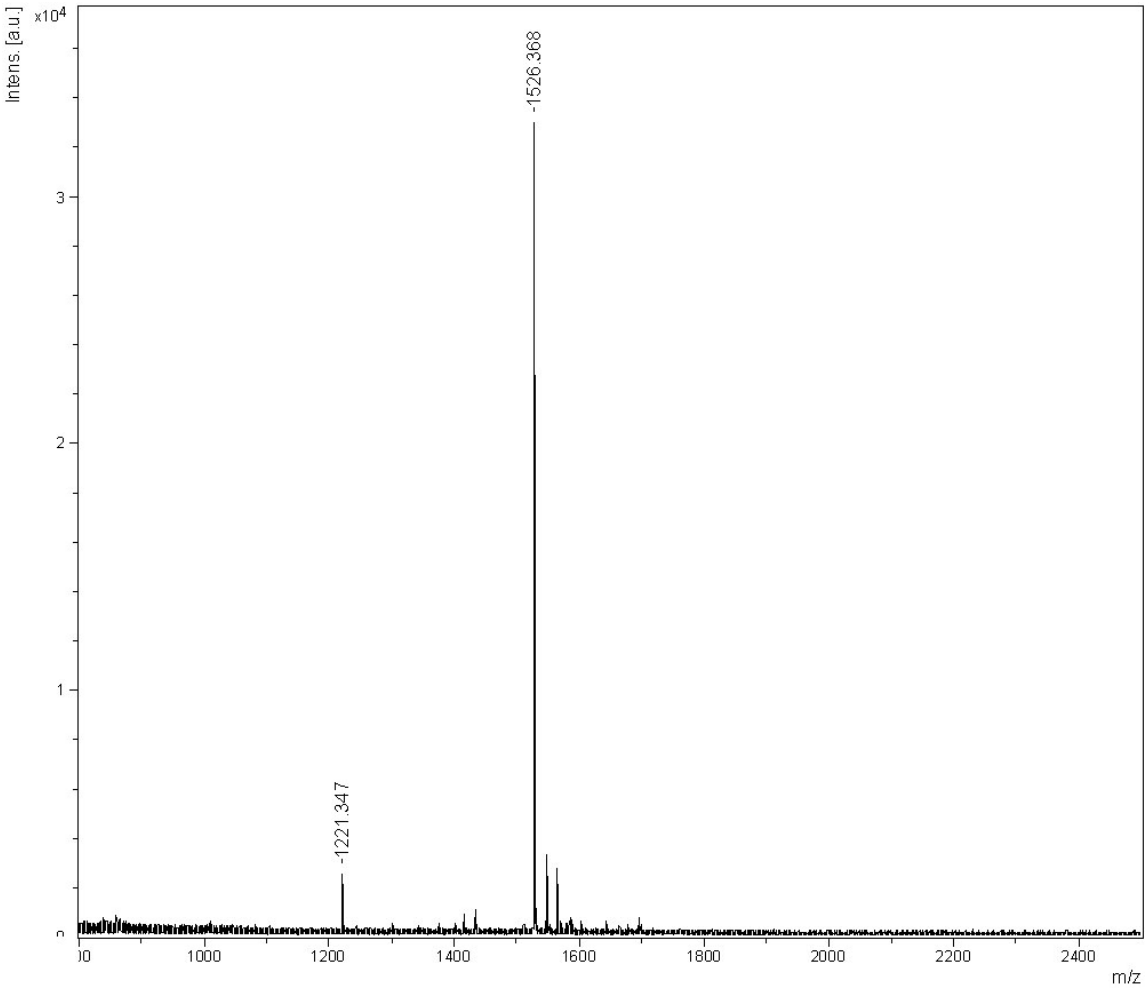

Figure S13(d4): Maldi-Tof mass-spectral analysis of the SMART™ RP-Hplc fraction at **R_T = 21.15** min in the **Fig S12(d2j).** Corresponding RP-Hplc fraction is **R_T = 21.23** min in the **Fig S12(d2)** [after **1h** of alkaline hydrolysis (pH 12.5 / 20ºC) of **5′-r(CACGCAC)-3′**, **8b**]. The main peak at m/z **1526.4** is for **5'-CGCAC-3'** [see Table S9(D)]**.**

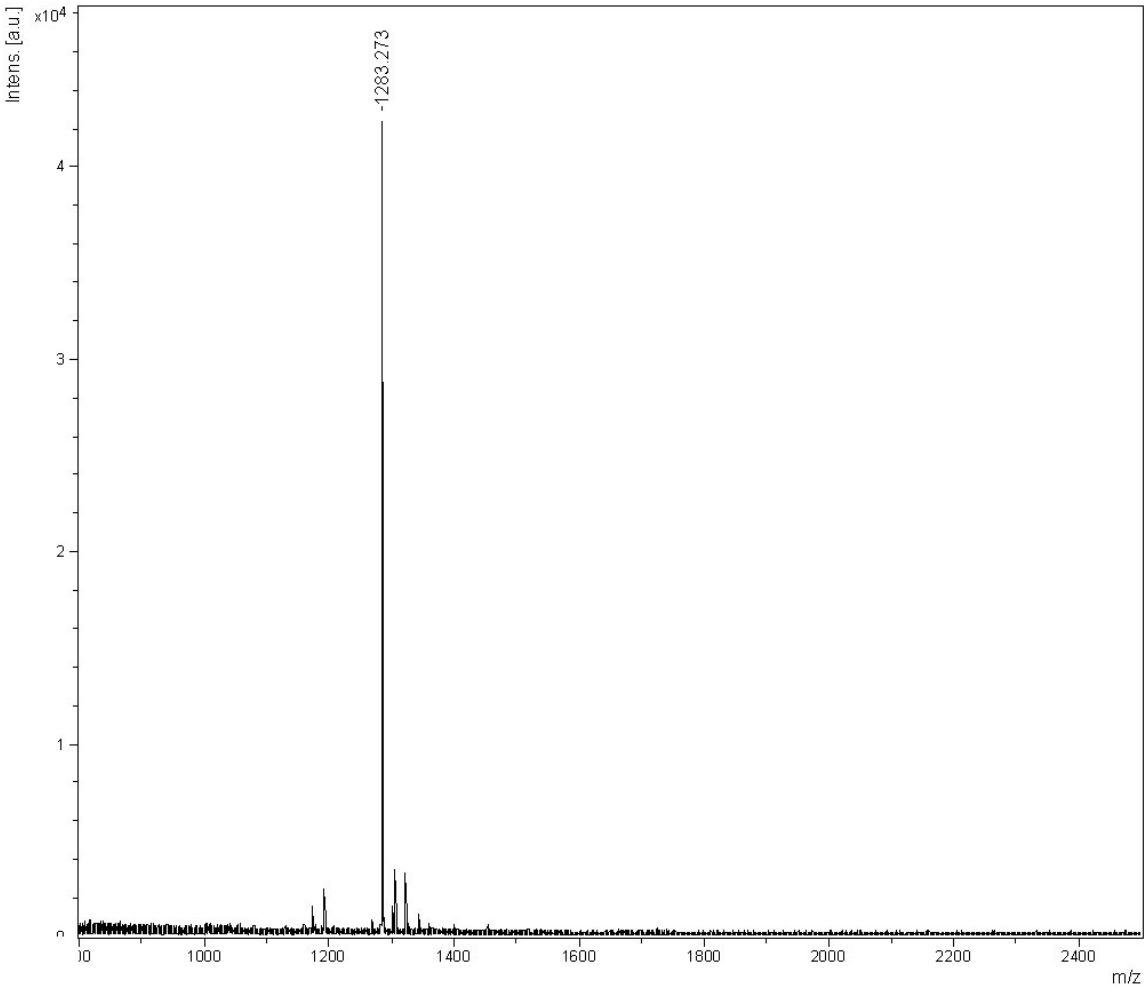

Figure S13(d5): Maldi-Tof mass-spectral analysis of the SMART™ RP-Hplc fraction at **R_T = 21.79** min in the **Fig S12(d2k).** Corresponding RP-Hplc fraction is **R_T = 24.14** min in the **Fig S12(d2)** [after **1h** of alkaline hydrolysis (pH 12.5 / 20ºC) of **5′-r(CACGCAC)-3′**, **8b**]. The main peak at m/z **1283.3** is for **5'-CACG$_{2', 3'\text{-cMP}}$** [see Table S9(D)]**.**

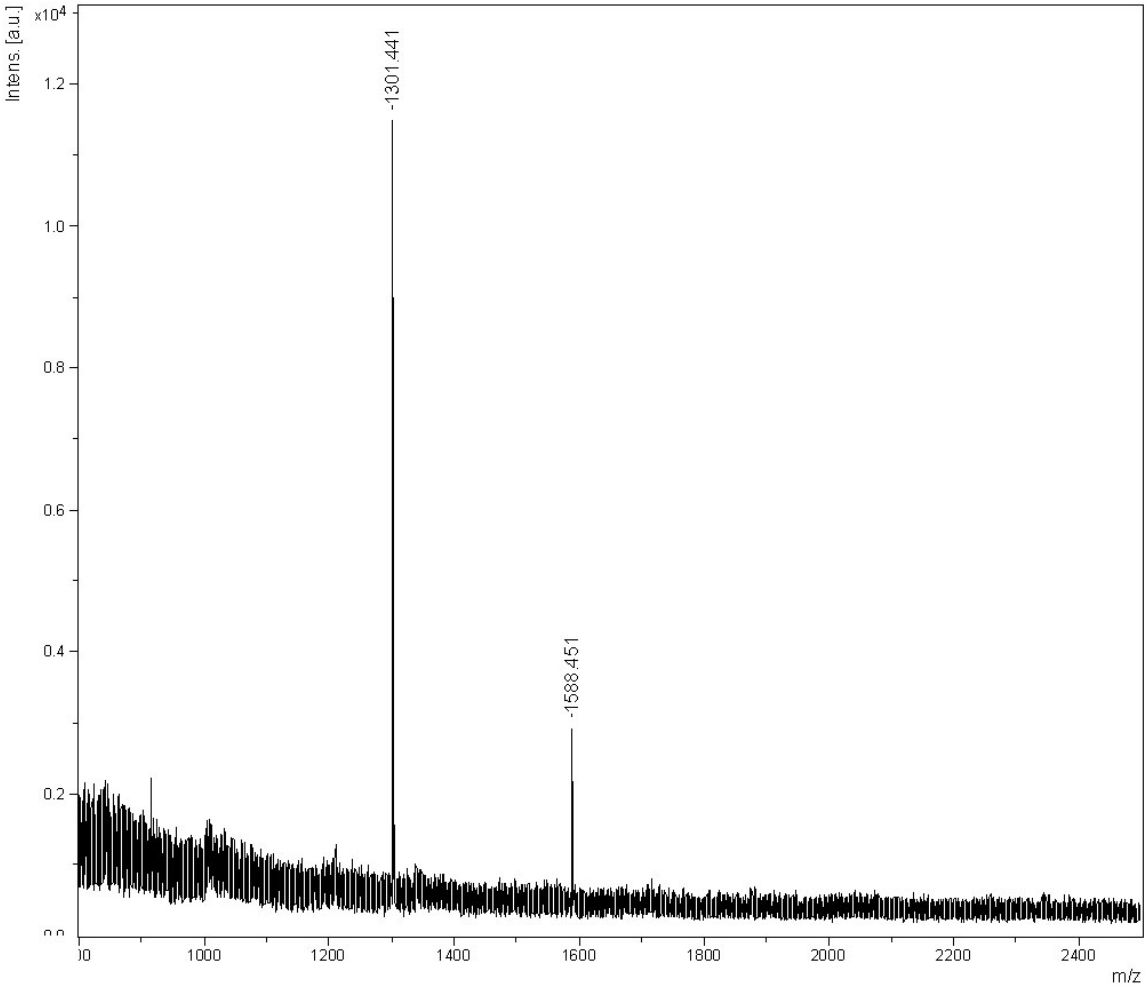

Figure S13(d6): Maldi-Tof mass-spectral analysis of the SMART™ RP-Hplc fraction at **R_T = 22.72** min in the **Fig S12(d2k).** Corresponding RP-Hplc fraction is **R_T = 24.14** min in the **Fig S12(d2)** [after **1h** of alkaline hydrolysis (pH 12.5 / 20ºC) of **5′-r(CACGCAC)-3′**, **8b**]. The main peak at m/z **1301.4** for **5'-CACG$_{2'/3'-P}$** and **1588.4** for **5'-CACGC$_{2', 3'-cMP}$** [see Table S9(D)]

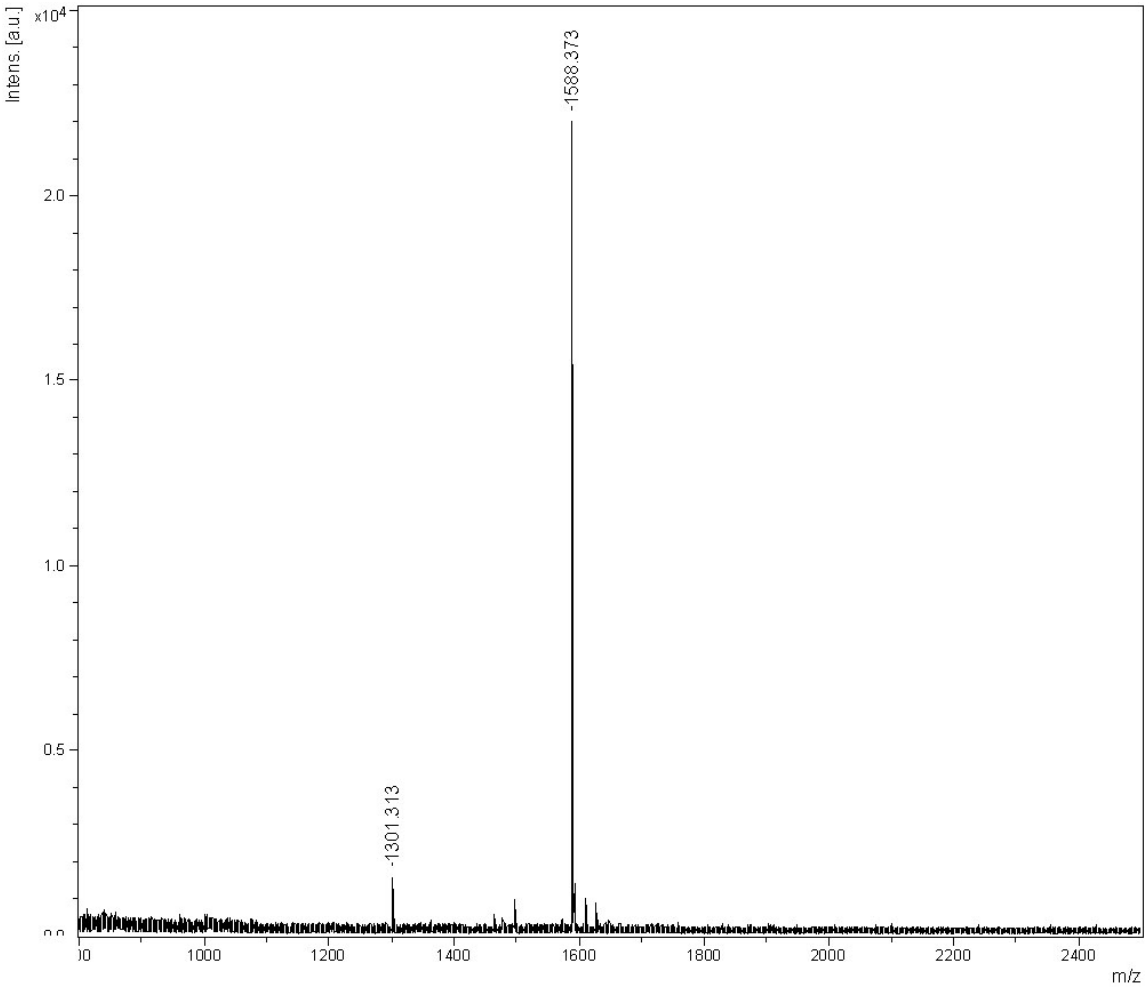

Figure S13(d7): Maldi-Tof mass-spectral analysis of the SMART™ RP-Hplc fraction at **R_T = 23.04** min in the **Fig S12(d2k).** Corresponding RP-Hplc fraction is **R_T = 24.14** min in the **Fig S12(d2)** [after **1h** of alkaline hydrolysis (pH 12.5 / 20ºC) of **5′-r(CACGCAC)-3′**, **8b**]. The main peak at m/z **1588.4** for **5'-CACGC$_{2', 3'\text{-cMP}}$** [see Table S9(D)]

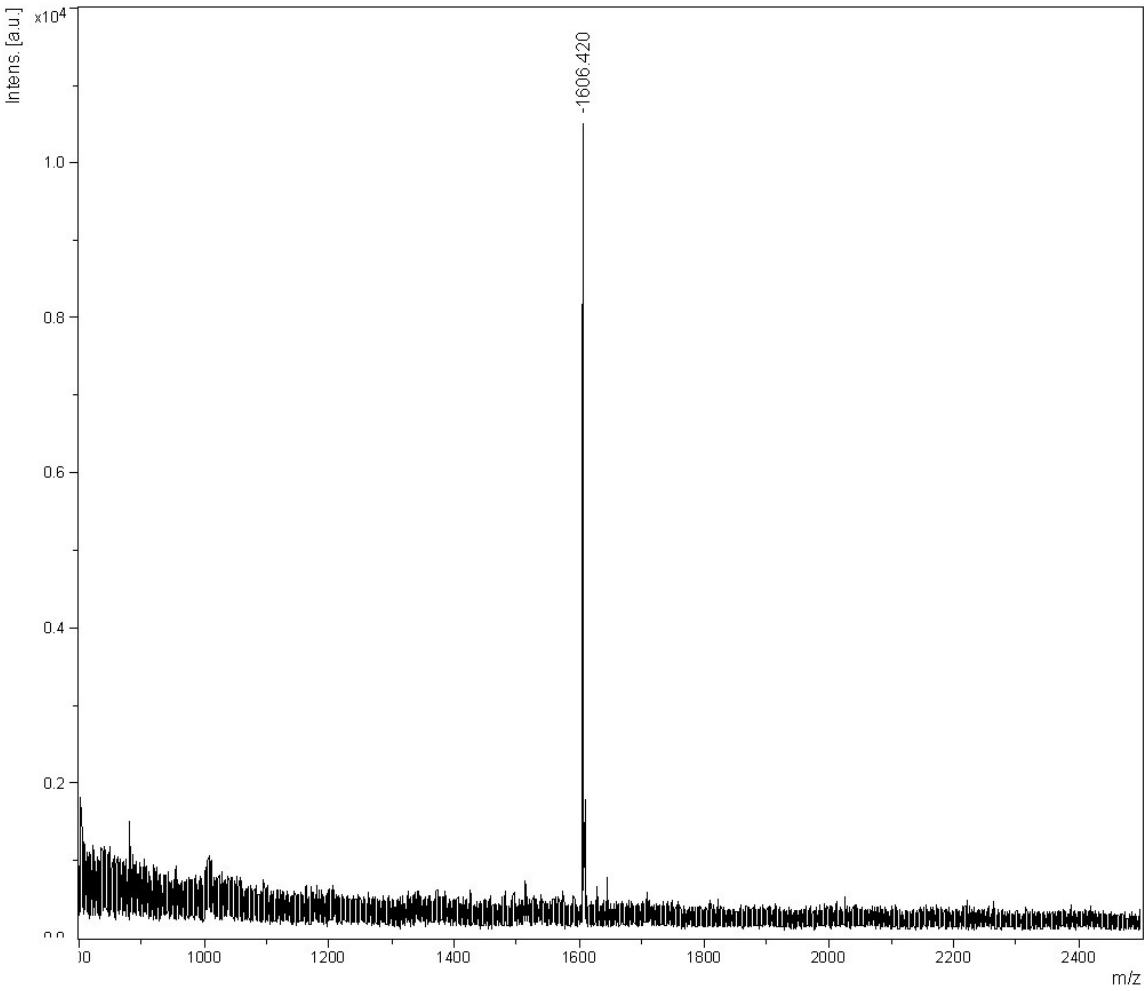
Intens. [a.u.]
x10^4
1.0
0.8
0.6
0.4
0.2
1606.420
1000
1200
1400
1600
1800
2000
2200
2400
m/z

Figure S13(d8): Maldi-Tof mass-spectral analysis of the SMART™ RP-Hplc fraction at **R_T = 24.16** min in the **Fig S12(d2k).** Corresponding RP-Hplc fraction is **R_T = 24.14** min in the **Fig S12(d2)** [after **1h** of alkaline hydrolysis (pH 12.5 / 20ºC) of **5′-r(CACGCAC)-3′**, **8b**]. The main peak at m/z **1606.4** for **5'-CACGC$_{2'/3'-P}$** [see Table S9(D)]

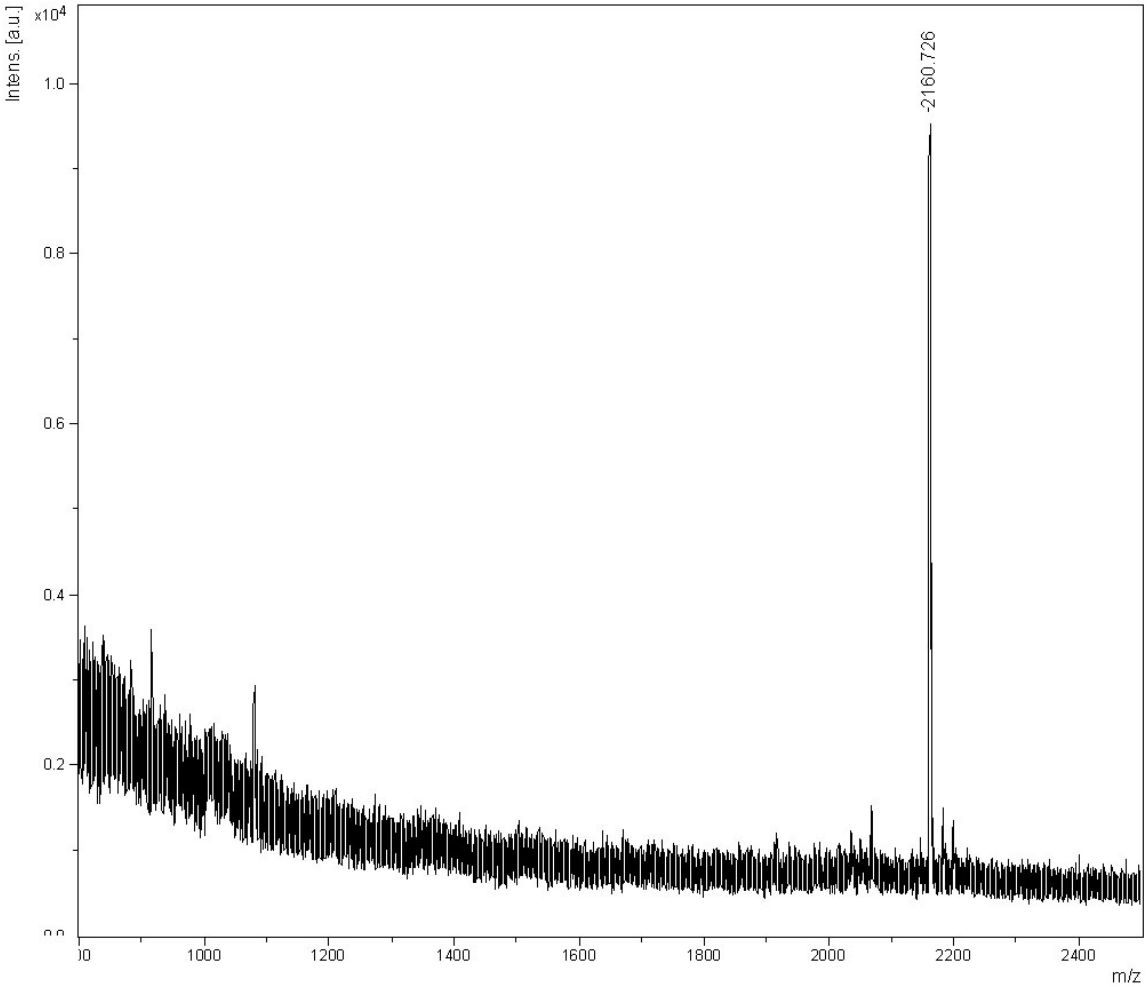

Figure S13(d9): Maldi-Tof mass-spectral analysis of the SMART™ RP-Hplc fraction at **R_T = 26.20** min in the **Fig S12(d2k).** Corresponding RP-Hplc fraction is **R_T = 24.14** min in the **Fig S12(d2)** [after **1h** of alkaline hydrolysis (pH 12.5 / 20ºC) of **5′-r(CACGCAC)-3′**, **8b**]. The main peak at m/z **2160.7** is for the parent heptamer [see Table S9(D)].

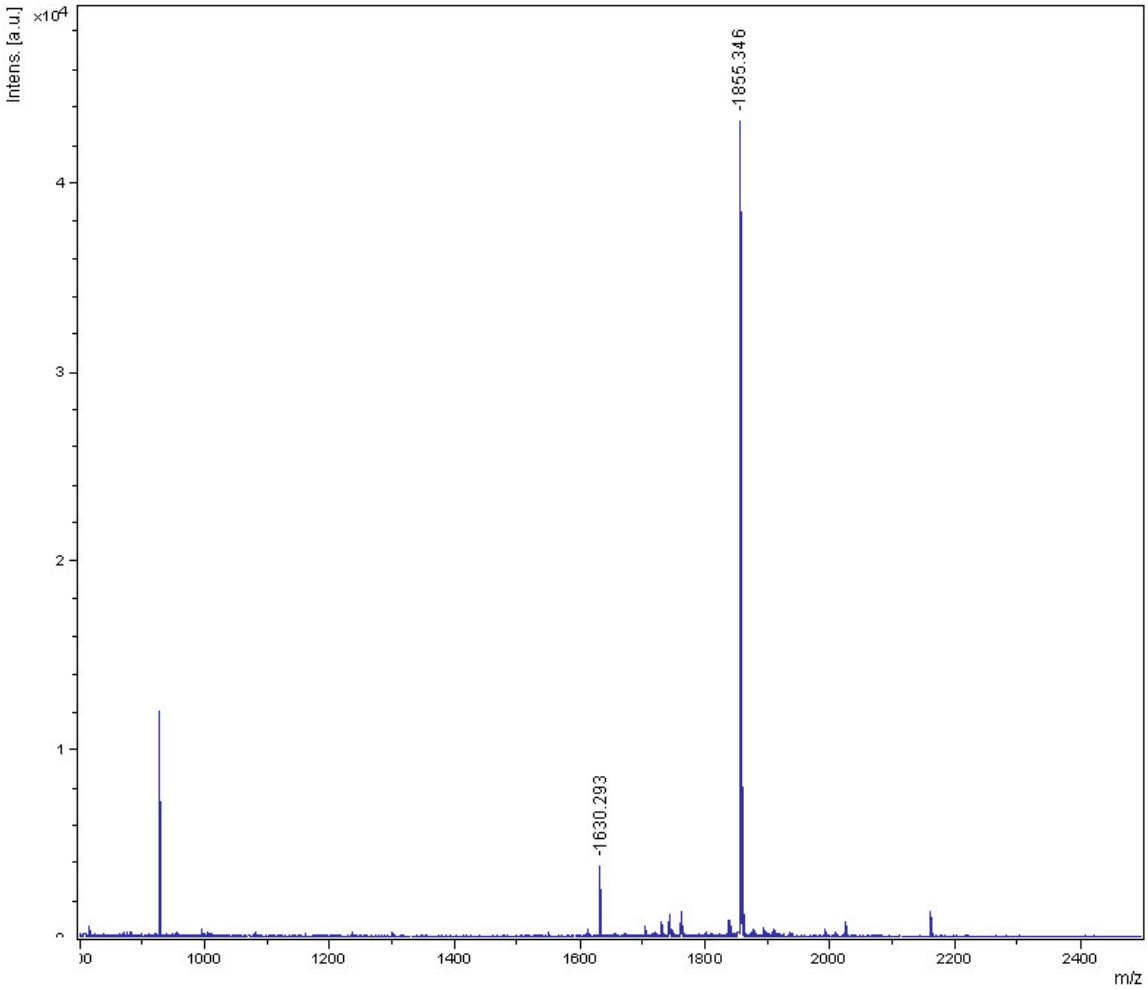

Figure S13(d10): Maldi-Tof mass-spectral analysis of the SMART™ RP-Hplc fraction at **R_T = 14.11** min in the **Fig S12(d2l).** Corresponding RP-Hplc fraction is **R_T = 25.39** min in the **Fig S12(d2)** [after **1h** of alkaline hydrolysis (pH 12.5 / 20ºC) of **5′-r(CACGCAC)-3′**, **8b**]. The main peak at m/z **1855.4** for **5'-ACGCAC-3'** [see Table S9(D)]

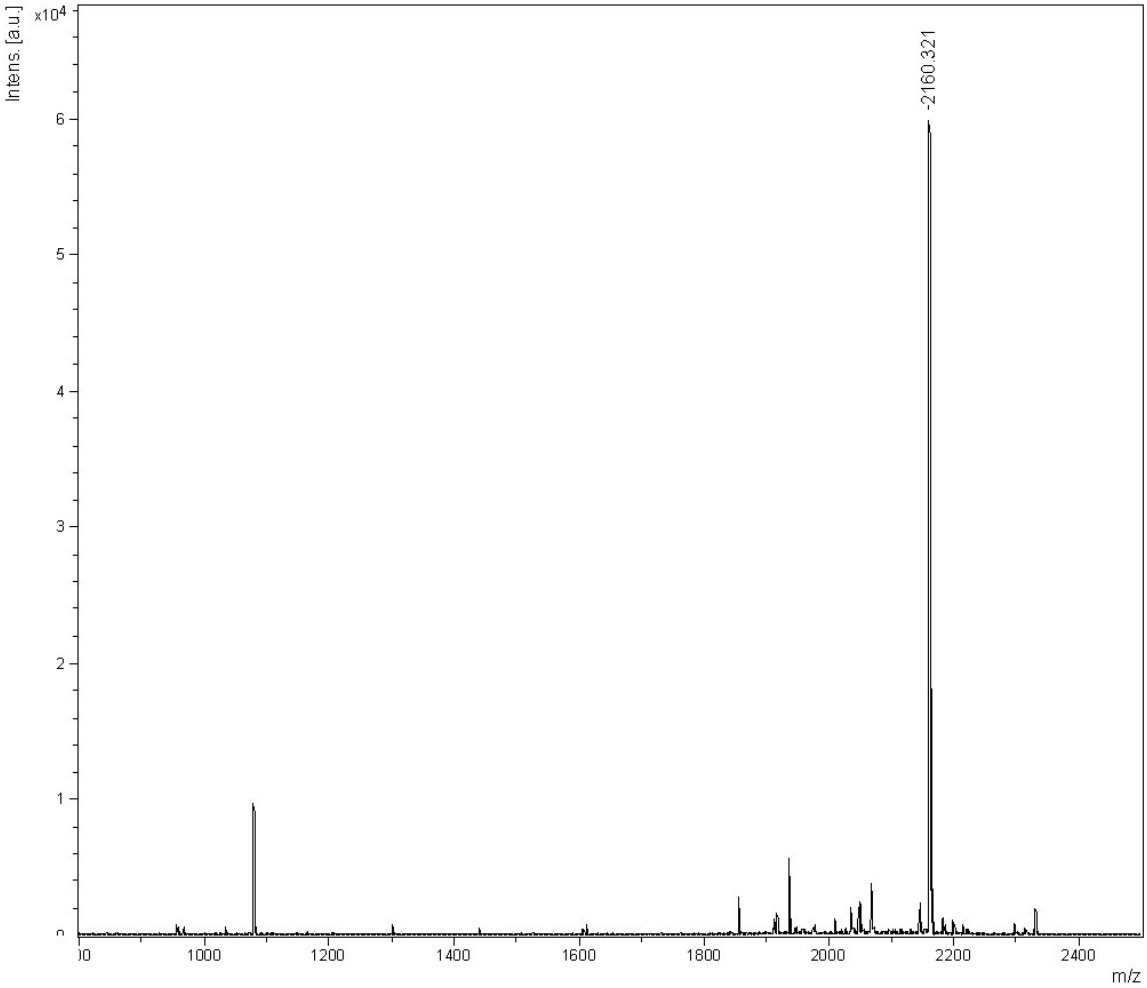

Figure S13(d11): Maldi-Tof mass-spectral analysis of the SMART™ RP-Hplc fraction at **R_T = 14.75** min in the **Fig S12(d2l).** Corresponding RP-Hplc fraction is **R_T = 25.39** min in the **Fig S12(d2)** [after **1h** of alkaline hydrolysis (pH 12.5 / 20ºC) of **5′-r(CACGCAC)-3′**, **8b**]. The main peak at m/z **2160.3** is for the parent heptamer [see Table S9(D)]

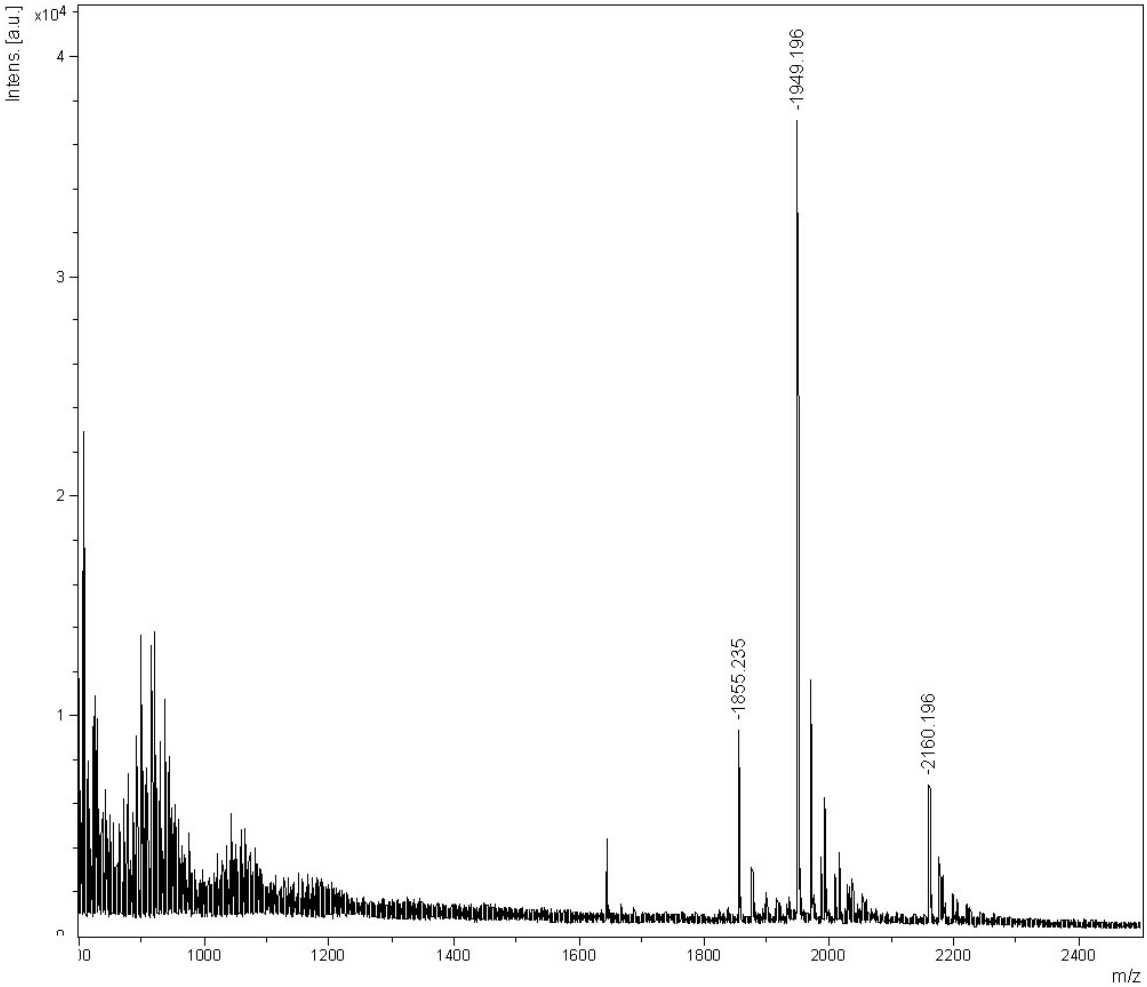

Figure S13(d12): Maldi-Tof mass-spectral analysis of the RP-Hplc fraction at **R_T = ~25.70** min for alkaline hydrolysis (pH 12.5 / 20ºC) of **5′-rCACGCAC-3′** (**8b**) after **1h** [for Hplc profile, see Fig

S12 (d2)] showing the main peak at m/z **1855.2** for **5'-ACGCAC-3'**, **1949.2** for non nucleos(t)idic fragment and **2160.2** for the parent heptamer [see Table S9(D)].

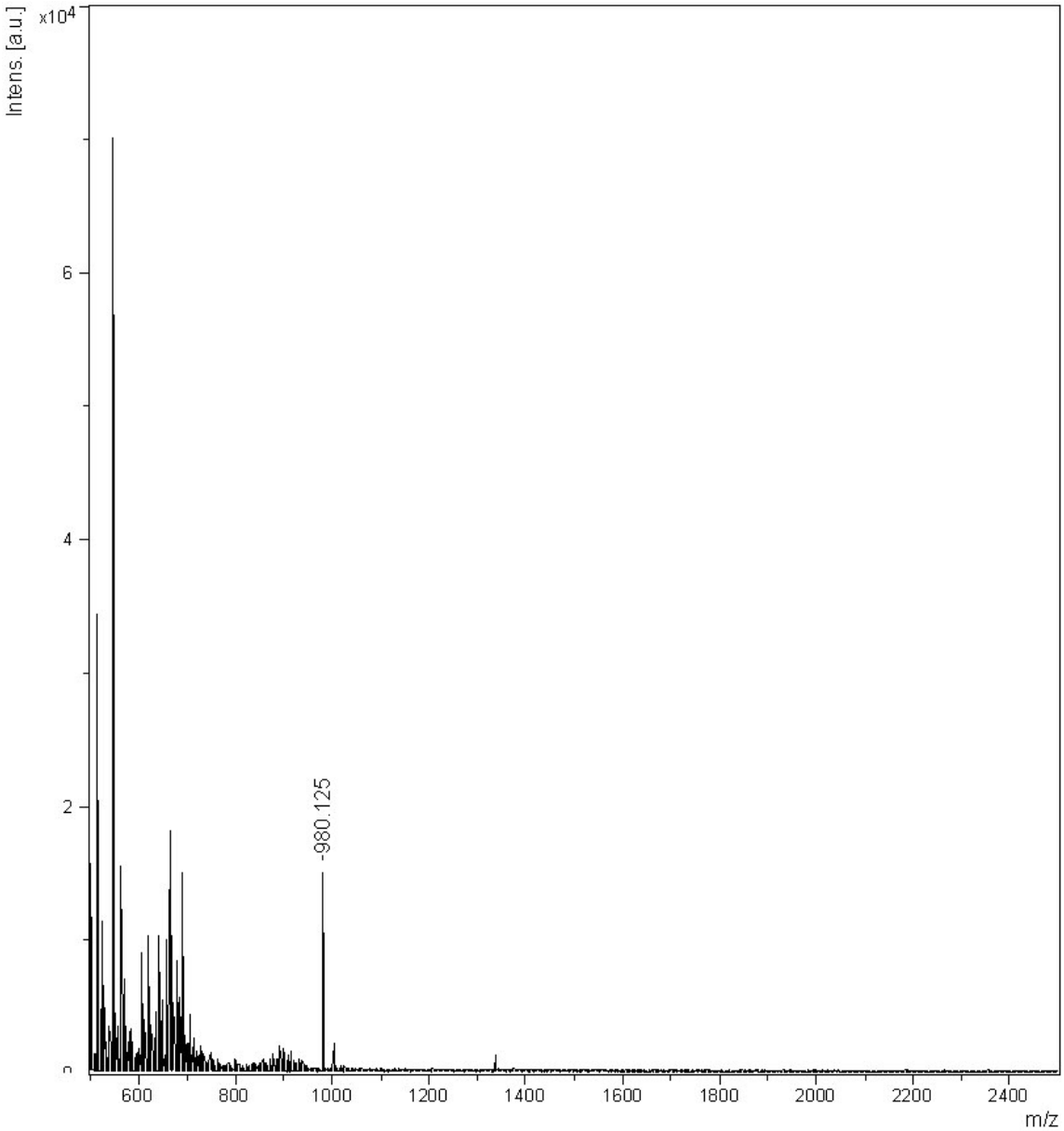

Figure S13(e1): Maldi Tof mass-spectral analysis of the RP-Hplc fraction at **R_T = 20.39** min for alkaline hydrolysis (pH 12.5 / 20ºC) of **5′-r(CAAG^{Me}AAC)-3′** (**5c**) after **1h** [for Hplc profile, see Fig **S12 (e2)**] showing the main peak at m/z **980.1** for **5′-CAA$_{2'/3'-P}$** [see Table S9(E)].

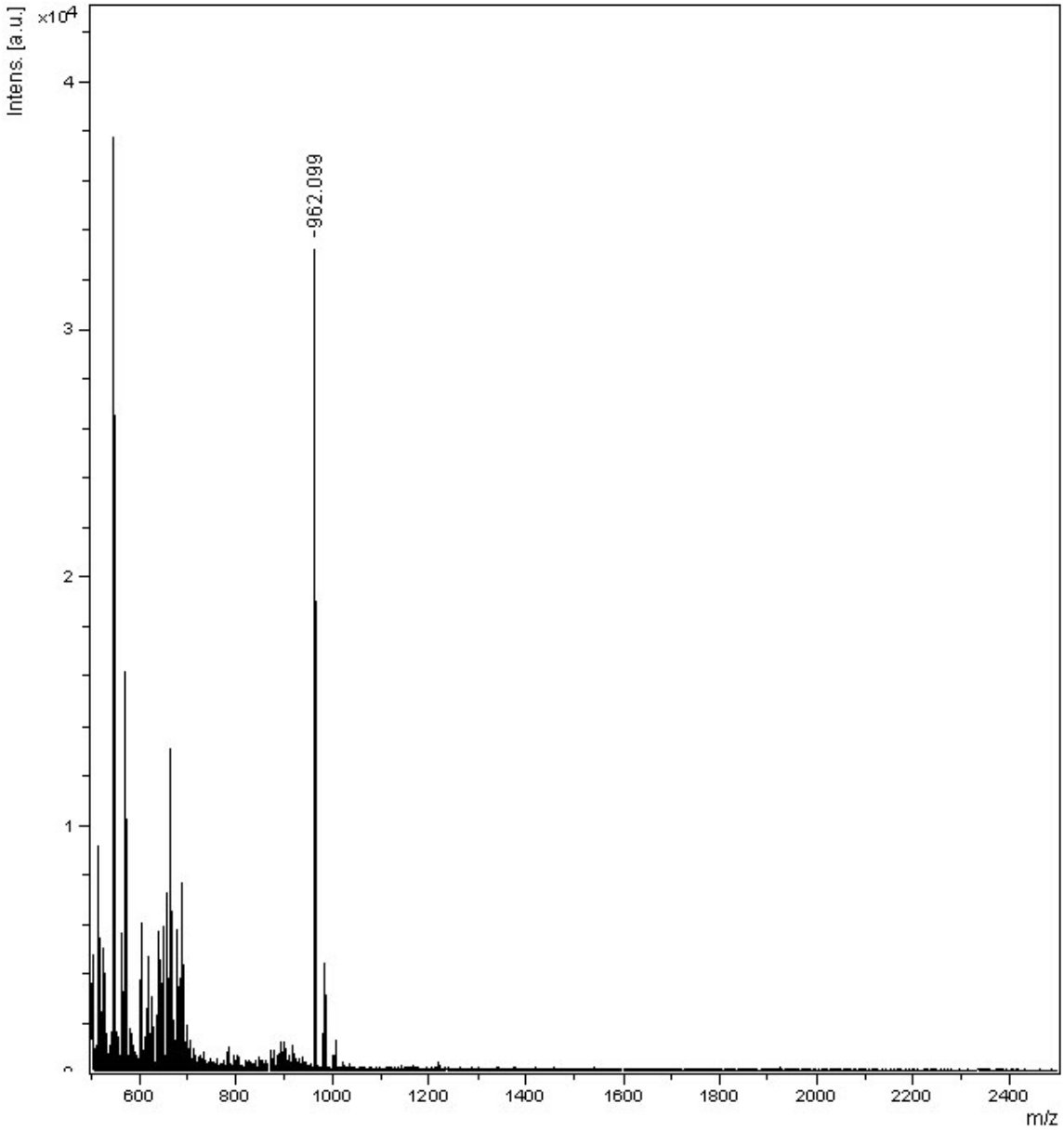

Figure S13(e2): Maldi Tof mass-spectral analysis of the RP-Hplc fraction at **R_T = 21.36** min for alkaline hydrolysis (pH 12.5 / 20ºC) of **5′-r(CAAG^{Me}AAC)-3′** (**5c**) after **1h** [for Hplc profile, see Fig **S12 (e2)**] showing the main peak at m/z **962.1** for **5′-CAA$_{2', 3'\text{-cMP}}$** [see Table S9(E)].

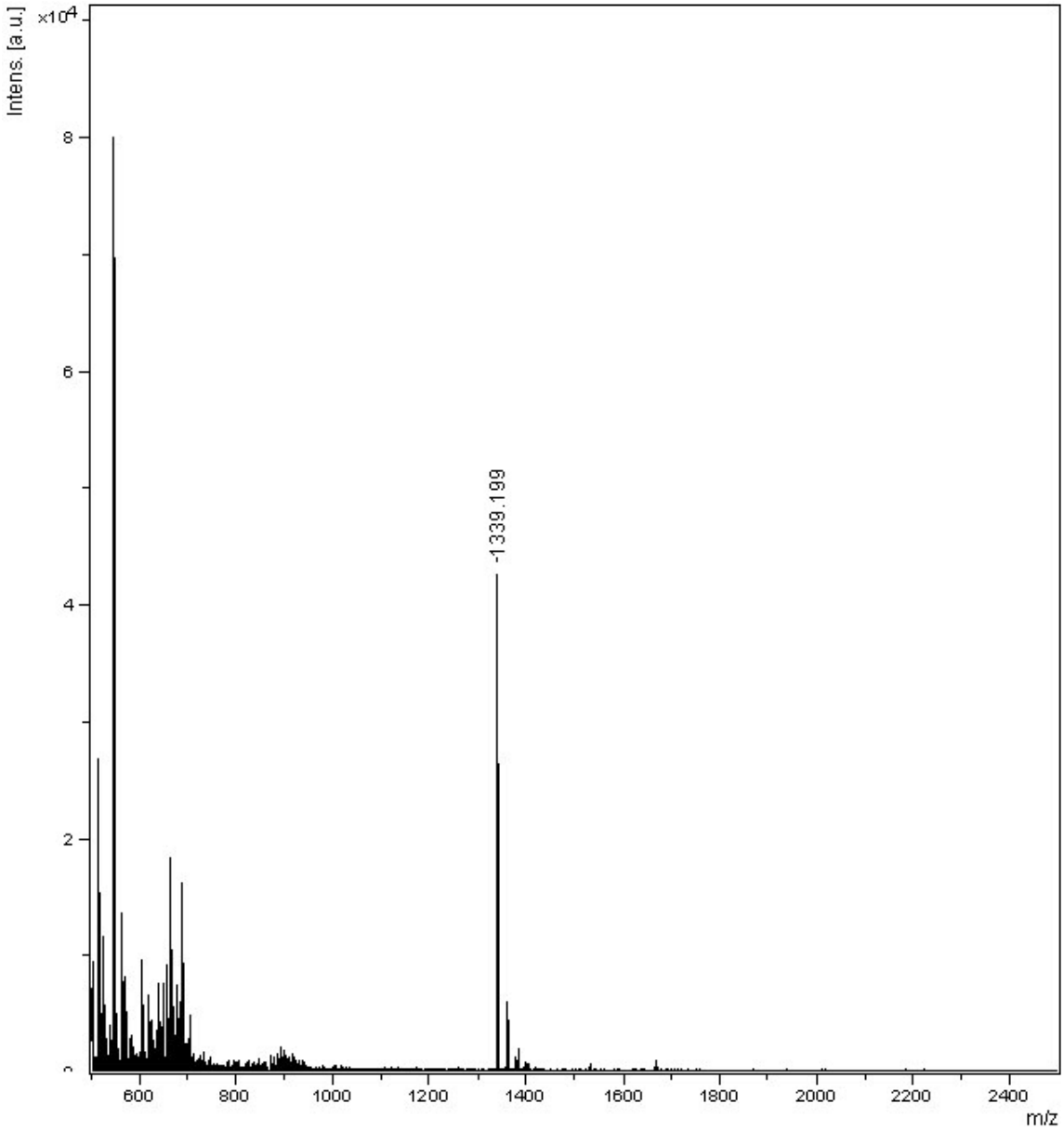

Figure S13(e3): Maldi Tof mass-spectral analysis of the RP-Hplc fraction at **R_T = 22.89** min for alkaline hydrolysis (pH 12.5 / 20ºC) of **5′-r(CAAG^{Me}AAC)-3′** (**5c**) after **1h** [for Hplc profile, see Fig **S12 (e2)**] showing the main peak at m/z **1339.2** for **5′-CAAG$^{Me}_{2'/3'-P}$** [see Table S9(E)].

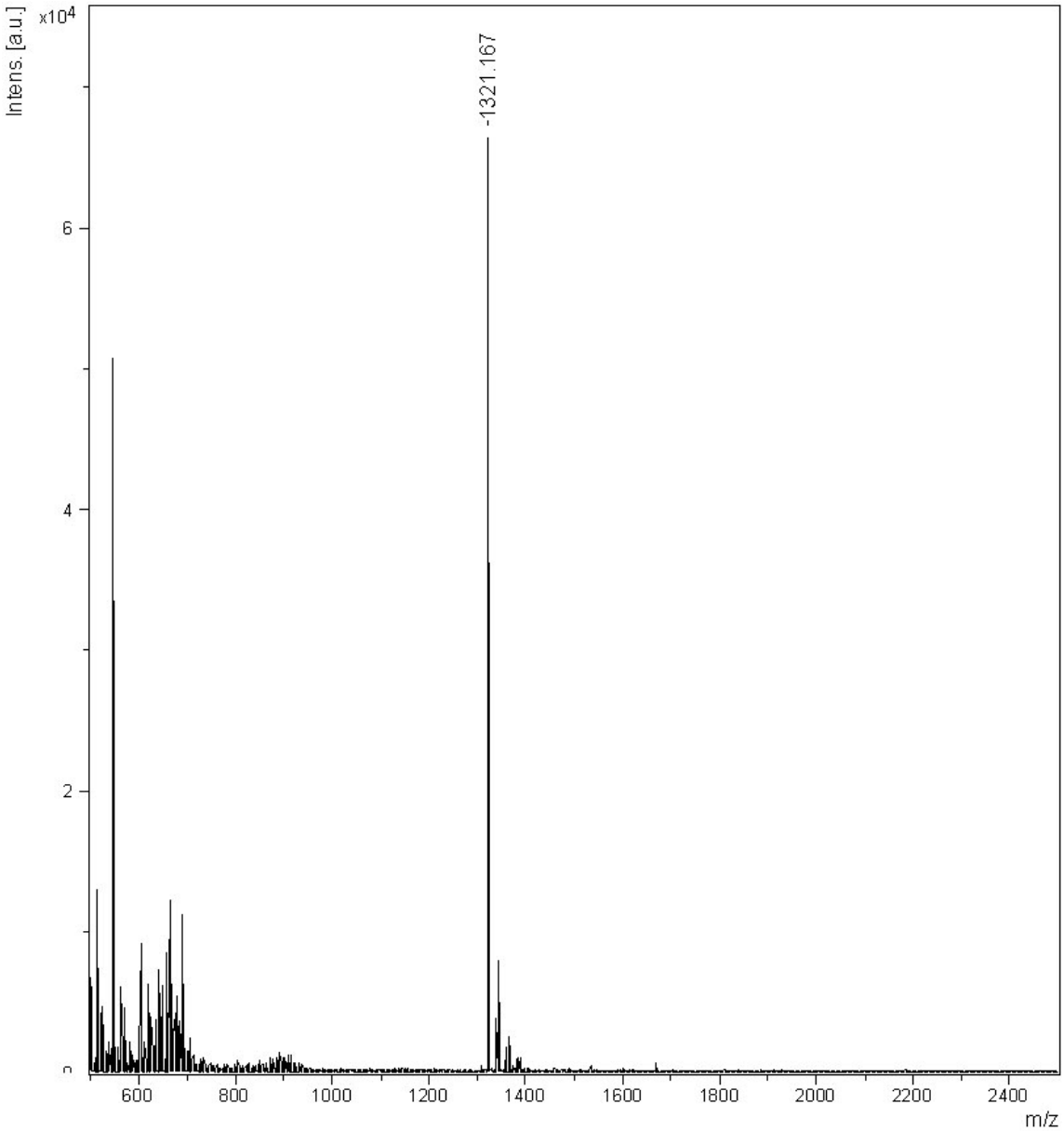

Figure S13(e4): Maldi Tof mass-spectral analysis of the RP-Hplc fraction at **R_T = 23.37** min for alkaline hydrolysis (pH 12.5 / 20ºC) of **5′-r(CAAG^{Me}AAC)-3′** (**5c**) after **1h** [for Hplc profile, see Fig **S12 (e2)**] showing the main peak at m/z **1321.2** for **5′-CAAG$^{Me}_{2',3'\text{-cMP}}$** [see Table S9(E)].

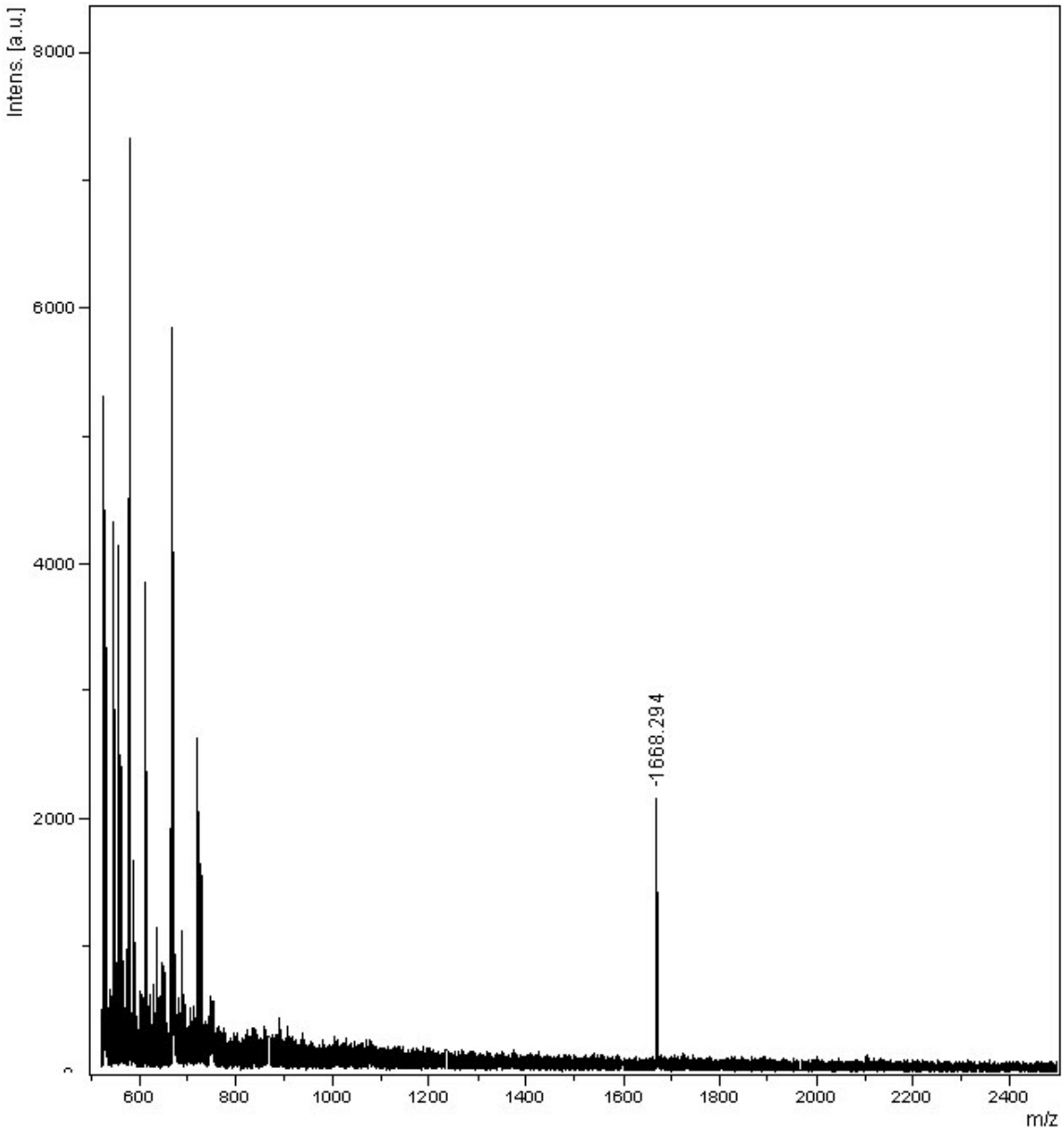

Figure S13(e5): Maldi-Tof mass-spectral analysis of the SMART™ RP-Hplc fraction at **R_T = 29.41** min in the **Fig S12(e2i).** Corresponding RP-Hplc fraction is **R_T = 25.50** min in the **Fig S12(e2)** [after

1h of alkaline hydrolysis (pH 12.5 / 20ºC) of **5′-r(CAAG^{Me}AAC)-3′**, **5c**] the main peak at m/z **1668.3** is for **5'-CAAG^{Me}A$_{2'/3'-P}$** [see Table S9(E)].

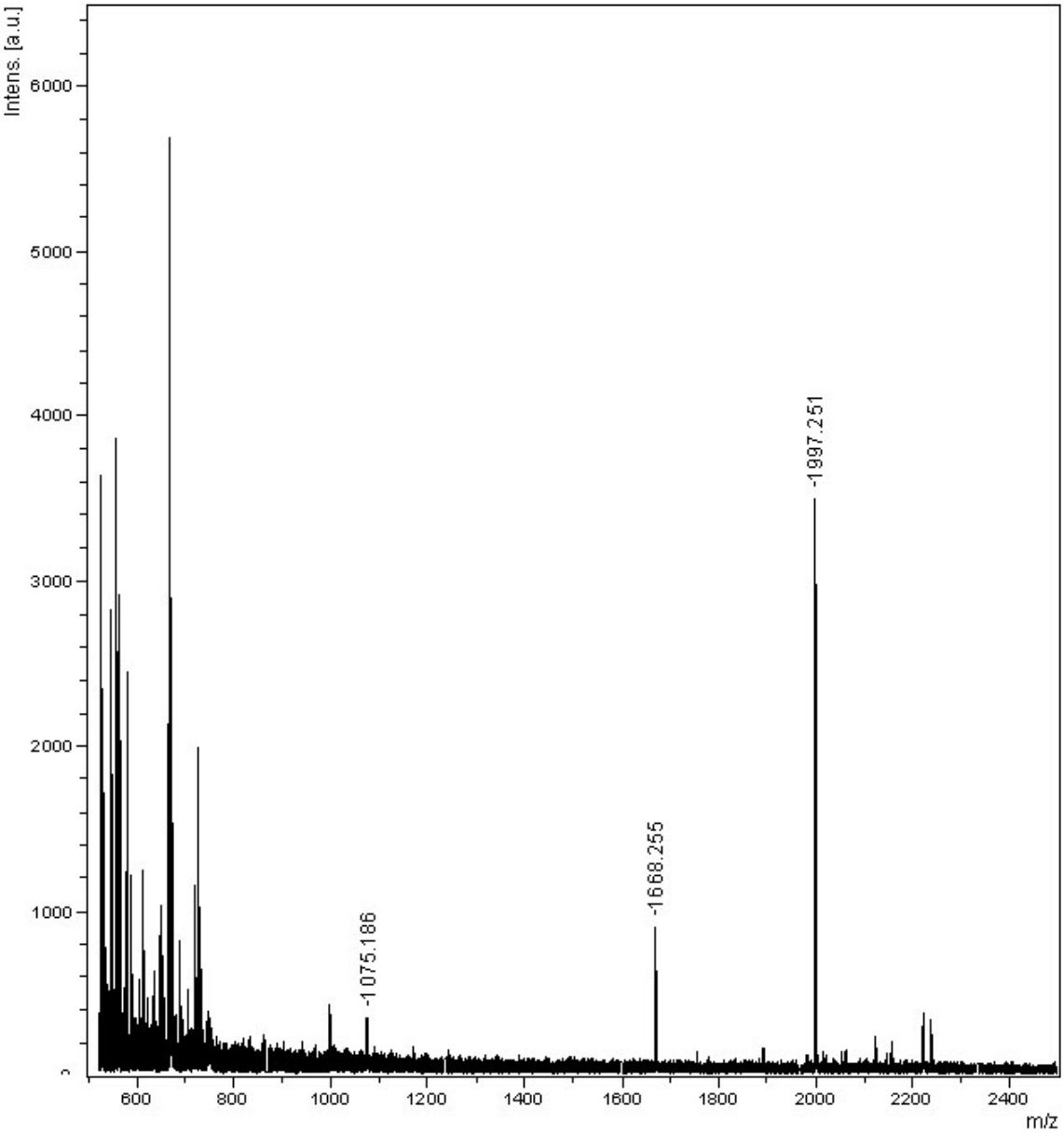

Figure S13(e6): Maldi-Tof mass-spectral analysis of the SMART™ RP-Hplc fraction at **R_T = 30.08** min in the **Fig S12(e2i).** Corresponding RP-Hplc fraction is **R_T = 25.50** min in the **Fig S12(e2)** [after **1h** of alkaline hydrolysis (pH 12.5 / 20ºC) of **5′-r(CAAG^{Me}AAC)-3′**, **5c**] the main peak at m/z **1997.3** is for **5'-CAAG^{Me}AA$_{2'/3'-P}$** [see Table S9(E)].

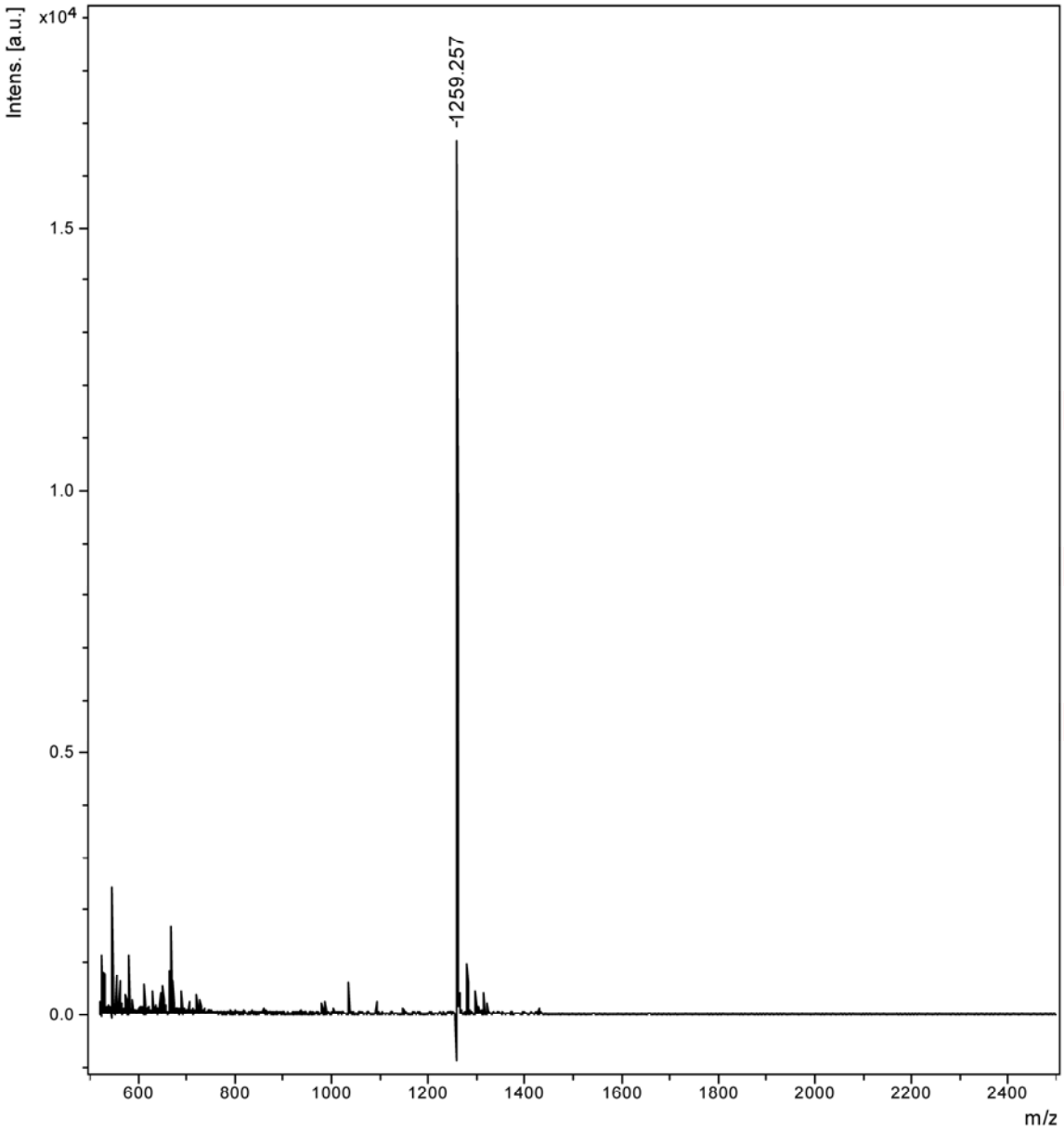

Figure S13(e7): Maldi-Tof mass-spectral analysis of the SMART™ RP-Hplc fraction at **R_T = 27.71** min in the **Fig S12(e2j).** Corresponding RP-Hplc fraction is **R_T = 25.70** min in the **Fig S12(e2)** [after **1h** of alkaline hydrolysis (pH 12.5 / 20ºC) of **5′-r(CAAG^{Me}AAC)-3′**, **5c**] the main peak at m/z **1259.3** is for **5'-CAAG^{Me}A$_{2', 3'\text{-cMP}}$** [see Table S9(E)].

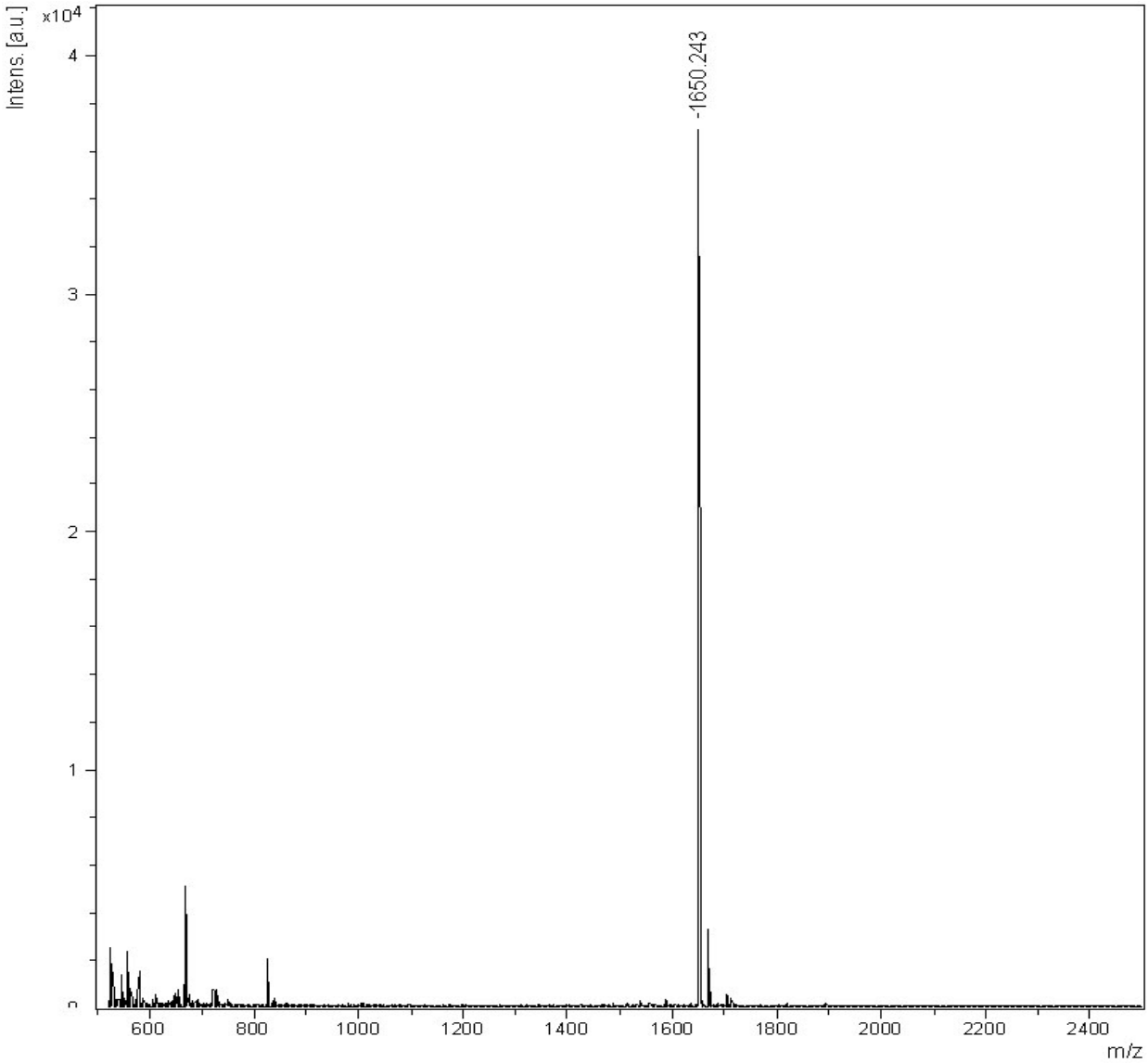

Figure S13(e8): Maldi-Tof mass-spectral analysis of the SMART™ RP-Hplc fraction at **R_T = 29.24** min in the **Fig S12(e2j).** Corresponding RP-Hplc fraction is **R_T = 25.70** min in the **Fig S12(e2)** [after **1h** of alkaline hydrolysis (pH 12.5 / 20ºC) of **5′-r(CAAG^{Me}AAC)-3′**, **5c**] the main peak at m/z **1650.2** is for **5′-G^{Me}AAC-3′** [see Table S9(E)].

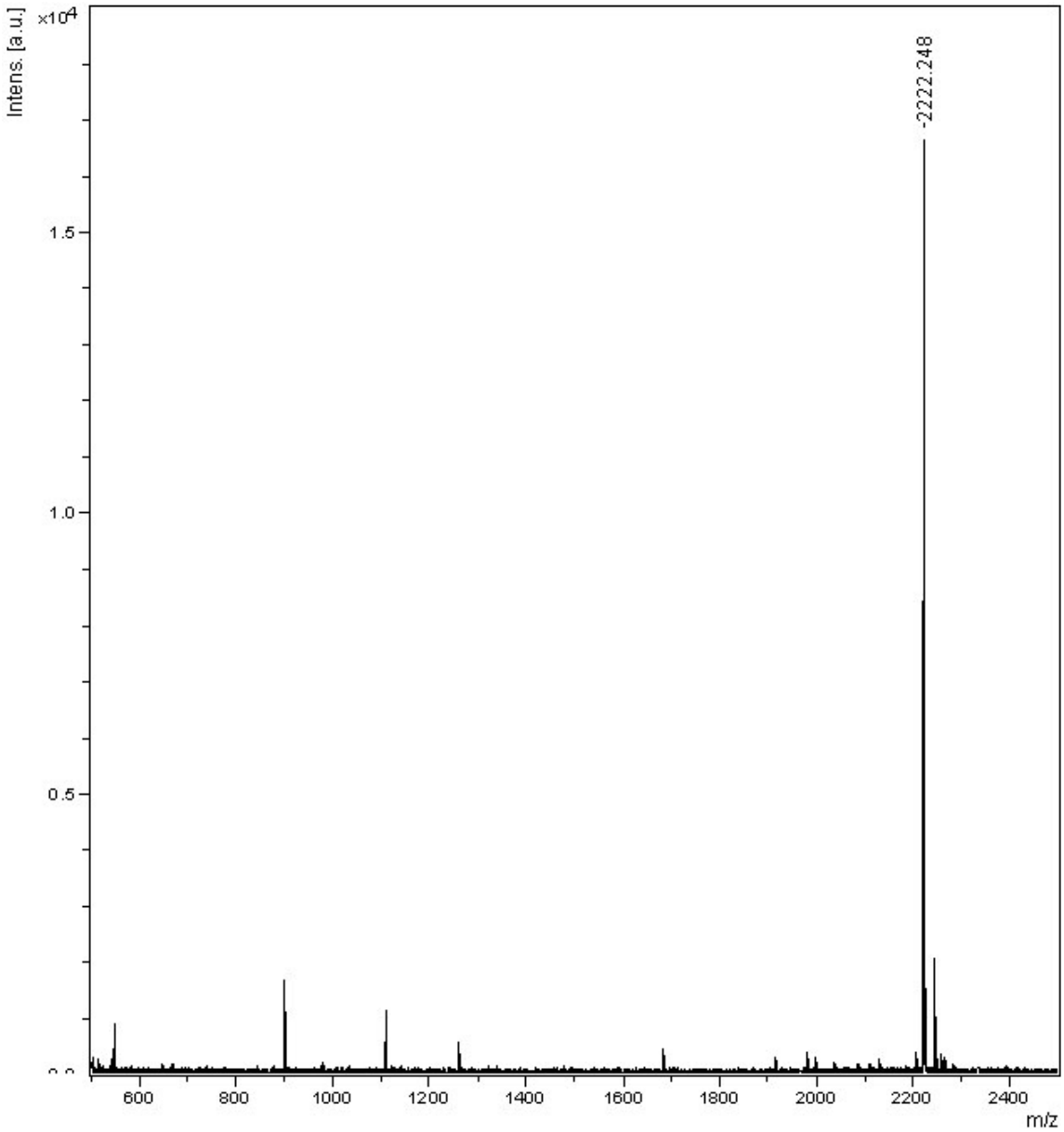

Figure S13(e9): Maldi Tof mass-spectral analysis of the RP-Hplc fraction at **R_T = 26.16** min for alkaline hydrolysis (pH 12.5 / 20ºC) of **5′-r(CAAG^{Me}AAC)-3′** (**5c**) after **1h** [for Hplc profile, see Fig **S12 (e2)**] showing the main peak at m/z **2222.2** for the parent heptameric peak [see Table S9(E)].

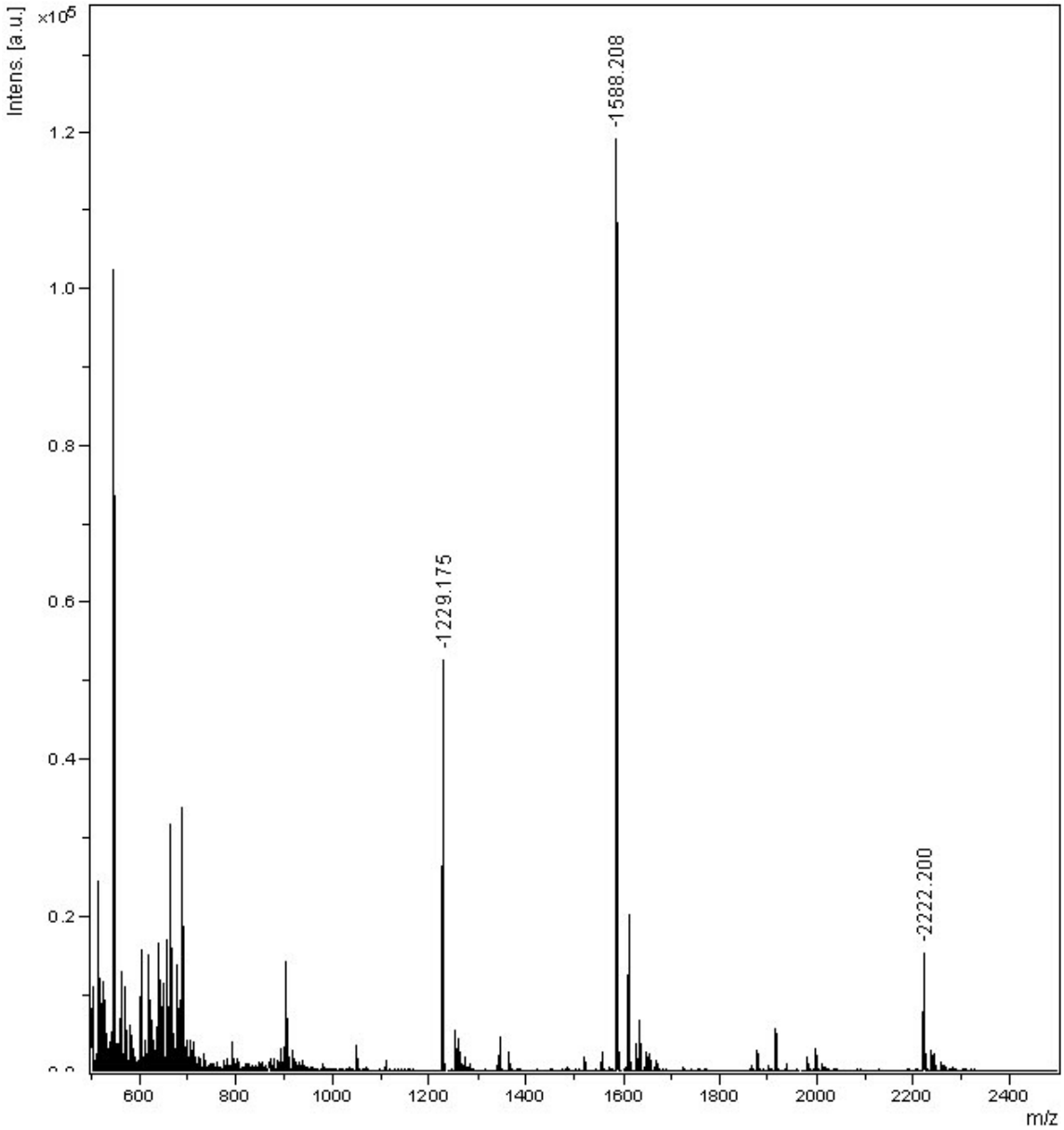

Figure S13(e10): Maldi Tof mass-spectral analysis of the RP-Hplc fraction at **R_T = 26.91** min for alkaline hydrolysis (pH 12.5 / 20ºC) of **5′-r(CAAG^{Me}AAC)-3′** (**5c**) after **1h** [for Hplc profile, see Fig **S12 (e2)**] showing the main peak at m/z **1588.2** for **5′-AG^{Me}AAC-3′** along with some non-nucleos(t)idic peak at m/z **1229.2** [see Table S9(E)].

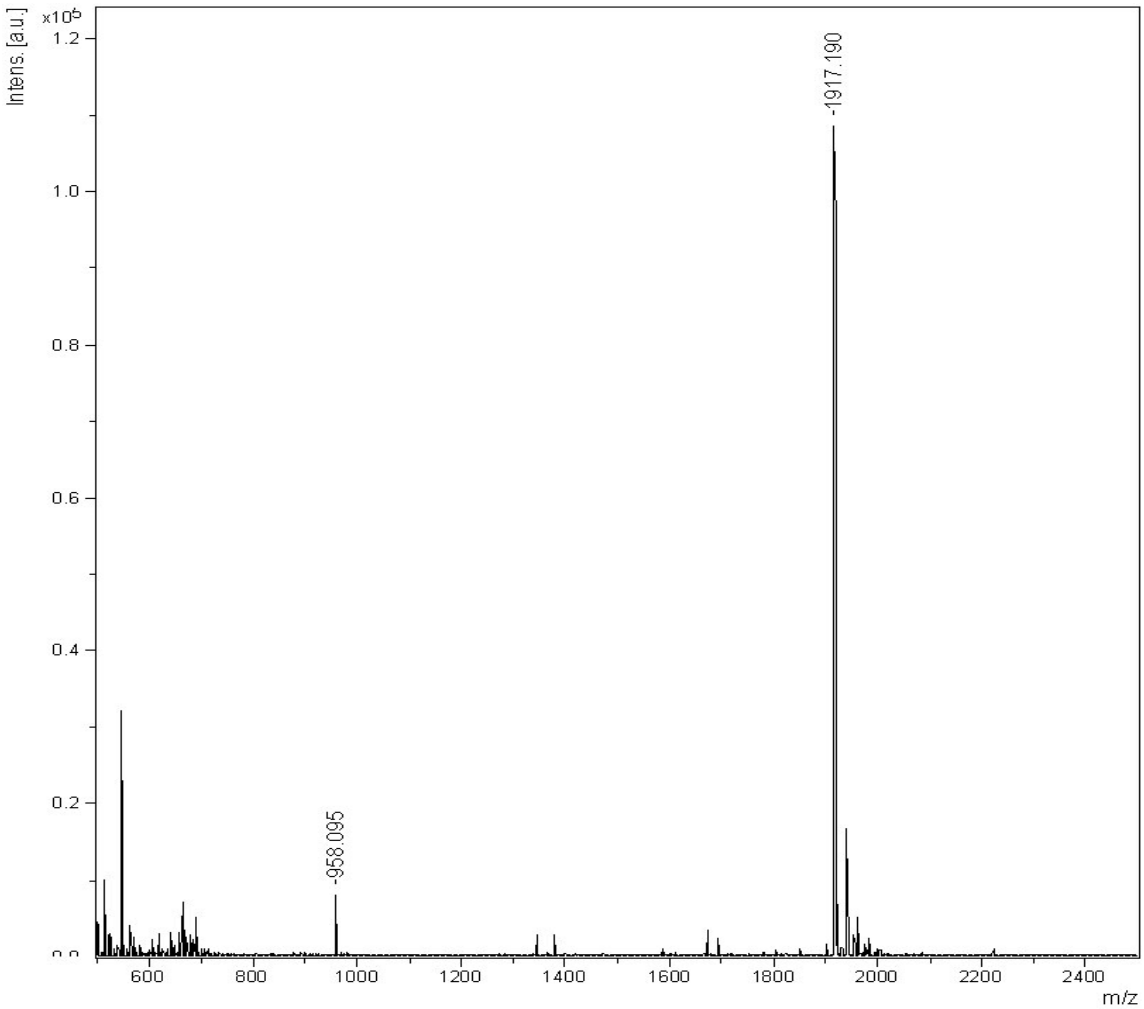

Figure S13(e11): Maldi Tof mass-spectral analysis of the RP-Hplc fraction at **R_T = 28.45** min for alkaline hydrolysis (pH 12.5 / 20ºC) of **5′-r(CAAG^{Me}AAC)-3′** (**5c**) after **1h** [for Hplc profile, see Fig **S12 (e2)**] showing the main peak at m/z **1917.2** for **5′-AAG^{Me}AAC-3′** [see Table S9(E)].

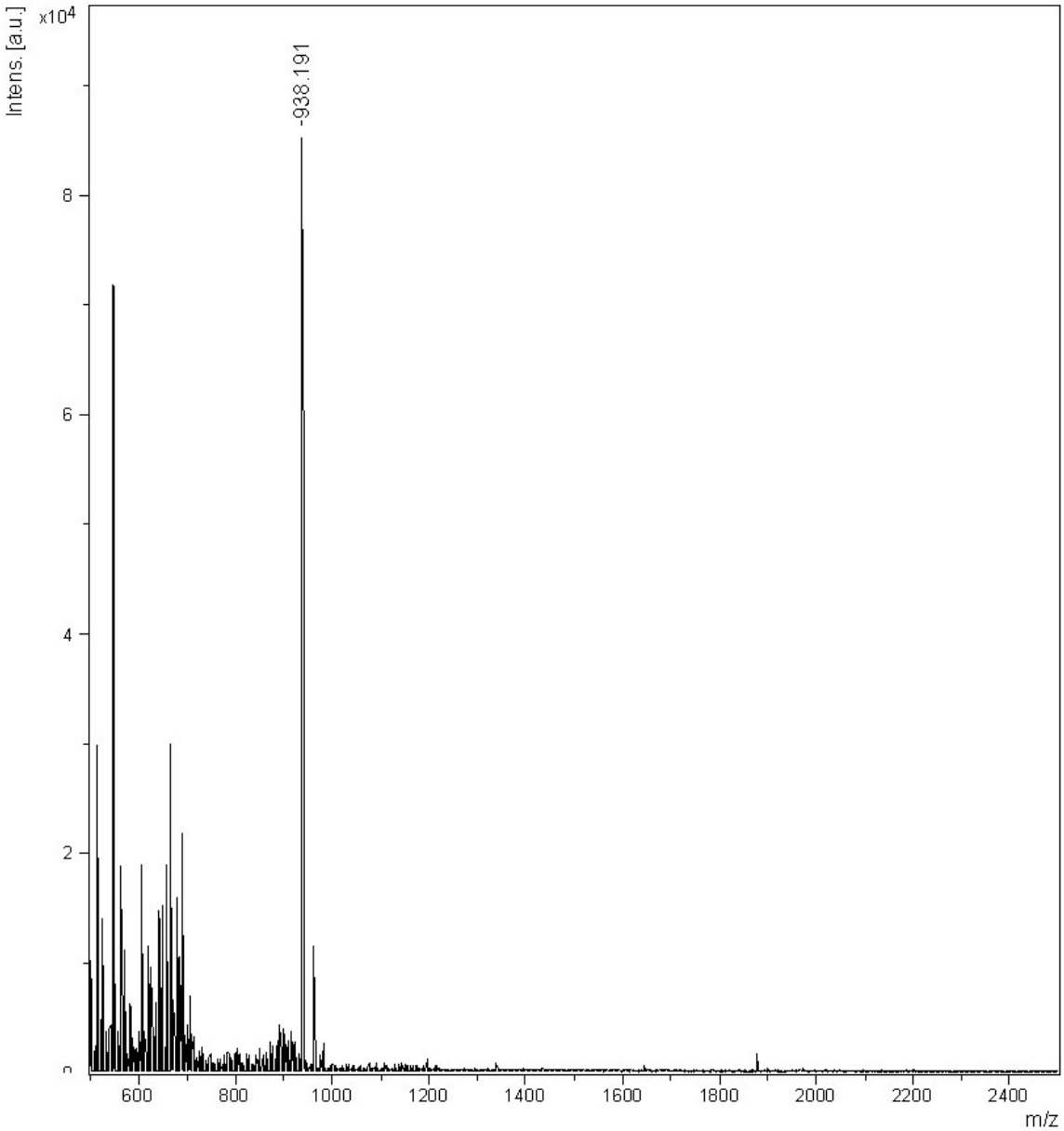

Figure S13(f1): Maldi Tof mass-spectral analysis of the RP-Hplc fraction at **R_T = 19.68** min for alkaline hydrolysis (pH 12.5 / 20ºC) of **5′-r(CACG^{Me}AAC)-3′** (**7c**) after **1h** [for Hplc profile, see Fig **S12 (f2)**] showing the main peak at m/z **938.2** for **5′-CAC$_{2′,3′\text{-cMP}}$** [see Table S9(F)].

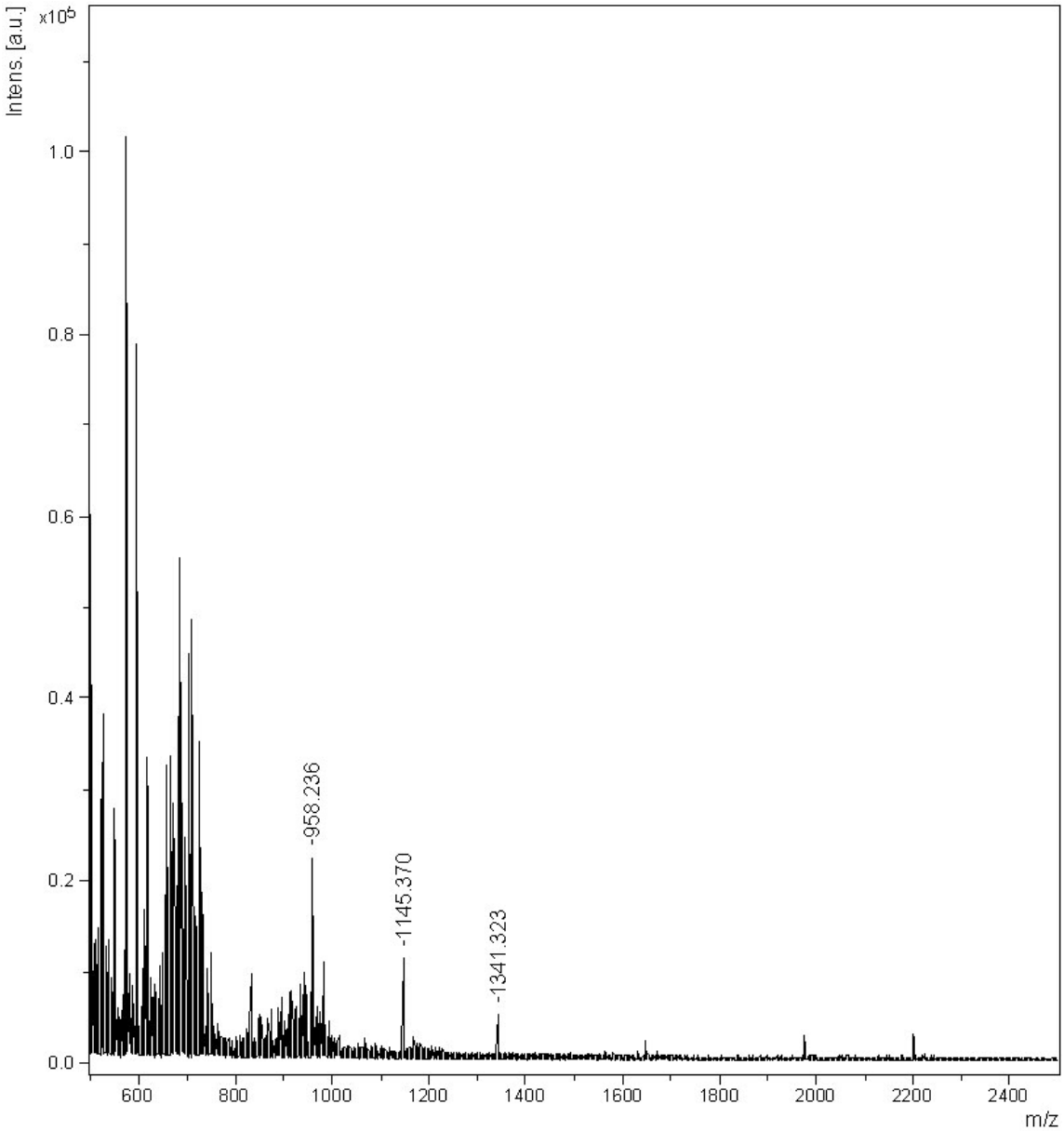

Figure S13(f2): Maldi Tof mass-spectral analysis of the RP-Hplc fraction at **R_T = 21.81** min for alkaline hydrolysis (pH 12.5 / 20ºC) of **5′-r(CACG^{Me}AAC)-3′** (**7c**) after **1h** [for Hplc profile, see Fig **S12 (f2)**] showing the main peak at m/z **958.2** for **5′-CAC$_{2'/3'-P}$** and other two peaks are non-nucleos(t)idic[see Table S9(F)].

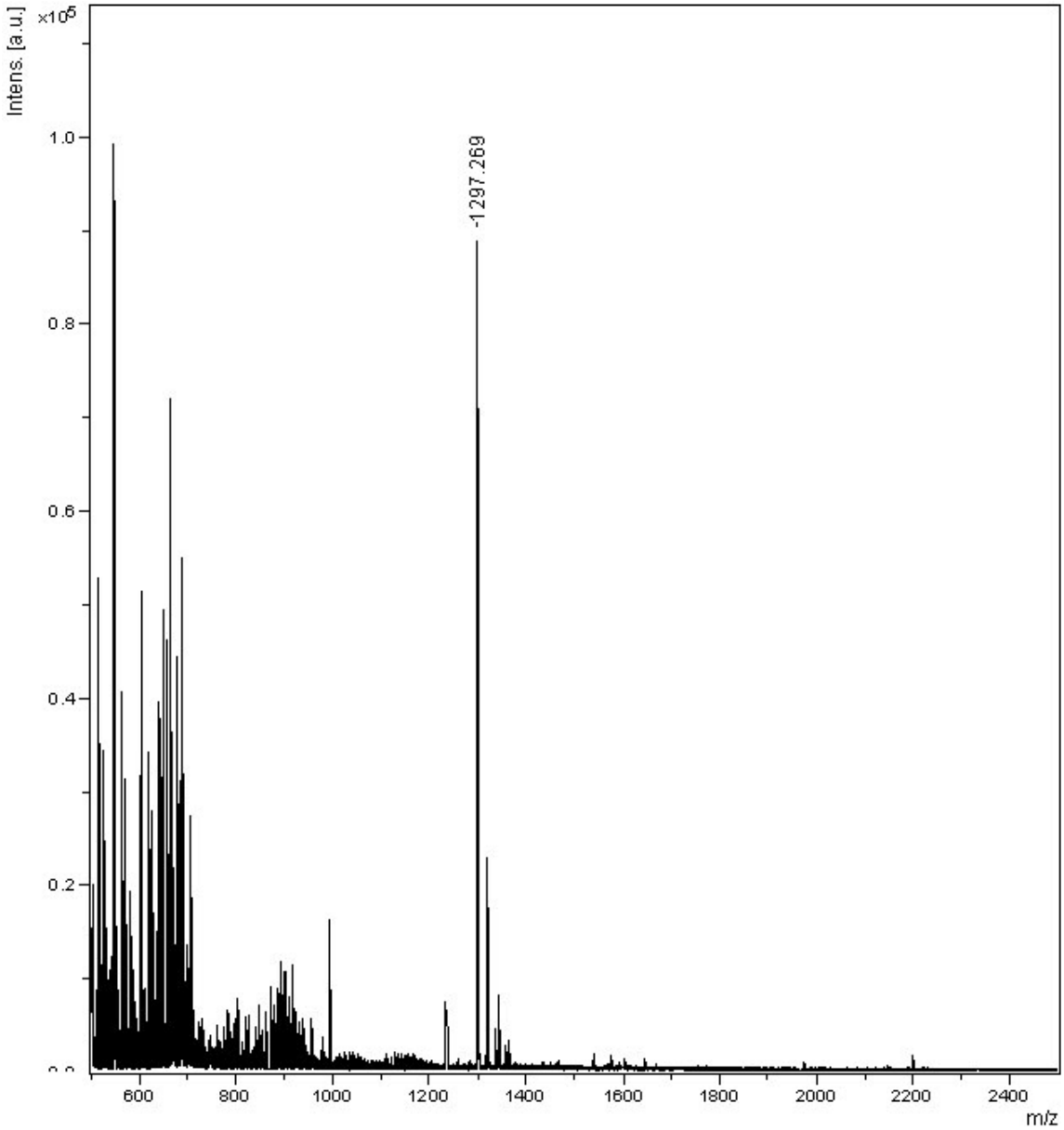

Figure S13(f3): Maldi Tof mass-spectral analysis of the RP-Hplc fraction at **R_T = 22.89** min for alkaline hydrolysis (pH 12.5 / 20ºC) of **5′-r(CACG^{Me}AAC)-3′** (**7c**) after **1h** [for Hplc profile, see Fig **S12 (f2)**] showing the main peak at m/z **1297.2** for **5′-CACG^{Me}$_{2',3'\text{-cMP}}$** [see Table S9(F)].

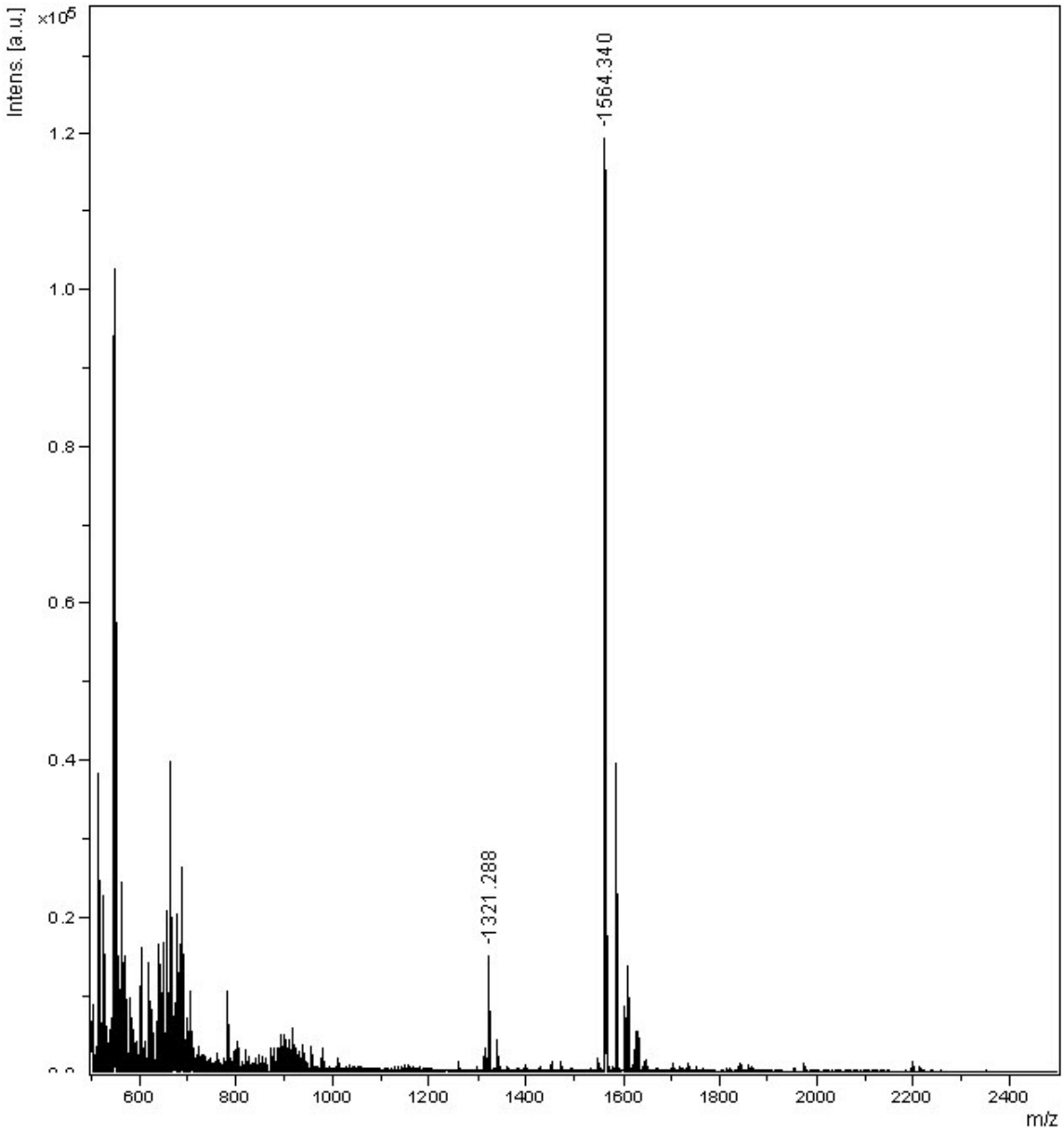

Figure S13(f4): Maldi Tof mass-spectral analysis of the RP-Hplc fraction at **R_T = 23.85** min for alkaline hydrolysis (pH 12.5 / 20ºC) of **5′-r(CACG^{Me}AAC)-3′** (**7c**) after **1h** [for Hplc profile, see Fig **S12 (f2)**] showing the main peak at m/z **1564.3** for **5′-CG^{Me}AAC-3′** [see Table S9(F)].

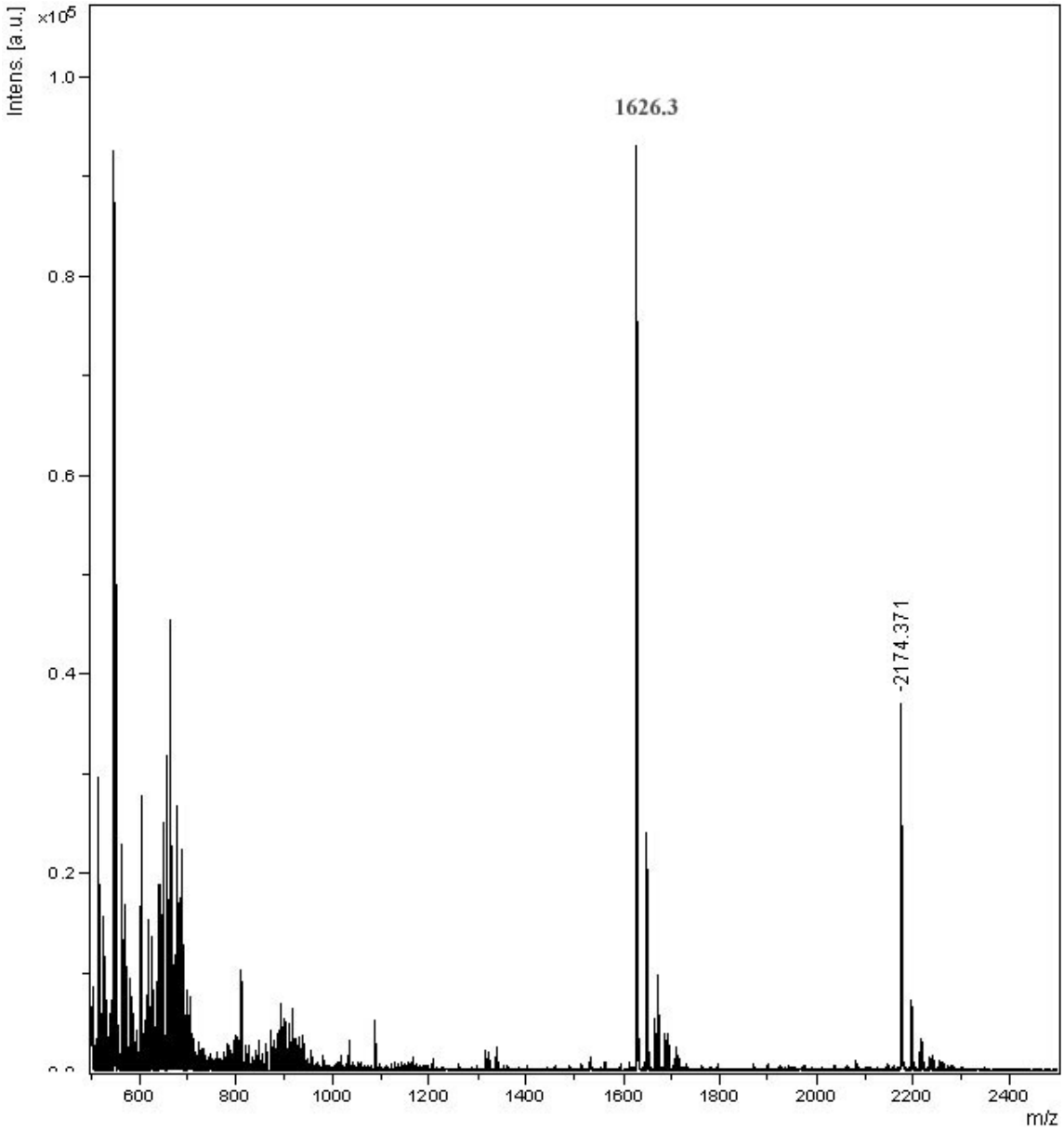

Figure S13(f5): Maldi Tof mass-spectral analysis of the RP-Hplc fraction at **R_T = 24.77** min for alkaline hydrolysis (pH 12.5 / 20ºC) of **5′-r(CACG^{Me}AAC)-3′** (**7c**) after **1h** [for Hplc profile, see Fig **S12 (f2)**] showing the main peak at m/z **1626.3** for **5′-CACG^{Me}A-3′** along with some non-nucleos(t)idic peak at m/z **2174.3.** [see Table S9(F)].

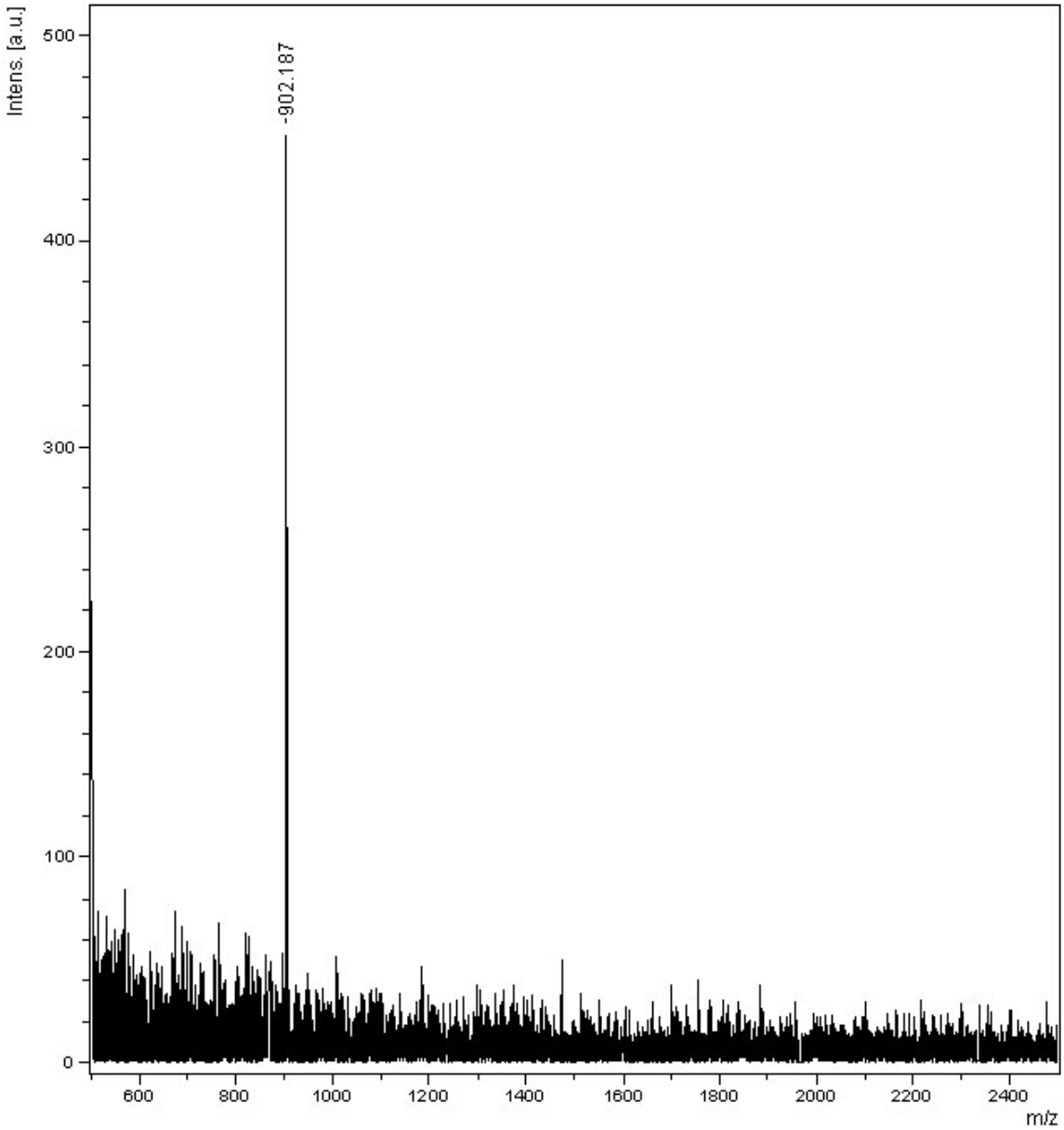

Figure S13(f6): Maldi-Tof mass-spectral analysis of the SMART™ RP-Hplc fraction at **R_T = 25.15** min and **R_T = 26.15** in the **Fig S12(f2i).** Corresponding mixed RP-Hplc fractions were at **R_T = 25.93** min and **R_T = 26.49** min in the **Fig S12(f2)** [after **1h** of alkaline hydrolysis (pH 12.5 / 20ºC) of **5′-r(CACG^{Me}AAC)-3′**, **7c**] showing the main peak at m/z **902.3** for **5'-AAC-3'** [see Table S9(F)].

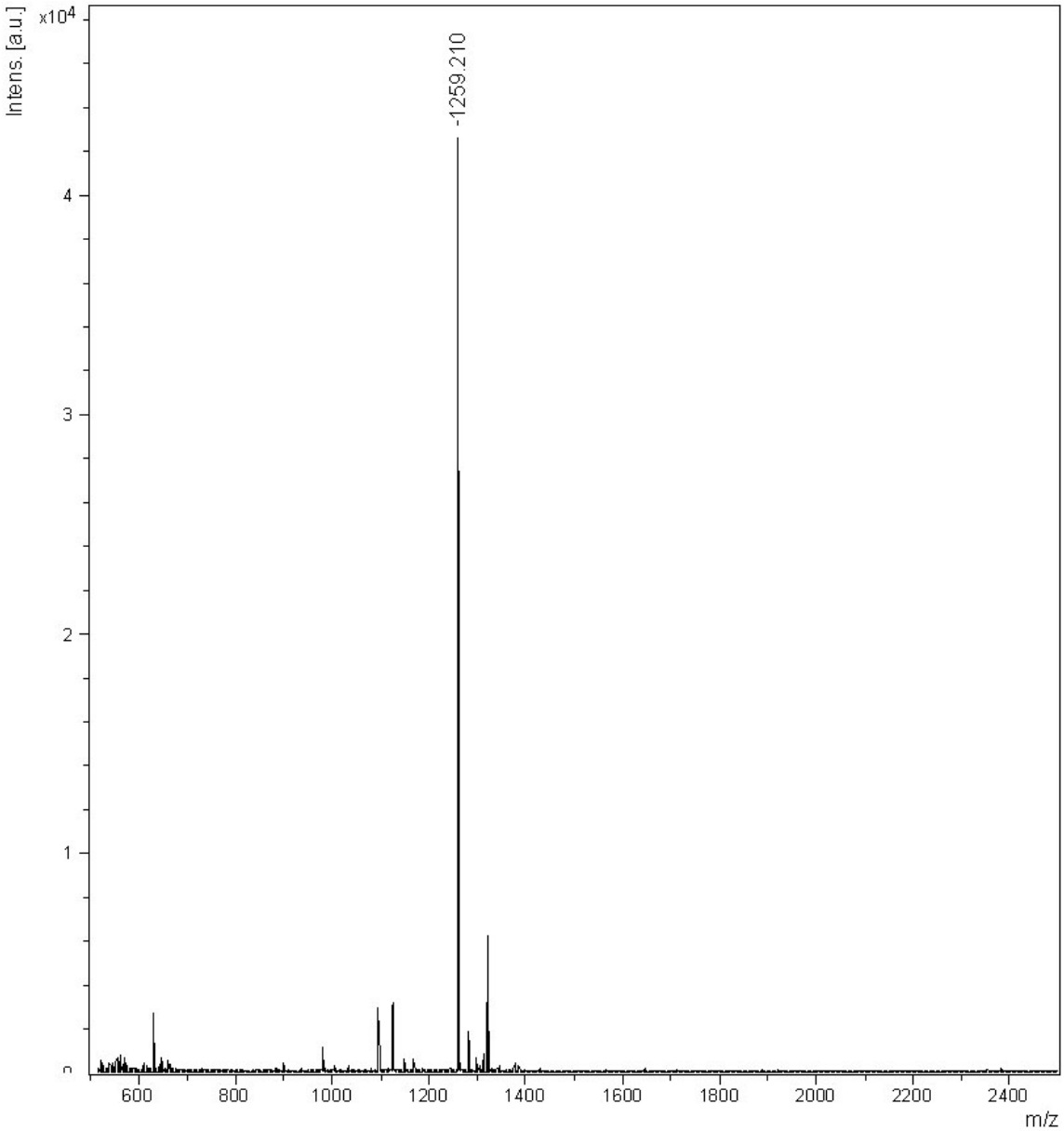

Figure S13(f7): Maldi-Tof mass-spectral analysis of the SMART™ RP-Hplc fraction at **R_T = 27.71** min in the **Fig S12(f2i).** Corresponding mixed RP-Hplc fractions were at **R_T = 25.93** min and **R_T = 26.49** min in the **Fig S12(f2)** [after **1h** of alkaline hydrolysis (pH 12.5 / 20ºC) of **5′-r(CACG^{Me}AAC)-3′**, **7c**] showing the main peak at m/z **1259.2** for **5′-G^{Me}AAC-3′** [see Table S9(F)].

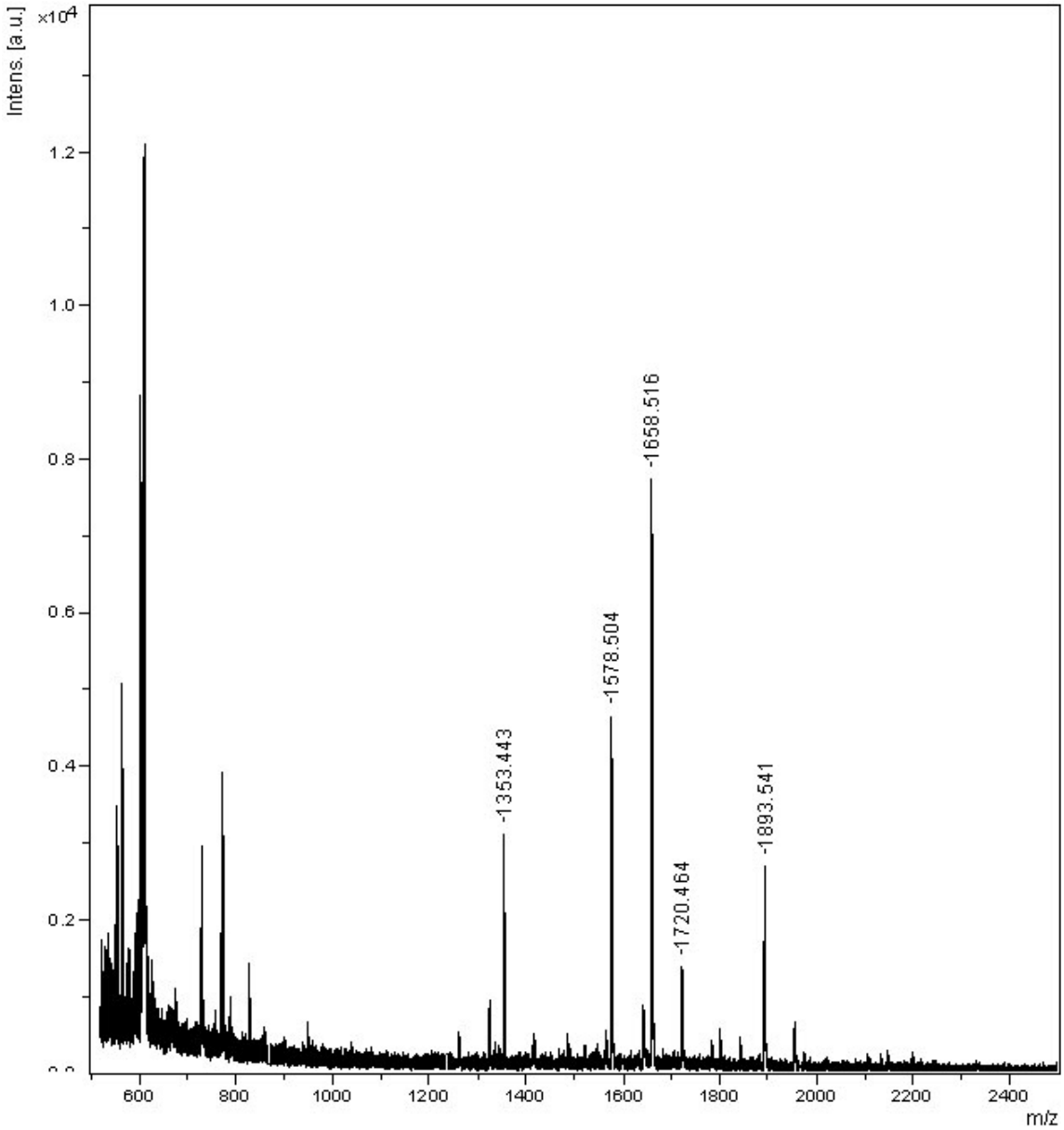

Figure S13(f8): Maldi-Tof mass-spectral analysis of the SMART™ RP-Hplc fraction at **R_T = 29.00** min in the **Fig S12(f2i).** Corresponding mixed RP-Hplc fractions were at **R_T = 25.93** min and **R_T = 26.49** min in the **Fig S12(f2)** [after **1h** of alkaline hydrolysis (pH 12.5 / 20ºC) of **5′-r(CACG^{Me}AAC)-3′**, **7c**] showing the peak at m/z **1894.5** for **5′-ACG^{Me}AAC-3′.** All other peaks are non-nucleos(t)idic.[see Table S9(F)].

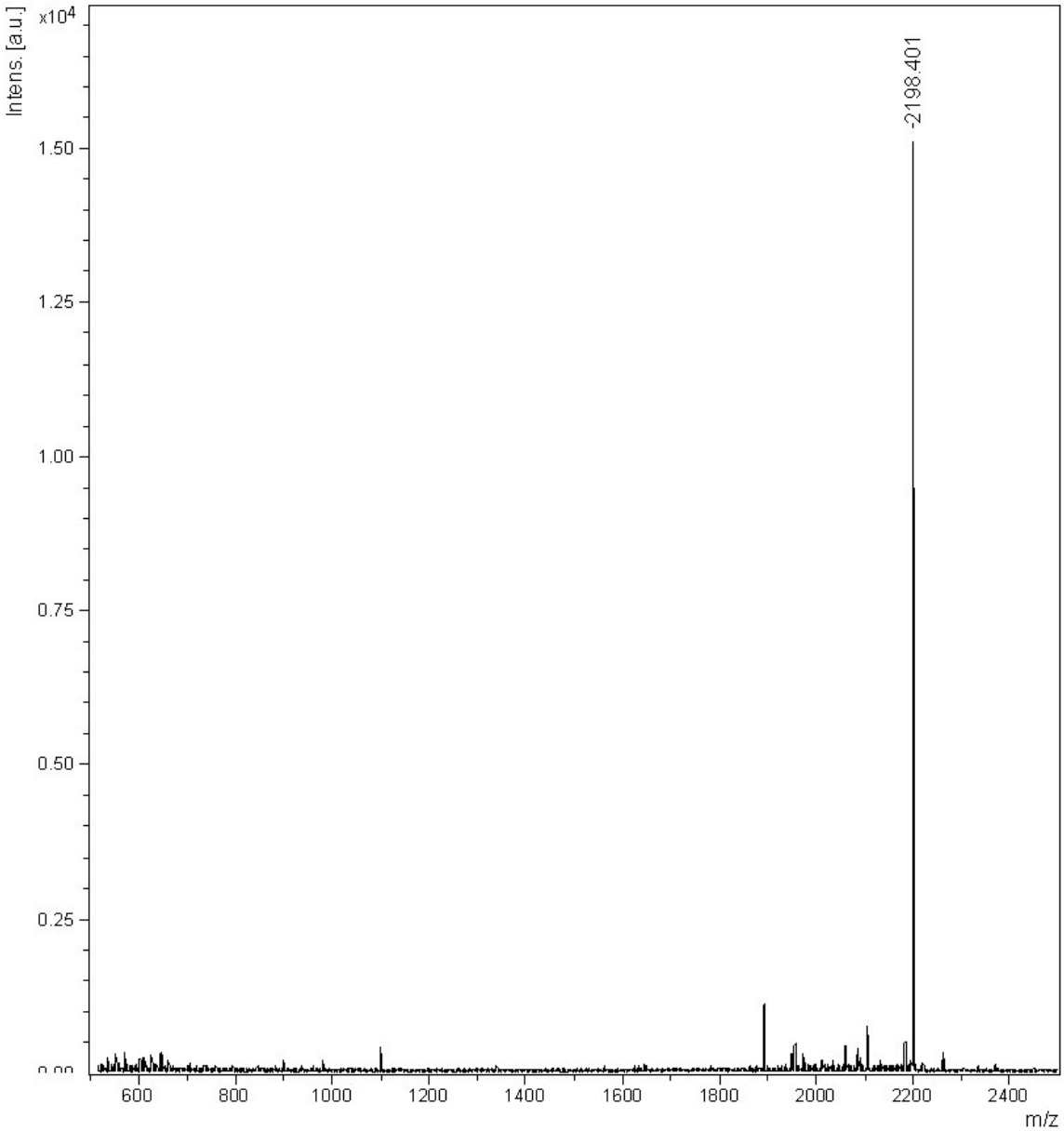

Figure S13(f9): Maldi-Tof mass-spectral analysis of the SMART™ RP-Hplc fraction at **R_T = 29.91** min in the **Fig S12(f2i).** Corresponding mixed RP-Hplc fractions were at **R_T = 25.93** min and **R_T = 26.49** min in the **Fig S12(f2)** [after **1h** of alkaline hydrolysis (pH 12.5 / 20ºC) of **5′-r(CACG^{Me}AAC)-3′**, **7c**] showing main the peak at m/z **2198.4** for **5′-CACG^{Me}AAC-3′**, the parent heptamer [see Table S9(F)].

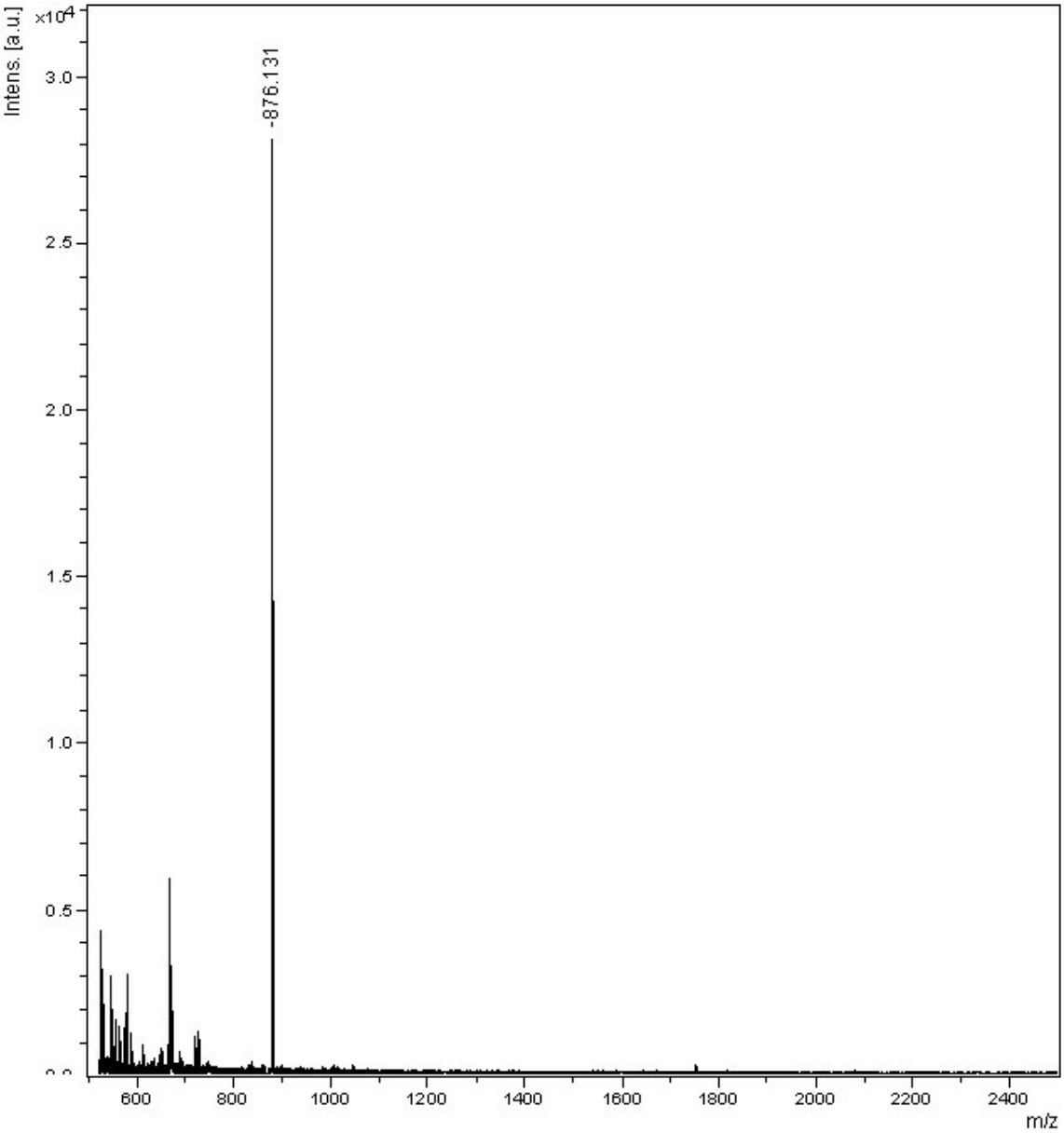

Figure S13(g1): Maldi-Tof mass-spectral analysis of the SMART™ RP-Hplc fraction at **R_T = 20.09** min in the **Fig S12(g2i).** Corresponding RP-Hplc fraction is **R_T = 19.68** min in the **Fig S12(g2)** [after **1h** of alkaline hydrolysis (pH 12.5 / 20ºC) of **5′-r(CACG^{Me}CAC)-3′**, **8c**]. The main peak at m/z **876.1** for **5'-CAC-3'** [see Table S9(G)]

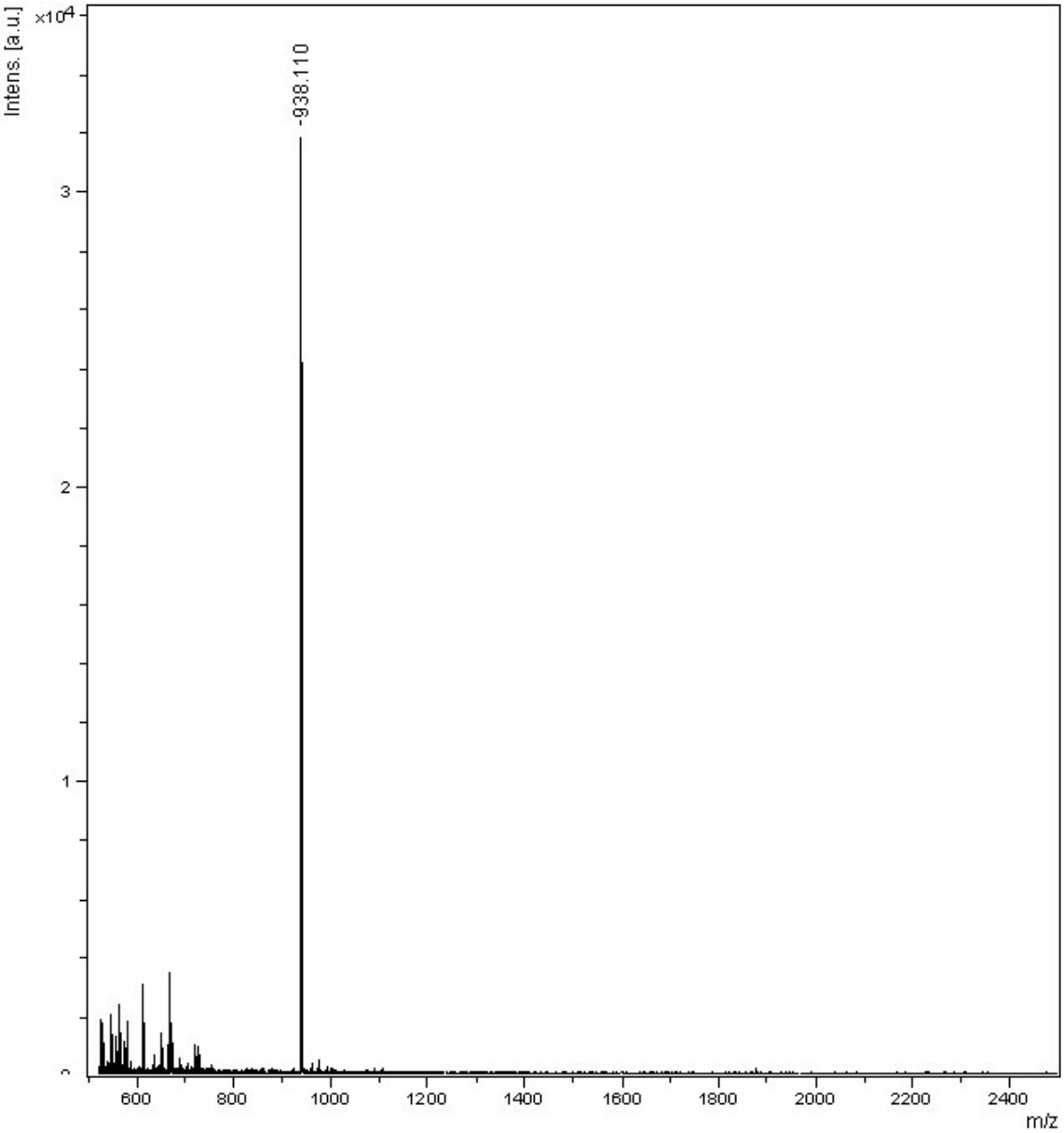

Figure S13(g2): Maldi-Tof mass-spectral analysis of the SMART™ RP-Hplc fraction at **R_T = 20.80** min in the **Fig S12(g2i).** Corresponding RP-Hplc fraction is **R_T = 19.68** min in the **Fig S12(g2)** [after **1h** of alkaline hydrolysis (pH 12.5 / 20ºC) of **5′-r(CACG^{Me}CAC)-3′**, **8c**]. The main peak at m/z **938.1** for **5′-CAC$_{2′,3′\text{-cMP}}$** [see Table S9(G)].

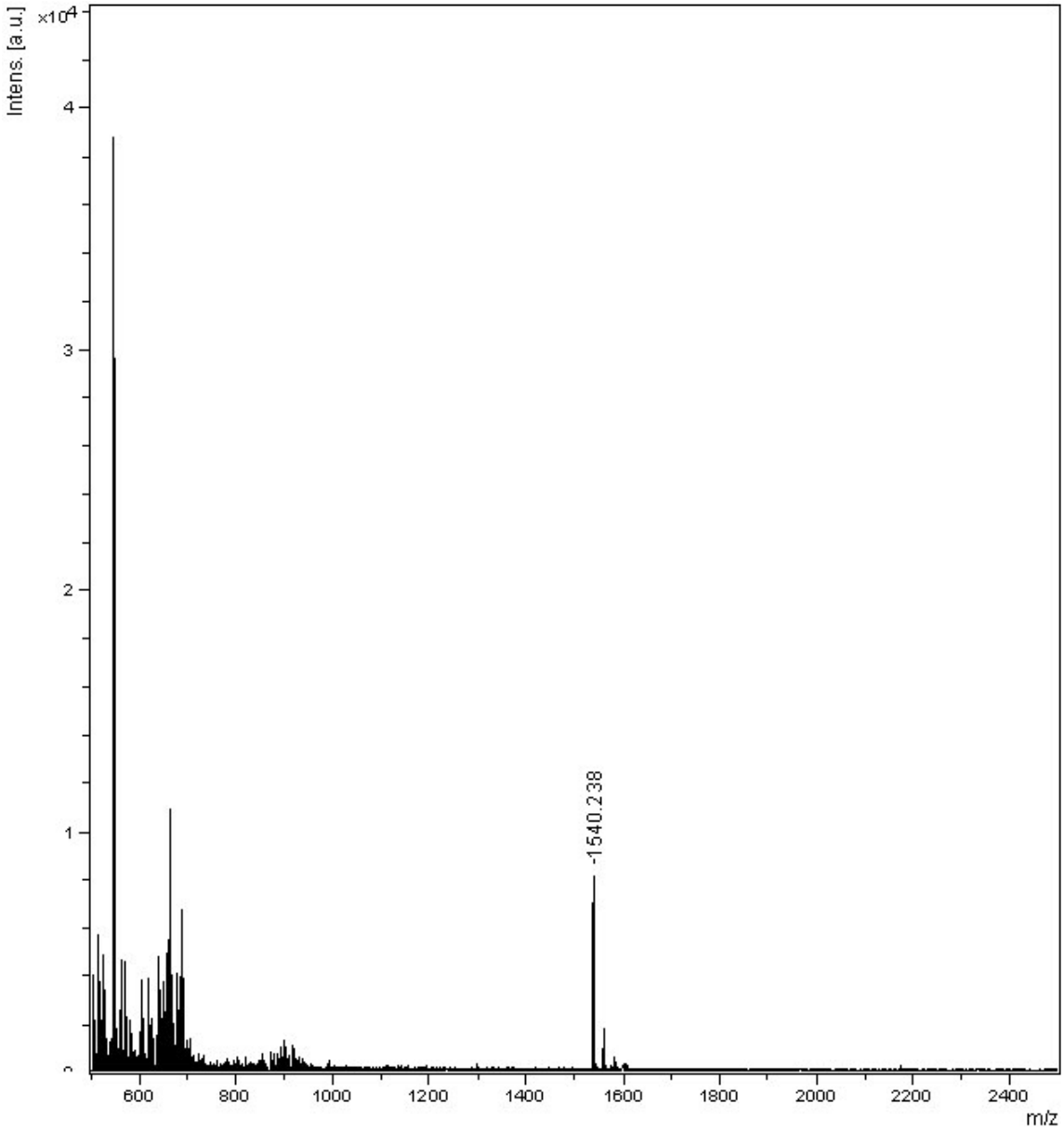

Figure S13(g3): Maldi Tof mass-spectral analysis of the RP-Hplc fraction at **R_T = 22.55** min for alkaline hydrolysis (pH 12.5 / 20ºC) of **5′-r(CACG^{Me}CAC)-3′** (**8c**) after **1h** [for Hplc profile, see Fig **S12 (g2)**] showing the main peak at m/z **1540.2** for **5′-CG^{Me}CAC-3′** [see Table S9(G)].

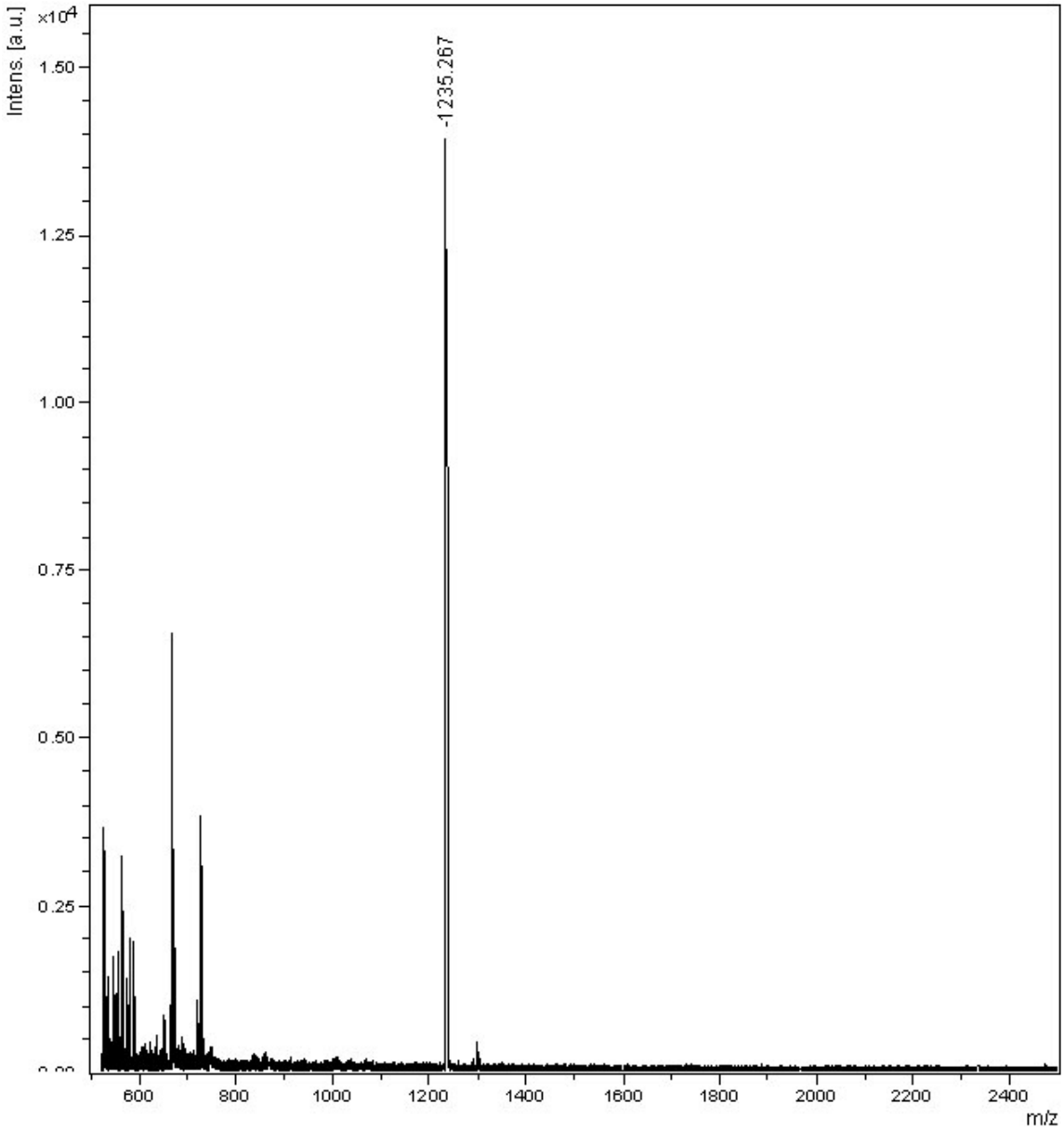

Figure S13(g4): Maldi-Tof mass-spectral analysis of the SMART™ RP-Hplc fraction at **R_T = 26.73** min in the **Fig S12(g2j).** Corresponding RP-Hplc fraction is **R_T = 23.15** min in the **Fig S12(g2)** [after **1h** of alkaline hydrolysis (pH 12.5 / 20ºC) of **5′-r(CACG^{Me}CAC)-3′**, **8c**]. The main peak at m/z **1235.2** for **5′-CACG$^{Me}_{2',3'\text{-cMP}}$** [see Table S9(G)].

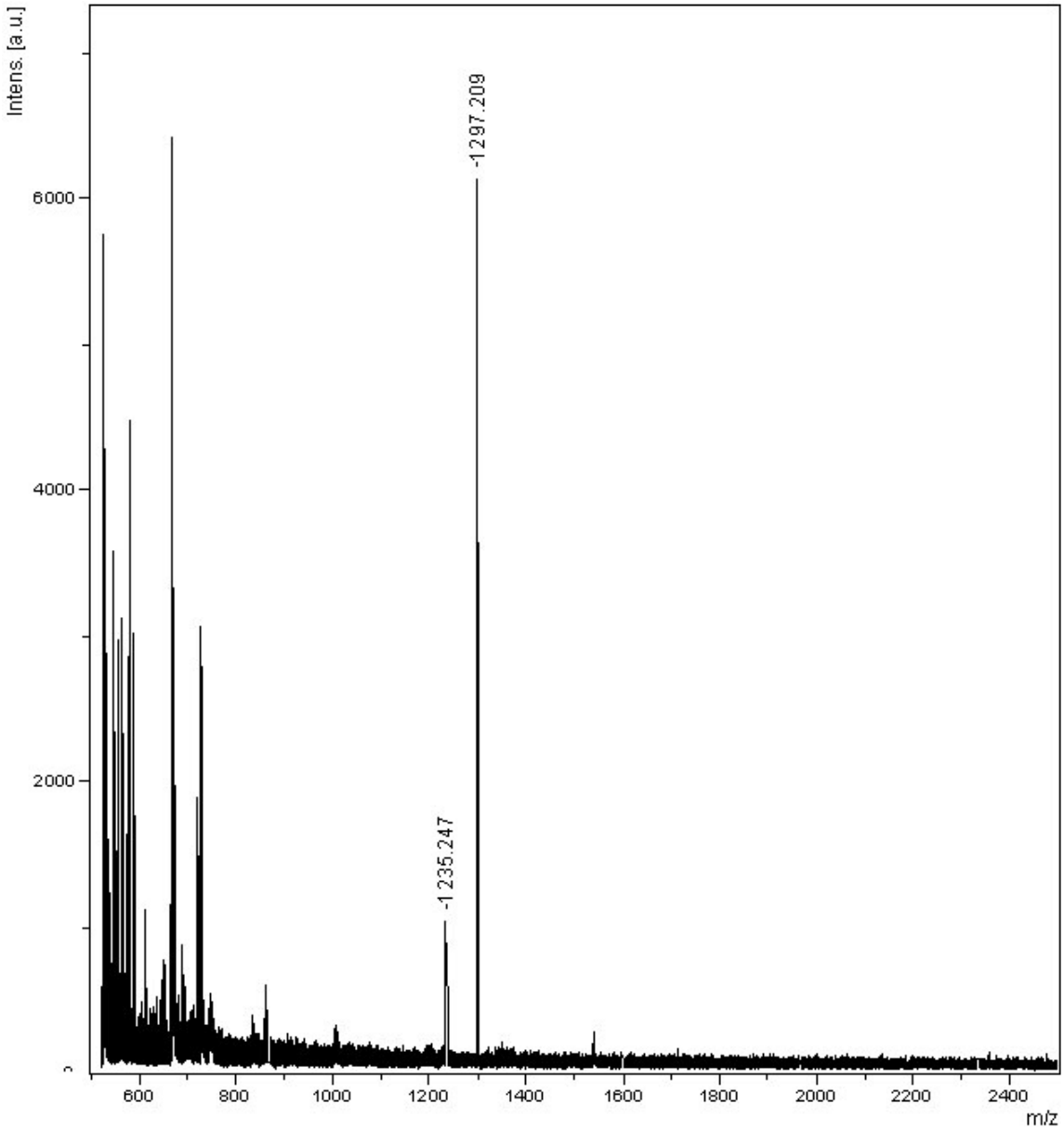

Figure S13(g5): Maldi-Tof mass-spectral analysis of the SMART™ RP-Hplc fraction at **R_T ≈ 27.00** min in the **Fig S12(g2j).** Corresponding RP-Hplc fraction is **R_T = 23.15** min in the **Fig S12(g2)** [after **1h** of alkaline hydrolysis (pH 12.5 / 20ºC) of **5′-r(CACG^{Me}CAC)-3′**, **8c**]. The main peak at m/z **1297.2** for **5′-G^{Me}CAC-3′** [see Table S9(G)].

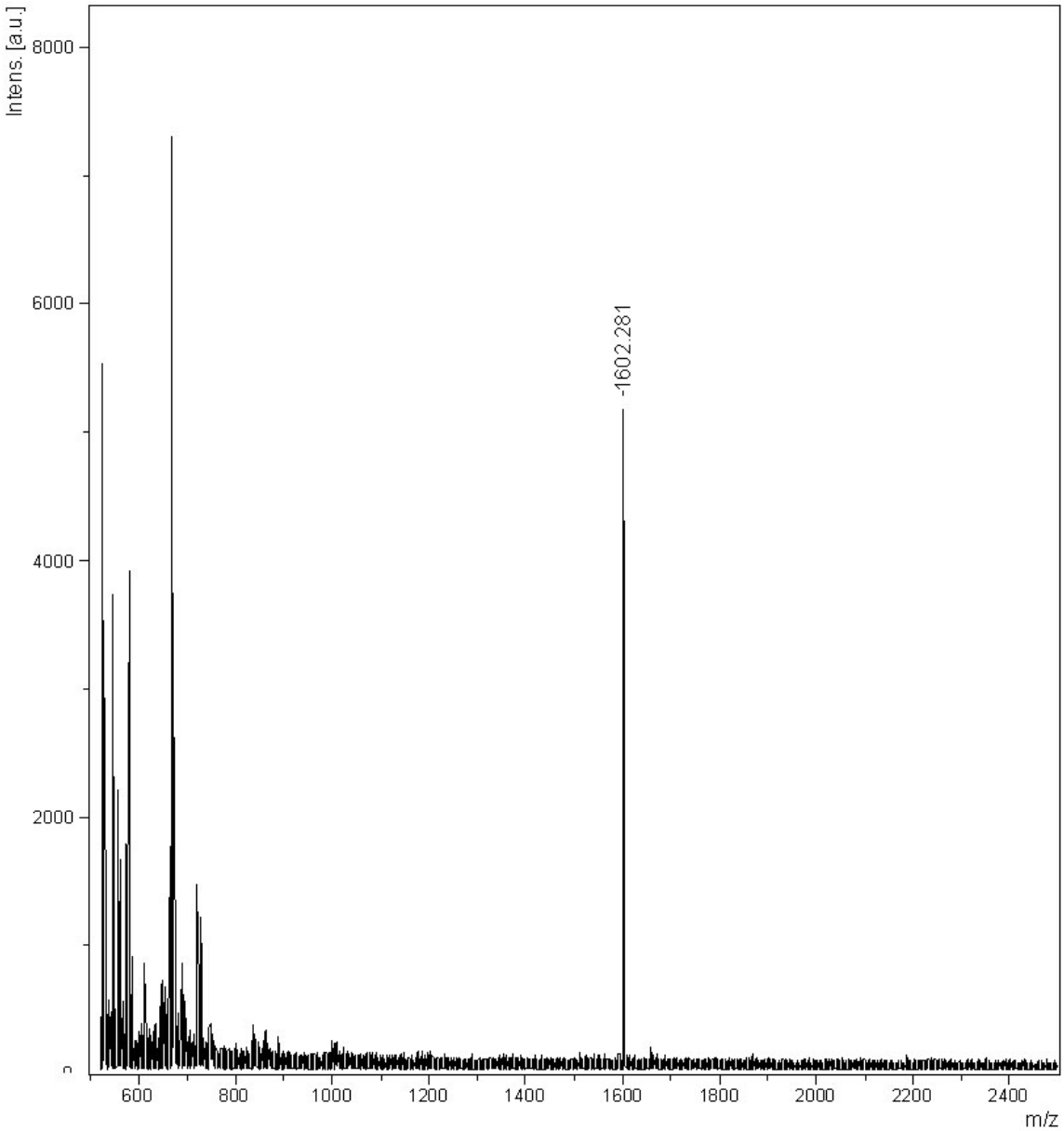

Figure S13(g6): Maldi-Tof mass-spectral analysis of the SMART™ RP-Hplc fraction at **R_T = 27.76** min in the **Fig S12(g2j).** Corresponding RP-Hplc fraction is **R_T = 23.15** min in the **Fig S12(g2)** [after **1h** of alkaline hydrolysis (pH 12.5 / 20ºC) of **5′-r(CACG^{Me}CAC)-3′**, **8c**]. The main peak at m/z **1602.2** for **5′-CACG^{Me}C$_{2′, 3′-cMP}$** [see Table S9(G)].

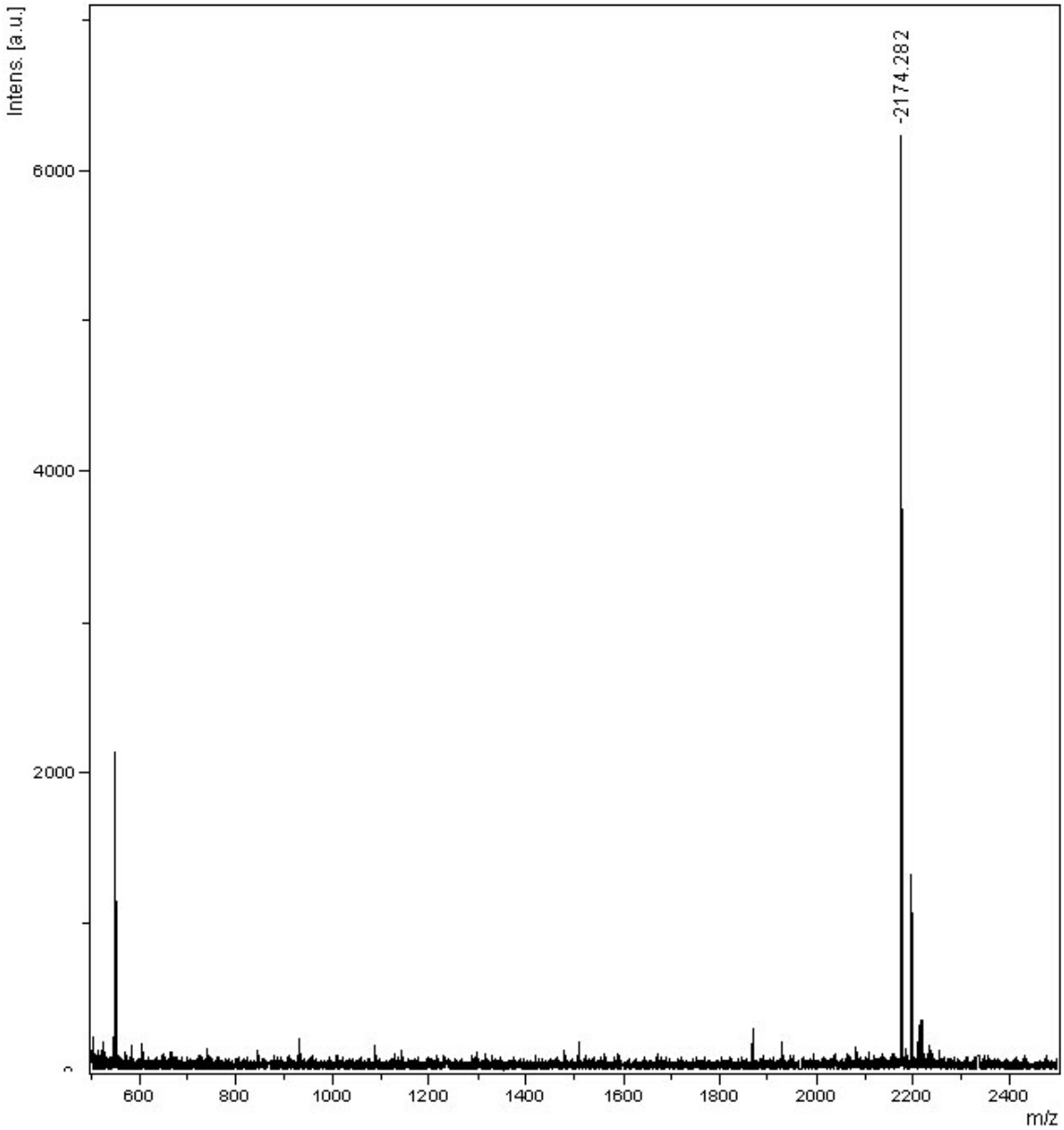

Figure S13(g7): Maldi Tof mass-spectral analysis of the RP-Hplc fraction at **R_T = 24.87** min for alkaline hydrolysis (pH 12.5 / 20ºC) of **5′-r(CACG^{Me}CAC)-3′** (**8c**) after **1h** [for Hplc profile, see Fig **S12 (g2)**] showing the main peak at m/z **2174.2** for the parent heptamer [see Table S9(G)].

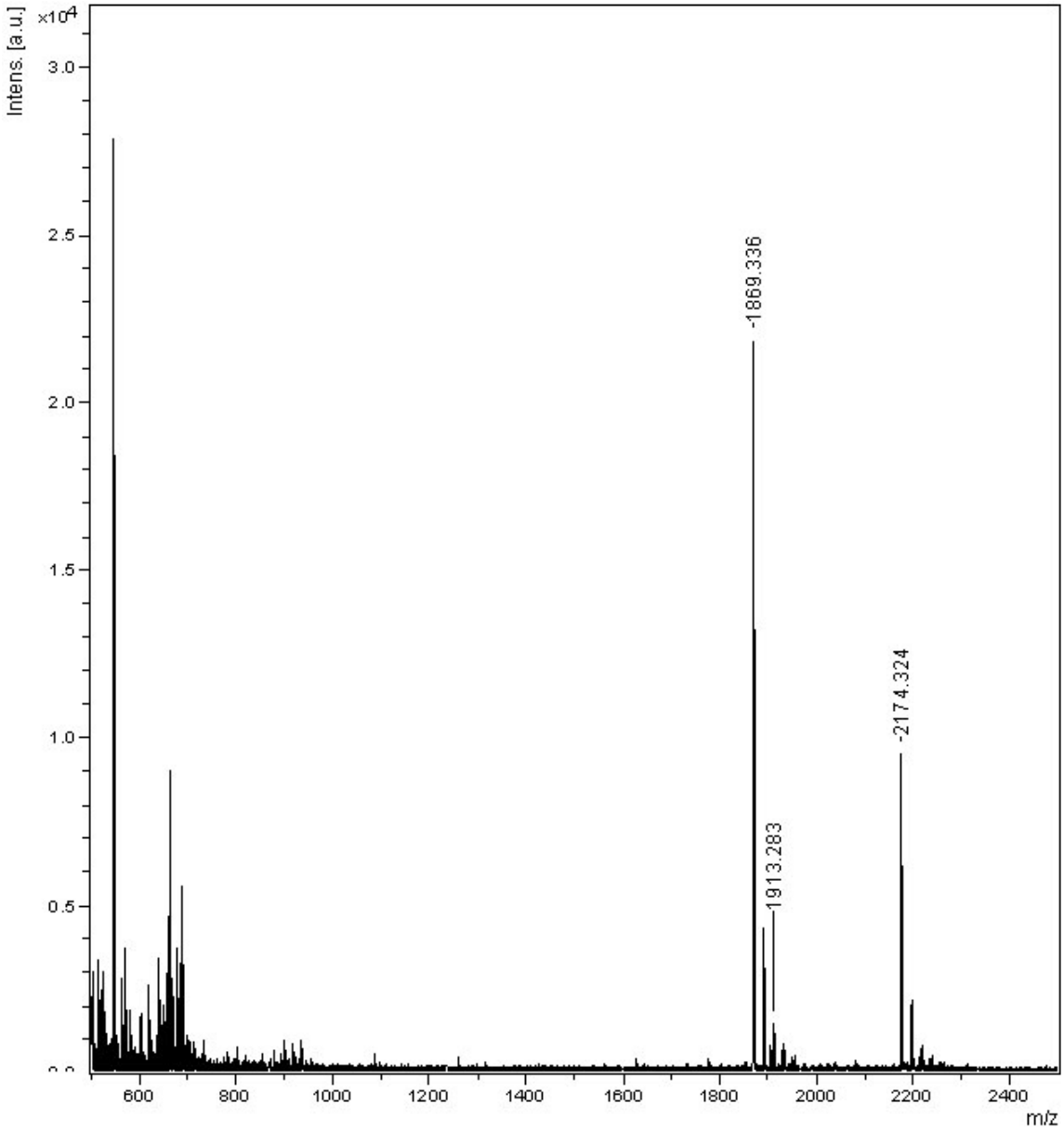

Figure S13(g8): Maldi Tof mass-spectral analysis of the RP-Hplc fraction at **R_T = 25.82** min for alkaline hydrolysis (pH 12.5 / 20ºC) of **5′-r(CACG^{Me}CAC)-3′** (**8c**) after **1h** [for Hplc profile, see Fig **S12 (g2)**] showing the main peak at m/z **1869.3** for **5′-ACG^{Me}CAC-3′** along with the parent heptameric peak[see Table S9(G)].